Established and Emerging Cardiovascular Magnetic Resonance Imaging Techniques in the Evaluation of Subclinical Cardiovascular Disease

Graham John Fent

Submitted in accordance with the requirements for the degree of Doctor of Medicine (MD)

The University of Leeds

Faculty of Medicine and Health

Leeds Institute of Cardiovascular and Metabolic Medicine

November 2017

Intellectual Property and Publication Statements

The candidate confirms that the work is his own, except where work which has formed part of jointly authored publications has been included. The contribution of the candidate and the other authors to this work has been explicitly indicated below. The candidate confirms that appropriate credit has been given within the thesis where reference has been made to the work of others:

Chapter 1

Publication:

Fent GJ, Greenwood JP, Plein S, Buch MH. The role of non-invasive cardiovascular imaging in the assessment of cardiovascular risk in rheumatoid arthritis: where we are and where we need to be. Ann. Rheum. Dis. 2016:annrheumdis-2016-209744. Available at: http://ard.bmj.com/lookup/doi/10.1136/annrheumdis-2016-209744 (epub ahead of print).

Authorship:

GF: Conception, design, literature search, drafting and revision of manuscript. **JG:** Revision of the manuscript. **SP:** Conception, design, drafting and revision of manuscript. **MB:** Conception, design, drafting and revision of manuscript

Chapter 3

Publication:

Fent GJ, Garg P, Foley JRJ, Swoboda PP, Dobson LE, Erhayiem B, Greenwood JP, Plein S, Treibel TA, Moon JC. Synthetic Myocardial Extracellular Volume Fraction. *JACC Cardiovasc Imaging* 2017;1–2. Available from: http://linkinghub.elsevier.com/retrieve/pii/S1936878X1631021X (epub ahead of print)

Authorship:

GF: Recruitment of patients, design, collection of data, data analysis and interpretation of data. Drafting and revision of manuscript. **PG**: Recruitment of patients, data analysis, collection and interpretation of data. Revision of manuscript. **JF:** Collection of data and revision of manuscript. **PS:** Recruitment of patients, collection of data and revision of manuscript. **LD:** Recruitment of patients, collection of data and revision of manuscript. **BE:** Recruitment of patients, collection of data **TT:** Design, data analysis and revision of manuscript. **JM:** Interpretation of data and revision of manuscript. **JG:** Interpretation of data and revision of manuscript. **SP:** Interpretation of data and revision of manuscript.

Chapter 4:

Authorship:

GF: Recruiting of patients, conception, data collection, data analysis and interpretation, drafting and revision of manuscript.

Chapter 5:

Publication:

Fent GJ, Garg P, Foley JRJ, Dobson LE, Musa TA, Erhayiem B, Greenwood JP, Plein S, Swoboda PP. The utility of global longitudinal strain in the identification of prior myocardial infarction in patients with preserved left ventricular ejection fraction. *Int J Cardiovasc Imaging*. 2017;0:0. Available from: http://link.springer.com/10.1007/s10554-017-1138-7 (epub ahead of print).

Authorship:

GF: Recruiting of patients, conception, data collection, data analysis and interpretation, drafting and revision of manuscript. **PG:** Recruiting of patients, revision of manuscript. **JF:** Interpretation of data and revision of manuscript **LD:** Interpretation of data and revision of manuscript **TM:** Interpretation of data and revision of manuscript. **BE:** Recruiting of patients, interpretation of data and revision of manuscript. **JG**: Interpretation of data and revision of manuscript. **SP:** Interpretation of data and revision of manuscript. **PS:** Conception, recruiting of pateints, data collection, interpretation of data, drafting and revision of manuscript.

Chapter 6:

Authorship:

GF: Recruiting of patients, conception, data collection, data analysis and interpretation, drafting and revision of manuscript. **BE:** Recruiting of patients and data analysis. **LAB:** Recruiting of patients and data analysis. **MB:** Interpretation of data and revision of manuscript. **JG:** Interpretation of data and revision of manuscript. **SP:** Interpretation of data and revision of manuscript

Chapter 7:

Authorship:

GF: Recruiting of patients, conception, data collection, data analysis and interpretation, drafting and revision of manuscript. . **BE:** Recruiting of patients and data analysis. **LAB:** Recruiting of patients and data analysis. **EH:** Statistical analysis. **MB:** Interpretation of data and revision of manuscript. **JG:** Interpretation of data and revision of manuscript. **SP:** Interpretation of data and revision of manuscript

Contributors initials/names:

GF: Graham Fent

BE: Bara Erhayiem

LAB: Lesley-Anne Bissell

TM: Tarique Al Musa

LD: Laura Dobson

PS: Peter Swoboda

JF: James Foley

PG: Pankaj Garg

EH: Elizabeth Hensor

JM: James Moon

TT: Thomas Treibel

MB: Maya Buch

JG: John Greenwood

SP: Sven Plein

Publications arising from this work

Papers:

1. Fent GJ, Greenwood JP, Plein S, Buch MH. The role of non-invasive cardiovascular imaging in the assessment of cardiovascular risk in rheumatoid arthritis: where we are and where we need to be. Ann. Rheum. Dis. 2016:annrheumdis-2016-209744. Available at: http://ard.bmj.com/lookup/doi/10.1136/annrheumdis-2016-209744 (epub ahead of print).
2. Fent GJ, Garg P, Foley JRJ, Swoboda PP, Dobson LE, Erhayiem B, Greenwood JP, Plein S, Treibel TA, Moon JC. Synthetic Myocardial Extracellular Volume Fraction. *JACC Cardiovasc Imaging* 2017;1–2. Available from: http://linkinghub.elsevier.com/retrieve/pii/S1936878X1631021X (epub ahead of print)
3. Fent GJ, Garg P, Foley JRJ, Dobson LE, Musa TA, Erhayiem B, Greenwood JP, Plein S, Swoboda PP. The utility of global longitudinal strain in the identification of prior myocardial infarction in patients with preserved left ventricular ejection fraction. *Int J Cardiovasc Imaging*. 2017;0:0. Available from: http://link.springer.com/10.1007/s10554-017-1138-7 (epub ahead of print).

Abstracts:

1. Fent GJ, Garg P, Dobson LE, Musa TA, Foley JRJ, Swoboda PP, Greenwood JP, Plein S. Quantitative myocardial perfusion and longitudinal strain by feature tracking in newly diagnosed, treatment naïve rheumatoid arthritis. Oral presentation at EuroCMR, Florence, Italy, May 2016.
2. Fent GJ, Garg P, Dobson L, et al. Global longitudinal strain using feature tracking identifies the presence of chronic myocardial infarction in patients with normal LV ejection fraction. Poster presentation at EuroCMR, Florence, Italy, May 2016.
3. Fent GJ, Swoboda PP, Foley JRJ, Garg P, Erhayiem B, Greenwood JP, Plein S. Radial and circumferential strain of the thoracic aorta measured by cardiovascular magnetic resonance feature tracking: a novel marker of aortic stiffness. Poster presentation at SCMR, Washington DC, USA, January 2017
4. Fent GJ, Hunt L, Mankia KS, Erhayiem B, Garg P, Swoboda PP, Andrews J, Greenwood JP, Emery P, Plein S, Buch M. Cardiovascular magnetic resonance imaging characterisation of cardiovascular abnormalities in individuals at risk of developing rheumatoid arthritis. Accepted for poster presentation at EULAR, Madrid, Spain, June 2017.

Acknowledgements

This work would not have been possible without the contribution and support of others. I would like to express my gratitude to Professor Sven Plein, Professor John Greenwood and Professor Maya Buch. Their leadership by example and academic guidance has been invaluable and is something that will stay with me through the rest of my career.

The working environment in the University of Leeds CMR Department has been fantastic and I would also like to express my thanks to the other staff involved in its day-to-day running. My colleagues Drs Swoboda, Garg, Foley, Chew, Brown, Biglands and Broadbent have provided creative thought, valuable experience and insight as well as a sense of humour when needed. I am grateful to the research nurses Petra, Lisa, Hannah and Fiona for their assistance in recruiting patients and smooth running of studies. Special thanks are due to the radiographers Gavin, Margaret, Caroline, Lisa, Georgina, Graham and Stephen for their technical know-how, scanning of patients and flexibility in accommodating my requests. I am also grateful to the assistants Debbie and Anne for their help

The greatest thanks of all go to the patients who participated in this research project. Their time and altruism has hopefully furthered our understanding of this field and may lead to improvements in patient care.

Lastly, I would like to acknowledge the support of my family- my wife Brenda for her patience and unrelenting positivity, my mum for teaching me to believe in myself and my dad for teaching me the value of quiet endeavour.

List of abbreviations

2Ch	2-chamber
4Ch	4-chamber
ACPA	Anti-cyclic citrullinated peptide antibody
AD	Aortic distensibility
anti-TNF	Anti-tumour necrosis factor α
AUC	Area undervla the curve
bDMARD	Biological disease modifying anti-rheumatic drug
BMI	Body mass index
BP	Blood pressure
BSA	Body surface area
bSSFP	Balanced steady state free precession
CAD	Coronary artery disease
CADERA	Coronary artery disease in early rheumatoid arthritis study
CMR	Cardiovascular magnetic resonance
CMR-FT	Cardiovascular magnetic resonance imaging feature tracking
CoV	Coefficient of variation
CRP	C-reactive protein
CSA	Cross-sectional area
csDMARD	Conventional synthetic disease modifying anti-rheumatic drug
CSPAMM	Complementary spatial modulation of magnetization
CT	Computed tomography
CV	Cardiovascular
CVD	Cardiovascular disease
DAS28	Disease activity score in 28 joints
DBP	Diastolic blood pressure
DCM	Dilated cardiomyopathy
DMARD	Disease modifying anti-rheumatic drug

ECG	Electrocardiogram
ECV	Extracellular myocardial volume fraction
EF	Ejection fraction
eGFR	Estimated glomerular filtration rate
ESR	Erythrocyte sedimentation rate
ETN	Etanercept
Gad-DTPA	Gadopentate-dimeglumine
GBCA	Gadolinium-based contrast agent
GLS	Global longitudinal strain
GLSR	Global longitudinal strain rate
GLSRe	Early diastolic global longitudinal strain rate
HCM	Hypertrophic cardiomyopathy
Hct	Haematocrit
HDL	High density lipoprotein
HFPEF	Heart failure with preserved ejection fraction
HFREF	Heart failure with reduced ejection fraction
IACON	Inflammatory arthritis disease continuum study
IL-1	Interleukin-1
IMH	Intramyocardial haemorrhage
LDL	Low density lipoprotein
LGE	Late Gadolinium enhancement imaging
ln	Natural logarithm
LV	Left ventricle
LVEDV	Left ventricular end diastolic volume
LVEDVi	Left ventricular end diastolic volume indexed to body surface area
LVESV	Left ventricular end systolic volume
LVMi	Left ventricular mass indexed to body surface area
MI	Myocardial infarction
MINOCA	Myocardial infarction with unobstructed coronary arteries

MOLLI	Modified Look-Locker inversion recovery
MR	Mitral regurgitation
MTX	Methotrexate
MV	Mitral valve
MVO	Microvascular obstruction
NO	Nitric oxide
NSF	Nephrogenic systemic fibrosis
PCI	Percutaneous coronary intervention
PD	Proton density
PET	Positron emission tomography
R1	Longitudinal relaxivity
RA	Rheumatoid Arthritis
ROC	Receiver-operating characteristic
ROI	Region of interest
RV	Right ventricle
RWMA	Regional wall motion abnormality
SBP	Systolic blood pressure
SD	Standard deviation
ShMOLLI	Shortened modified Look-Locker inversion recovery
SPAMM	Spatial modulation of magnetization
SPECT	Single positon emission computerised tomography
STEMI	ST-elevation myocardial infarction
SWT	Systolic wall thickening
T	Tesla
T2STIR	T2 short T1 inversion recovery
T2T	Treatment to target
TE	Echo time
TNF α	Tumour necrosis factor alpha
TNFi	Tumour necrosis factor α inhibitor

TOF	Time of flight
TR	Repetition time
TSA	Torsion sheer angle
US	Ultrasound
VEDERA	Very early versus delayed Etanercept in rheumatoid arthritis study
VLA	Vertical long axis
WMA	Wall motion abnormality

Abstract

Introduction: Cardiovascular disease (CVD) remains the number one cause of mortality in the world for both men and women, thus improving its diagnosis and treatment is a priority. Rheumatoid Arthritis (RA) is a common auto-immune disease associated with high rates of CVD. Cardiovascular magnetic resonance (CMR) offers a multi-parametric, quantitative approach to the assessment of the heart and cardiovascular system with a host of techniques allowing assessment of anatomy, ventricular function, myocardial composition, myocardial perfusion, vascular performance and myocardial metabolism during a single scan. Its quantitative nature and lack of ionising radiation lend themselves ideally to the longitudinal study of subclinical CVD.

Aims: To assess 1) whether blood longitudinal relaxation (T1) can be used to estimate blood haematocrit value to allow calculation of extracellular myocardial volume fraction (ECV), 2) whether CMR feature tracking (CMR-FT) is a feasible means of assessing aortic stiffness, 3) whether global longitudinal strain (GLS) is reduced in patients with prior MI with preserved left ventricular ejection fraction versus healthy controls, 4) whether aortic stiffness is present at all time points in the disease course of RA and 5) whether subclinical CV abnormalities in newly diagnosed RA improve with treatment and if the anti-tumour necrosis α Inhibitor Etanercept offers additional benefit over standard treatment.

Methods: Patients were recruited between and February 2011 and February 2017. All patients underwent a comprehensive, multi-parametric CMR study including cine and late Gadolinium enhancement imaging at either 1.5 or 3.0T.

Results: 1) estimation of blood haematocrit from blood T1 value provides accurate estimation of 'synthetic' ECV, 2) CMR-FT assessment of aortic stiffness is feasible and provides reproducible values for descending and ascending aortic strain values, 3) GLS is reduced in prior MI patients versus healthy controls (-17.3 ± 3.7% versus -19.3 ± 1.9% respectively, p=0.012). A GLS cut-off value of 18% correctly identifies prior MI with a sensitivity of 60% and specificity of 72.5%, 4) Aortic stiffness is evident in at risk RA individuals, newly diagnosed RA as well as established RA and 5) Aortic distensibility and left ventricular mass improve significantly in newly diagnosed RA patients following treatment. Etanercept appears to offer additional benefit over standard treatment evidenced by numerical improvements in aortic distensibility.

Table of contents

List of figures

List of Tables

List of equations

1. General Introduction

1.1. Background

Since the first reports of *in vivo* fluoroscopic imaging of the heart in the late nineteenth century(1), non-invasive cardiovascular imaging has progressed to become an indispensable means of assessing the function of the heart and wider cardiovascular (CV) system.

Cardiovascular disease (CVD) remains the number one cause of mortality in the world for both men and women(2), thus improving its diagnosis and treatment is a worldwide priority. As our understanding of the epidemiology of cardiovascular disease has evolved over time, there has been increased interest in characterising the way in which these diseases develop before they manifest clinically.

A multitude of factors are driving these efforts towards the characterisation of subclinical cardiovascular disease. Most significantly, the diagnosis of a disease before it becomes clinically apparent offers the potential to delay or halt its progression before morbidity or mortality ensue, through treatments and/or lifestyle changes. Identifying evidence of cardiovascular disease earlier than has previously been demonstrated and before the onset of clinical symptoms potentially offers the opportunity to bring forward the initiation of treatment.

The study of subclinical cardiovascular disease identification of 'biomarkers' of a disease (measurable indicators of its presence and/or severity) may improve not only its diagnosis, but also assess treatment effectiveness, patients most likely to benefit from particular treatments as well as assessing their prognosis over time(3). Biomarkers may be defined as 1) *biological biomarkers* – objective, measurable indicators of normal, pathological or pharmacological responses to disease or a therapeutic agent, or 2) *surrogate markers* – where a biomarker serves as a substitute for a clinically important outcome and therefore it's level is expected to reflect the effect of a disease or therapeutic agent(4). A scheme of validation has been proposed by which new and emerging biomarkers are evaluated and developed(5). Initially the clinical relevance of a biomarker must be proven, for instance demonstration of its ability to reflect a plausible and rational physiological or pathological change in a biological system. Additionally, its sensitivity and specificity to detect a significant morbidity or mortality outcome within a target

population must be demonstrated. Its reliability must also be demonstrated in terms of accuracy, precision and reproducibility (across different assessors, within the same assessor and at different time points). Lastly, a biomarker's utility in terms of practicality and feasibility (ease and resource intensiveness of performing the test) as well as the acceptability of the test to patients needs to be proven.

The study of subclinical cardiovascular disease, aside from its role in development of biomarkers, offers the opportunity to elucidate the pathophysiological mechanisms by which it develops into *clinical* disease, which in turn may provide insight into potential therapeutic targets to treat that disease.

Whereas early non-invasive cardiovascular imaging techniques assessed the heart and cardiovascular systems on a gross macroscopic level, cardiovascular magnetic resonance imaging (CMR) is able to offer in vivo assessment at tissue and even cellular levels. It provides a comprehensive assessment of cardiac structure and function with broad applications in both clinical and research settings.

Key advantages of CMR include the lack of use of either ionising radiation, radioactive isotopes or iodinated contrast agents as are used by alternative modalities such as computed tomography (CT), single positron emission computed tomography (SPECT) and positron emission tomography (PET)(6). Images can be acquired in any desired plane, without many of the limitations imposed by patient habitus or pre-existing lung disease (both key limitations of transthoracic echocardiography). CMR offers a multi-parametric, quantitative approach to the assessment of the heart and cardiovascular system with a host of techniques allowing assessment of anatomy, ventricular function, myocardial composition, myocardial perfusion, vascular performance and myocardial metabolism(7) during a single scan. Measuring quantitative CMR parameters affords accurate comparison of these parameters in the same patient over time, comparisons within different patient groups, as well as between patients with and without a particular disease. Furthermore, a quantitative approach (as opposed to qualitative visual analysis) potentially allows for the detection of more subtle abnormalities of cardiac structure and function, as well as improved reproducibility.

CMR is used extensively in the assessment of the effectiveness of treatments in the form of surrogate endpoints which are expected to predict clinical benefit or harm. Accordingly, these may be used to supplement or even replace 'hard' clinical outcomes such as mortality and measures of morbidity(8). Examples where CMR provides useful and reliable surrogate endpoints in clinical trials include acute ST segment elevation infarct (STEMI). Here, the quantitative parameters 'area at risk,

‘infarct size’ and salvage index (discussed later in this chapter) can be assessed(9, 10). Numerous other potential CMR surrogate endpoints for clinical trials have been proposed including dilated cardiomyopathy (DCM)(11) and amyloid heart disease(12).

Key clinical applications of CMR include the assessment of patients with known or suspected cardiomyopathy, assessment of the thoracic aorta, characterisation of anatomy and cardiac function in congenital heart disease, the evaluation of known or suspected coronary artery disease and the assessment of pericardial disease and cardiac masses(13).

Limitations of CMR include its relative expense and contraindications for patients with either retained metal objects or older metallic medical prostheses. The use of Gadolonium based contrast agents (GBCA) in patients with severe renal disease (eGFR <30ml/min) is contra-indicated as this is associated potentially fatal nephrogenic systemic fibrosis(NSF)(14). Nevertheless, since the introduction of routine screening of renal function prior to patients undergoing CMR requiring GBCA and restricting its use to patients with acceptable renal function (eGFR ≥30ml/min), the worldwide incidence of NFS is now extremely low(15). More recently however, additional concerns have been raised over the use GBCA. Repeated use of linear GBCA compounds have been associated with long-term retention of these compounds in areas of the brain including the globus pallidus and dentate nucleus(16). However, the clinical consequence, if any, of this phenomenon is not known and further investigation in this area is ongoing. More research is needed before any change is made to clinical guidelines and protocols.

This chapter aims to discuss current and emerging CMR techniques used to evaluate subclinical disease as well as to synthesise and evaluate the key current literature surrounding the epidemiology and pathogenesis of both prior myocardial infarction (MI) and rheumatoid arthritis (RA), both of which are investigated in subsequent results chapters.

1.2. Assessing subclinical cardiovascular disease with CMR

1.2.1. Cine imaging by CMR

Cardiovascular magnetic resonance (CMR) is considered the current reference standard for quantitation of left ventricular (LV) and right ventricular (RV) mass, volumes and systolic function(7) due to its accuracy and reproducibility. Aside from ventricular volumes, cine imaging provides detailed structural and morphological information relating to the cardiovascular system, both of which are key elements of clinical CMR reporting.

CMR methods have undergone considerable evolution and standardisation over the past two decades. Today, balanced steady state free precession (bSSFP) is the standard for acquisition of cine CMR images as it provides improved endocardial border delimitation, shorter scan times and higher signal to noise ratios than the formerly used spoiled gradient echo methods(17). The overall better image quality of bSSFP acquisition and the ability to more clearly differentiate trabeculation from the endocardial border leads to different estimates of LV and RV chamber size, with typically larger volumes and lower mass(18). Parallel imaging may be used to improve temporal resolution, in-plane spatial resolution and/or breath hold times of bSSFP cine acquisitions and works by undersampling raw image data in the phase encoding direction(19). However, its use is also associated with reduction of signal to noise ratio as well as an increase in image artefact.

Typically cine imaging is acquired using retrospective electrocardiogram (ECG) gating, where continuous acquisition of images and ECG signal occurs and is then used to reconstruct images by grouping them sequentially according to their relation to the R wave on the ECG and thus according to cardiac phase(20). This ensures that all phases of the cardiac cycle are included in cine acquisitions and allows corrections to be made to allow for beat to beat variations in heart rate. Disadvantages with a retrospective gating technique are reduced image quality when the ECG R-R interval is irregular (in the case of arrhythmia) and difficulty in acquiring images when the R wave amplitude is low, which is a particular issue on 3.0 tesla (T) systems. When image quality is markedly compromised by either of these issues, real-time imaging may be used which does not require ECG gating(21). However, this technique is currently severely limited by reduced spatial and temporal resolution.

1.2.2. Strain imaging by CMR

CMR may be used in the assessment of myocardial strain. Myocardial deformation imaging or *strain imaging* is the assessment of myocardial shortening or lengthening at either segmental or wider global level during systole or diastole(22). Myocardial shortening is assigned a negative value, whereas lengthening is expressed as a positive value. Strain (equation 1) may be assessed in one of three cardiac axes; longitudinal, radial or circumferential(23).

Equation 1 Strain equation

$$Strain = (L - Lo) / Lo$$

Where L= length in a specific direction after deformation (e.g. radial, circumferential, longitudinal planes) and Lo = original length

Traditionally, quantitation of ventricular function has been assessed by expressing LV or RV ejection fraction (EF) which is later discussed in the methods chapter. Regional ventricular function is typically assessed visually, by describing individual LV or RV segments as contracting normally or abnormally. When regional myocardial contraction is visually abnormal this is referred to as a regional wall motion abnormality (RWMA). However, strain imaging offers the potential to detect abnormalities in myocardial function at either global or regional level before they manifest clinically or are apparent in traditional measures of abnormal myocardial function such as ejection fraction, RWMA or ventricular remodelling(24). Clinical applications of strain imaging to date have predominantly been demonstrated using speckle tracking echocardiography. Examples include the demonstration of global longitudinal strain (GLS) as a better predictor of mortality than LVEF in heart failure with patients with LVEF≥40% (25). Longitudinal strain is also demonstrably lower in patients with early hypertrophic cardiomyopathy (HCM) and, in combination with other clinical parameters, may be of use in screening asymptomatic family members of affected patients(26). In patients treated with cardiotoxic chemotherapy agents, GLS may be reduced before LVEF, potentially allowing earlier adjustments to treatment regimens thereby halting the development of clinical heart failure(27).

Strain indices are conventionally assessed using CMR by ‘tagging’, which is widely considered to be the reference standard non-invasive imaging technique in the assessment of myocardial deformation. The most commonly used CMR tissue tagging techniques are referred to as ‘spatial modulation of magnetization’ (SPAMM) or ‘complementary spatial modulation of magnetization’ (CSPAMM)(28). These require acquisition of specialised images where a grid-like magnetised pattern of two orthogonally intersecting lines are superimposed over the imaging slice (short or long axis) over the course of the cardiac cycle allowing tracking of the pattern in space and time in order to calculate strain values. The grid-like magnetisation effect in SPAMM is achieved with a CMR pulse sequence resulting in selective radiofrequency saturation of the ‘tagged’ myocardium through the cardiac cycle with a temporal resolution in the region of 15-20ms(29). The use of CSPAMM improves the fading of the grid tags due to longitudinal T1 recovery which occurs using SPAMM, at the expense of doubling the required scan time(30). Although CMR tissue tagging produces accurate and reproducible values for both regional and global deformation indices, the technique is limited by the need for a dedicated image acquisition scheme and its requirement of time-consuming post-processing analysis in order to extract these values; factors which potentially limit its use in clinical practice(31).

CMR feature tracking (CMR-FT) is a newer technique which, rather than requiring a specific image acquisition scheme, is able to calculate strain values comparable to those obtained with CMR tagging or echocardiographic speckle tracking from SSFP (or other) cine acquisitions. The underlying methodological principles of the technique are comparable to speckle tracking echocardiography and use post-processing computer software to identify features (typically the size of a few pixels) appearing within a small window of an image, identifying a comparable feature within subsequent image frames and assessing its displacement through space and time(32). This technique works better at endocardial borders than within compacted myocardium, probably due to the homogeneity of water content and relative lack of distinctive features within myocardium(32).

Although few studies have compared CMR tissue tagging directly with CMR FT, tissue tagging has been demonstrated to be more reproducible for the measurement of segmental strain parameters(33). However, CMR-FT reproducibility is good for global strain indices (both long and short axis) and no significant differences are observed between measurements obtained at 1.5 and 3.0T field strength bSSFP cine acquisitions(34).

1.2.3. Assessment of myocardial perfusion by CMR

Chronic myocardial ischaemia can be assessed using CMR by either visual or computerised quantitative assessment of blood flow to the LV myocardium by intravenous injection of GBCA and observation of resultant myocardial uptake both at rest and during pharmacological vasodilator stress(35). Hyperaemia is most commonly brought about by use of intravenous adenosine infusion. Adenosine is a naturally occurring endogenous cardiovascular signalling molecule which acts on A2A and A2B receptors(36). The half-life of adenosine is short (in the region of 10 seconds) with very few contra-indications and an excellent safety profile. Alternative vasodilator agents which have been used in CMR myocardial perfusion assessment include Regadenason and Disopyramide, though these are seldom used in the context of CMR perfusion in either clinical practice or research in the UK. Regadenason is used in some centres in the USA (37).

Images are acquired in 3 short axis slices through the LV to ensure coverage of the LV base, mid and apex, a detailed explanation for which is given in the methods chapter. Spoiled gradient T1-weighted echo sequences are the most commonly used pulse sequences in CMR perfusion imaging(38) and can be used in combination with acceleration techniques such as *kt*-sense or *kt*-blast based on spatio-temporal undersampling to maximise in-plane spatial resolution of acquired data(39), while still enabling acquisition of all 3 short axis slices with each heartbeat. Acquiring images with each heartbeat is crucial to ensure adequate temporal resolution and full capture of myocardial uptake of GBCA during its first pass through the coronary circulation. GBCAs shorten T1 time, appearing as areas of high signal when present. Spatial resolution of CMR perfusion analysis without the use of acceleration techniques is around 2-3mm, but with acceleration and at 3.0T field strength (which offers improved contrast and signal to noise ratios) may be lower than 2mm(37).

Uptake of contrast agent may be impaired during vasodilator stress either due to epicardial coronary artery disease or more distally in the coronary tree in the form of microvascular disease. The presence of flow-limiting, functionally significant epicardial coronary artery disease in the clinical setting is conventionally determined by qualitative visual assessment. Abnormally perfused areas of myocardium appear as a relatively dark area of myocardium in a coronary

distribution. Conversely, neighbouring normally-perfused myocardium appears lighter, with high signal intensity due to higher uptake of contrast agent.

CMR is commonly used in the assessment of clinical patients with suspected stable coronary artery disease. Meta-analysis has demonstrated that this technique has a high sensitivity and specificity for the detection of significant epicardial coronary artery disease, estimated at 89 and 76 % respectively for sensitivity and sensitivity(40). Direct comparison of CMR to SPECT suggests that CMR offers a higher degree accuracy than SPECT in identifying significant coronary artery stenosis on subsequent x-ray coronary angiography(41).

Besides visual assessment, myocardial perfusion may be assessed in a quantitative manner using computer software (normally as a post-processing technique applied after the scan has taken place). Numerous mathematical algorithms exist by which to compute myocardial blood flow in ml/min/g, which work by equating signal intensity curves through first pass perfusion of blood pool and myocardium to GBCA concentration. Of the algorithms available, Fermi deconvolution correlates best with animal model studies of myocardial perfusion using fluorescent microspheres as the validation technique(42). A ‘dual-bolus’ technique may improve myocardial perfusion quantification, where a 10% dilute GBCA bolus is first infused, followed by a concentrated GBCA bolus. Perfusion quantification relies on a linear relationship between signal intensity and GBCA concentration, however, GBCA infusion can induce T-1 saturation and signal attenuation in the LV cavity(43). Use of a dilute GBCA bolus serves to maintain linearity of the LV signal intensity, improving the accuracy of blood flow algorithms.

Quantitative perfusion may circumvent some limitations to visual assessment of myocardial perfusion using CMR. Once such limitation is ‘balanced ischaemia’, where globally impaired perfusion is misinterpreted as normal. This may occur due to widespread epicardial coronary disease, since visual analysis relies on comparing normally perfused areas of myocardium with abnormal areas, yet when only abnormal areas are seen, this may be misinterpreted as ‘normal’(10). Furthermore, quantitative perfusion may allow more accurate assessment of coronary microcirculation dysfunction which typically manifests as a global myocardial process(44). Subclinical impairment of coronary microcirculatory function has been demonstrated in a variety of diseases including HCM(45), dilated cardiomyopathy(46) and aortic stenosis(47).

The reference standard technique for quantitative myocardial perfusion is PET(44, 48), however, good agreement has been shown between PET and quantitative

myocardial perfusion by CMR(49) as well as invasively measured fractional flow reserve(50).

1.2.4. CMR Tissue Characterisation Techniques

A key advantage of CMR lies in its ability to provide ‘tissue characterisation’ of the myocardium; detailed information regarding the structure and composition of the ventricular myocardium allowing detection and diagnosis of a wide range of myocardial diseases(51).

1.2.4.1. Late Gadolinium Enhancement Imaging

The most established tissue characterisation technique is late Gadolinium enhancement imaging (LGE) whereby a contrast agent is administered to the patient allowing visualisation of characteristic patterns of myocardial hyperenhancement, which in turn reflect areas of infarction or focal fibrosis(52). Contrast diffuses passively into and is retained within infarcted or fibrotic myocardium and appears as confluent areas of high signal on LGE due to the T1 shortening properties of GBCAs (time taken for protons to return to their resting alignment after aligning in the longitudinal plane following a ‘saturation’ or ‘inversion’ pulse) . The Gadolinium component of GBCAs is bound to a chelate, the purpose of which is to reduce toxicity and limit the distribution of GBCAs to the extracellular compartment of tissues in the body(53). In normal tissues with intact cellular membranes, this extracellular space is relatively small, however, if acute cellular necrosis occurs (e.g. in acute MI) contrast is able to passively diffuse into the intracellular space, or if healthy myocardial cells are replaced by substances such as collagen as occurs in chronic MI or conditions leading to myocardial fibrosis, the extracellular compartment is larger relative to normal which increases the distribution of GBCA. Fibrosis itself can be considered as pathological remodelling of the extracellular space surrounding cardiac myocytes involving deposition of collagen into this space, often leading to stiffness of these myocytes(54).

CMR pulse sequences for acquisition of late Gadolinium enhancement images use inversion recovery gradient echo pulse sequences . Images are acquired 10-15 minutes following GBCA injection. Firstly, a variable inversion time scout sequence or ‘Look Locker’ sequence is performed allowing selection of the optimal inversion time at which the myocardium becomes ‘nulled’ i.e. devoid of signal and appearing dark, thus maximising the contrast between normal low signal myocardium and high signal areas where GBCA has been retained. Images are then acquired after

applying the appropriate inversion time. A more recent alternative technique termed ‘phase sensitive inversion recovery’ removes the dedicated variable inversion time scout sequence needed to determine the optimal inversion time of nulled myocardium (and operator dependence on its interpretation) while retaining excellent image quality(55).

In the clinical setting, LGE is useful in the diagnosis and differentiation of numerous cardiomyopathies, each of which have characteristic patterns of hyperenhancement (56) as well as in the detection of myocardial infarction in both the acute and chronic setting.

Quantification of LGE can be performed using semi-automated post-processing software. These use signal intensity thresholding techniques which incorporate mathematical cut-off points to determine normal versus hyperenhancing myocardium and have been validated against histology slides from explanted hearts and myomectomy tissue demonstrating good agreement between the two(57). Each technique differs in performance and reproducibility, though no consensus exists as to the optimal method to use(58).

The main limitations of LGE are its requirement of GBCA (limiting its use to patients with eGFR >30ml/kg/min), its relative inability to demonstrate diffuse as opposed to focal fibrotic processes and its inability to differentiate active inflammation from chronic, inactive scar(59). Most of these limitations can be overcome through the use of additional assessment of CMR tissue characteristics.

1.2.4.2. T1 Mapping and Extracellular Volume Fraction Calculation

CMR generates images by recording and displaying relative pixel intensity according to the relaxation of hydrogen protons in a static magnetic field. T1 relaxation time represents the intrinsic spin-lattice magnetic relaxation property of tissue or relaxation recovery time of protons in the longitudinal plane after excitation with an inversion pulse(60). Precise T1 values can be calculated of myocardium and blood on a pixel-wise basis in the form of ‘T1 maps’ allowing comparison between patients and pre-defined normal values (which are vendor and field strength dependent). T1 times vary greatly in different body tissues and to a lesser degree within the myocardium itself. T1 maps represent a composite image comprised of individual images at different T1 recovery times(61). The intensity of pixels in the composite image correspond to the T1 time within the corresponding

voxel – the brighter the pixel, the longer the T1 recovery time. Myocardial T1 mapping provides additional diagnostic information in the form of the magnetic relaxation properties of the myocardium on a pixel by pixel basis and may reveal a more subtle, diffuse myocardial fibrosis process not evident on LGE imaging, without the requirement of contrast agent(62). A high T1 value may be seen in the presence of diffuse myocardial fibrosis, but may also also be elevated in the context of myocardial protein deposition and oedema(63). Conversely, low T1 values are typically seen in iron or lipid deposition(63).

Three main types of pulse sequence can be used to generate T1 maps. Messroghli et al. devised the commonly used Modified Look-Locker Inversion recovery scheme (MOLLI) which merges SSFP single shot read-out images at end-diastole from multiple Look-Locker experiments at conducted at differing, consecutive inversion times to generate maps within a single breath-hold of around 15-20 seconds(64). Following on from this work, Piechnik et al. described the shortened MOLLI or 'ShMOLLI' sequence which is a simplified, shortened pulse sequence with fewer SSFP readouts and requires a shorter (approximately 10 second) breath-hold to acquire(65). Agreement in values between the two methods is good(65). SASHA is a third, newer pulse sequence and stands for 'saturation recovery single-shot acquisition'. This uses 10 ECG triggered single shot bSSFP images in a single breath hold with a shorter breath hold time than MOLLI. Performance in phantom studies and in vivo is good(66).

T1 mapping techniques in combination with administration of GBCA provide an estimate of myocardial extracellular volume fraction (ECV), which expresses the relative volume of cardiac tissue not occupied by cells. ECV can be useful in demonstrating more diffuse forms of fibrosis where the post GBCA myocardial signal intensity may be isointense and therefore not evident on LGE, which highlights localised areas of fibrosis(67). ECV is estimated from the concentration of GBCA within the LV myocardium relative to the blood concentration of GBCA in a dynamic steady state(67) and therefore may be derived from an equation incorporating myocardial and blood T1 (ms) adjusted for the patient's haematocrit (which influences both of these values). Full details of myocardial ECV volume fraction calculation are provided in the methods chapter.

The relative balance of the cellular and extracellular volumes may be altered by varying degrees by various physiological and pathophysiological processes(60, 68–

70). ECV measured by CMR has been validated against histologically derived myocardial ECV(71). Furthermore, ECV calculated by CMR shows promise in prognostication of mortality and morbidity(68, 72). Current limitations of the technique include 'partial voluming' occurring at the myocardial: blood pool interface, where a given voxel or voxels comprise T1 values from both myocardium and blood pool and therefore represents the average T1 value of the two. This may be obviated by measuring myocardial T1 values from a region of interest in the midwall and blood region of interest well away from the myocardium. However, doing so may not detect a true pathological process such as subepicardial or subendocardial fibrosis(67).

1.2.4.3. T2 weighted Imaging

T2 weighted imaging is most commonly performed using short TI triple inversion recovery prepared fast spin echo pulse sequences (T2 STIR images). This technique allows acquisition of still images taken in a desired imaging plane with bright areas corresponding to areas of high T2 signal with relative suppression of signal from both the blood pool and fat. T2 (or spin-spin relaxation time) itself refers to the exponential time constant for the decay in magnetisation occurring in the transverse plane following application of a radiofrequency excitation pulse(73). This time constant is dependent on interactions of the spin of neighbouring protons, hence the term 'spin-spin relaxation time'(73). Areas of high water content or oedema appear as areas of high signal. For this reason, this technique is particularly useful in and may improve diagnosis of diseases associated with acute increases in myocardial oedema such as myocardial infarction, Takotsubo cardiomyopathy and myocarditis(74).

In acute myocardial infarction, the total area of high T2 signal has been shown to correspond to the 'area at risk' i.e. the volume of myocardium liable to be irreversibly infarcted should revascularisation not occur(75). This can be assessed retrospectively (up to one week after the onset of myocardial infarction) so as not to delay urgent revascularisation(74). When the 'infarct size' (volume of LV LGE as a proportion of the overall LV myocardial volume) is subtracted from the area at risk, this corresponds to the amount of myocardium recovered by revascularisation; known as the 'salvage index'. Both area at risk and infarct size are independent predictors of mortality in STEMI patients(9) and provide a means of quantifying the severity of an MI.

T2 weighted imaging suffers a number of potential limitations. The first of these limitations is regional myocardial T2 signal variation relating to the use of phased array coils; the T2 signal may appear less intense the further away it is from the surface coil. Additionally, image quality may be limited by low contrast to noise ratio between normal and abnormal myocardium. Lastly, 'slow flow artefact' may be present where the blood pool adjacent to less well contracting LV segments appears bright due to misregistration between the dark blood preparation and image readout imaging phases(76). These potential limitations need to be considered when interpreting CMR T2 images, but may also be in part circumvented by T2 mapping.

T2 maps can be generated by using a pulse sequence which includes a T2 preparation pulse which is followed by 3 SSFP readouts taken at consecutive increasing echo times(77). These 3 images are then processed to fit the T2 decay curve at each pixel within the imaging field in the form of a pixel-wise T2 maps. Alternative pulse sequences have also been proposed for the generation of T2 maps(78). T2 mapping assessment of patients with proven active myocarditis on endomyocardial biopsy has been shown to be more accurate than T1 mapping and other CMR parameters in predicting active myocarditis(79).

1.2.4.4. T2* Imaging Using CMR

T2* imaging using CMR is used primarily in the assessment of patients at risk of iron overload and resultant siderotic cardiomyopathy due to disease states such as thallasaemia major, sickle cell anaemia and other conditions where patients are transfusion dependent. Intracellular iron has strong paramagnetic properties (as occurs in iron overload states) and causes shortening of the T2* decay constant due to inhomogeneities in the magnetic field(38). T2* relaxation time can be measured using a gradient echo pulse sequence and correlates very strongly with invasively measured in vivo iron concentrations, allowing longitudinal, non-invasive assessment of iron loading and adjustments to iron chelation therapy as appropriate(80).

1.2.5. CMR Assessment of Vascular Performance

Arterial stiffness is a recognised surrogate measure of increased CVD risk(81) and reflects a generalised process of vascular ageing and atherosclerosis, meaning (CMR) quantitation may be a useful biomarker in diseases leading to arterial

stiffness. Increased stiffness within the aortic arterial wall leads to increased aortic pulse pressure and increased left ventricular afterload(82). End-organ damage is thought to occur as a result of failure of dampening of the systolic waveform by the aortic wall, exposing the low vascular resistance cerebral, cardiac and renal vascular systems to increased haemodynamic load(82). This has been proposed to lead to arterial remodelling, thickening of the arterial wall and eventual atherosclerotic plaque formation(83).

A number of techniques exist by which to quantitatively assess arterial stiffness. Aortic stiffness is most commonly measured by aortic pulse wave velocity and augmentation index(84). These have conventionally been assessed by 'applanation tonometry' using use a transcutaneous device such as the Sphygmocor device(85) to record the pulse pressure waveform in order to derive these values.

Pulse wave velocity is the 'propagation speed of the pressure or the velocity wave along the artery…calculated as the distance separating two locations and the transit time needed for the wave to cover this distance'(86). CMR may be used to calculate pulse wave velocity in a simple fashion, requiring phase-contrast acquisitions planned perpendicular to the proximal ascending and descending aorta, as well as the distance between these two sites of aortic waveform measurement(87).

Augmentation index is measured either at the radial or carotid artery and is defined as the change in pressure between the first and second systolic peaks of the arterial waveform as a percentage of the pulse pressure(88). Using meta-analysis, augmentation index has been demonstrated to predict cardiovascular mortality independently of peripheral blood pressure(89).

An alternative means of assessing aortic stiffness is aortic distensibility (AD) which can be measured by CMR and has been validated against the reference standard technique(90). Using CMR to assess aortic stiffness as a research application is particularly attractive, as its multi-parametric approach allows for simultaneous assessment of other cardiovascular abnormalities. Aortic distensibility measures the elastic property of the large arteries and is determined by the difference in systolic and diastolic blood pressure and changes in cross-sectional aortic area between diastole and systole(91). Although AD naturally decreases with age, it has been shown to be significantly reduced in patients with renal disease(92) and significant coronary artery disease(93) versus age-matched controls. Furthermore,

aortic distensibility has been shown to be an independent predictor of mortality in hypertensive patients(94).

1.3. Epidemiology and Pathogenesis of Myocardial Infarction

1.3.1. Epidemiology of Myocardial Infarction

Myocardial infarction is a leading cause of mortality worldwide, defined as 'myocardial death due to prolonged ischaemia'(95). In the UK alone, over 915,000 people are estimated to have previously had an MI and coronary artery disease was responsible for 73,500 deaths in 2012, representing 16% of all male and 12% of all female deaths(96). NHS spending on treating coronary artery disease is estimated at £6.8 billion pounds each year, representing a significant proportion of the total spending budget(96).

1.3.2. Pathogenesis of Myocardial Infarction

The onset of MI is classically heralded by typical symptoms of chest pain, diaphoresis and dyspnoea. Nevertheless, a proportion of patients may have either vague symptoms or absence of any symptoms; frequently in these instances MI is unrecognised at the time of its occurrence(97). Myocardial cell death can occur in as little as 20 minutes after ischaemia begins, with complete necrosis occurring after between 2 and 4 hours(95). The pattern of myocardial damage caused by MI has been termed the 'wavefront phenomenon' where distal tissues within the coronary vascular bed are affected first (endocardial), followed by more proximal tissues (epicardial)(98). Interruption to myocardial blood supply resulting in myocardial infarction can be caused by one of a number of mechanisms. These are summarised in the following table:

Table 1-1 Classification of Myocardial Infarction

(adapted from Thygeson et al. Third Universal Definition of Myocardial Infarction. JACC 2012. 60 (16); 1581-98)

MI Classification	Description
Type 1	Spontaneous plaque rupture or dissection within an epicardial coronary artery.
Type 2	MI secondary to 'ischaemic imbalance' – myocardial oxygen supply is temporarily outstripped by demand as a result of brady- or tachycardia, hypotension, respiratory failure etc.
Type 3	Myocardial infarction resulting in death
Types 4a/4b/5	Myocardial infarction resulting from PCI (4a) or thrombosis of existing coronary stent (4b) or coronary artery bypass grafting (5)

Following myocardial infarction, the heart undergoes a complex process of post-infarction remodelling. Necrotic myocardium becomes replaced by fibrotic scar, while non-infarcted myocardium serves to maintain adequate cardiac output in order to compensate for the reduced contribution to this by infarcted regions of the heart(99). Autopsy studies suggest this process may take around 6 weeks(100). CMR has shown a 40% reduction in infarcted LV mass measured by LGE at 4 months compared with at the time of infarction, with little interval change at 12 months, suggesting the majority of the remodelling process is largely complete within 4 months(101). Over the days and weeks following MI, depending on the size of infarction, the LV may dilate; with larger infarcts and those involving the anterior as opposed to inferior or circumflex coronary territories associated with greater LV dilatation(102). LV chamber enlargement is thought to occur due to a combination of thinning with concurrent expansion along the circumferential length of infarcted myocardium, coupled with circumferential lengthening of the remote (unaffected) myocardium(103).

1.4. CMR assessment in myocardial infarction

CMR offers a comprehensive assessment of cardiovascular function following myocardial infarction, providing detailed prognostication and the potential to guide clinical decision-making. Firstly, assessment of left ventricular function aids both in long-term prognostication(104) (primarily through assessment of LVEF) and in making treatment decisions in terms of heart failure management(105) and complex device therapy(106). CMR may be used to investigate patients with chest pain, raised troponin and normal/near normal findings on invasive coronary angiography (termed 'Myocardial Infarction with Non-Obstructed Coronary Arteries' or MINOCA(107)), arriving at a conclusive diagnosis in a high proportion of patients(108). Ordinarily, left ventricular function following myocardial infarction is assessed using transthoracic echocardiography, though CMR may be used where this is not feasible(105). Additionally CMR may be used to assess the functional significance of residual coronary lesions following myocardial infarction(105).

CMR is frequently used in the assessment of myocardial viability in patients with chronic ischaemic heart disease. In a landmark paper, Kim et al.(109) demonstrated that an increasing transmural degree of myocardial hyperenhancement on LGE corresponded inversely with the likelihood of successful functional recovery of myocardial contractility following revascularisation with coronary artery bypass grafting or percutaneous coronary intervention (PCI). Where no hyperenhancement by LGE was noted in a myocardial segment with reduced contractility, contractility improved in 78% of patients, whereas >75% transmural hyperenhancement corresponded with functional improvement in under 2% of patients. Meta-analysis of studies using similar LGE-guided revascularisation with PCI demonstrated a weighted sensitivity of 87% and specificity of 68% to detect hibernating myocardium using a cut-off of 50% transmurality of LGE(110). However, any potential mortality benefit resulting from such LGE-guided revascularisation remains to proven in a large scale prospective study.

Parameters measurable by CMR other than LVEF alone may improve prognostication of patients post myocardial infarction. Parameters which are useful in this setting include the presence of microvascular obstruction (MVO),

intramyocardial haemorrhage (IMH) and LGE. MVO may occur soon after the onset of MI and refers to a cascade of deleterious events within small vessels which prevent perfusion of the myocardium(111). This process is linked to factors including small vessel vasoconstriction, myocardial oedema, swelling of capillary endothelial cells and micro-embolisation of debris leading to plugging of small vessels(112). Intramyocardial haemorrhage represents an extreme form of MVO resulting in damage to small vessel endothelium and extra-vasation of red blood cells into the core of the infarction(113). MVO appears as an island of hypo-enhancement within the bright, hyper-enhanced areas of infarction on LGE imaging whereas IMH appears as a hypo-enhancement on T2 STIR or T2* imaging within surrounding areas of infarction and oedema(114). Both MVO and IMH are now established independent predictors of CV mortality in patients with MI(112). In the context of prior, unrecognised infarction, the proportion of infarcted myocardium on LGE correlates strongly with mortality and adverse CV events. Even a small amount of infarcted myocardium (mean 1.4% infarcted myocardium on LGE) corresponded to a 7-fold increase in mortality in a cohort of patients with unrecognised prior MI(115).

1.5. Epidemiology and Pathogenesis of Cardiovascular Disease in Rheumatoid Arthritis

1.5.1. Epidemiology of CVD in RA

Rheumatoid arthritis is a chronic autoimmune inflammatory arthritis which affects not just the joints, but multiple organ systems including the heart and cardiovascular system.

Rheumatoid arthritis affects up to 1% of the general population and is associated with increased mortality. This is predominantly, though not exclusively due to an accelerated process of atherosclerosis affecting the coronary and cerebral arterial systems(116). Overall, there is a 50% increase in cardiovascular mortality amongst patients with RA(117), similar in magnitude to that associated with diabetes(118). The increased relative risk of CVD compared with the general population appears to be most profound in younger patients(119).

The process of accelerated atherosclerosis seen in RA typically manifests as coronary artery disease (CAD)(120) which in turn predisposes to myocardial infarction (MI), heart failure due to reduced ejection fraction and sudden cardiac death due to heart arrhythmia. Patients may already have developed

cardiovascular disease by the time RA has been diagnosed; patients with RA are three times more likely to have had either an acute MI or unrecognised MI in the two years preceding formal diagnosis than age and sex matched individuals without RA. This risk continues after diagnosis as patients with RA have a twofold higher risk of acute MI compared with those without the disease(121). Acute MI in patients with RA is associated with a more severe presentation compared with the general population and worse short term outcomes(122).

For this reason, both the European League Against Rheumatism(123) and European Society of Cardiology(124) recognise RA as a CVD risk factor and advocate risk stratification with a view to primary CVD prevention medication in patients deemed at high CVD risk. Non-invasive imaging including measures of arterial stiffness may be used to predict CVD risk, particularly when patients are on the border of decisional thresholds(125).

Aside from CVD relating to accelerated atherosclerosis, RA is associated with a constellation of other disease processes affecting the heart including myocarditis, pericarditis, aortitis, left ventricular dysfunction and valvular disease(figure 1-1).

Figure 1-1 Pathogenic mechanisms of CVD in RA

Coronal SSFP still frame image depicting the pathogenic mechanisms causing cardiovascular disease in Rheumatoid Arthritis

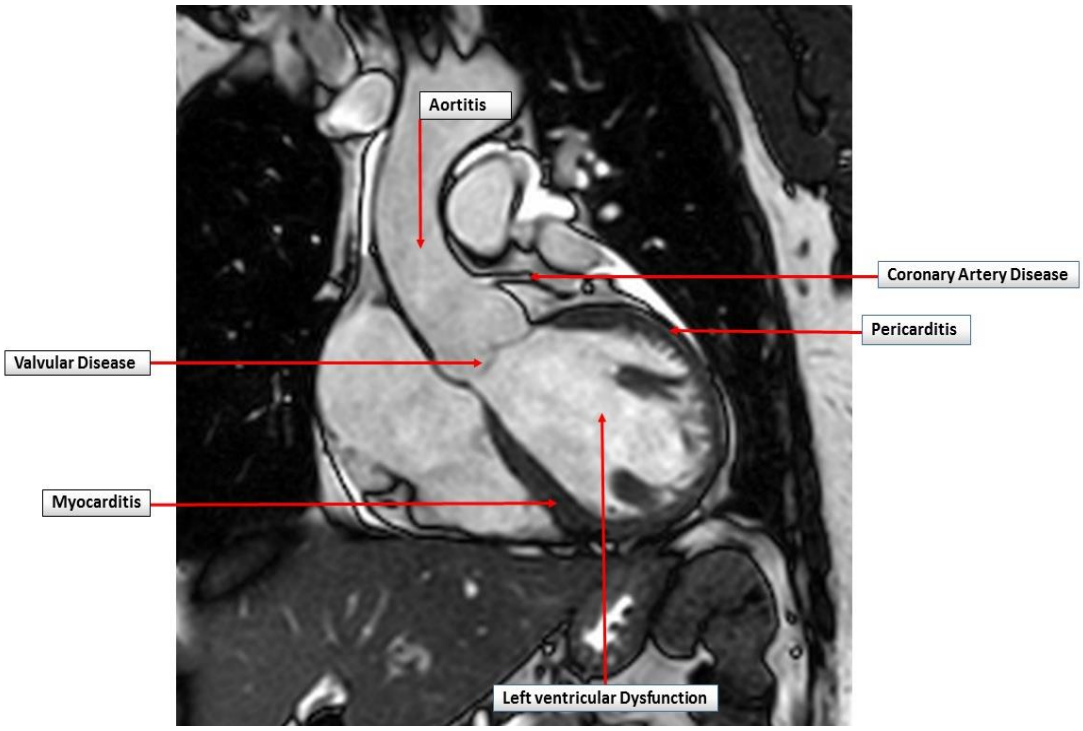

Myocarditis is inflammation of the myocardium and is a common finding of RA at autopsy(126, 127). Although rarely clinically significant it can infrequently cause significant morbidity or even death(128).

Pericarditis, a pathological process involving inflammation of the pericardial layers surrounding the heart, is a frequent finding in RA(129) present in a high proportion of patients at autopsy(126). Often this is clinically silent, but may rarely cause significant symptoms due either to pericardial effusion or pericardial constriction where the pericardial layer becomes thickened and encases the heart leading to ventricular interdependence, reduced cardiac output and eventually to breathlessness and overt heart failure.

Clinically apparent large vessel vasculitis including aortitis in RA is uncommon, occurring in 1-3% of patients(130). Nevertheless low-grade, clinically silent aortic inflammation may be a common feature of RA and contribute to both

atherosclerosis and endothelial dysfunction seen in this disease(131). Histological analysis of arterial biopsy specimens from patients with inflammatory rheumatic disease undergoing coronary bypass surgery has revealed high rates of inflammatory cell infiltrates(132). Furthermore, 18-fluorodeoxyglucose PET imaging has shown increased uptake of radiotracer in the aortic wall of RA patients versus controls, which remained significant after adjustment for CVD risk factors(133). In the same study, radiotracer uptake in the aortic wall correlated strongly with synovial activity in RA patients(133).

Left ventricular dysfunction is a common finding in RA, occurring in both diastolic (impaired ventricular relaxation) and systolic forms (impaired ventricular contraction). RA patients frequently develop heart failure but often without displaying the common symptoms and clinical signs as patients in the general population and mortality is worse in RA patients as compared with non-RA patients(134).

Patients with RA frequently have higher rates of valvular heart disease than the general population, predominantly in the form of mitral regurgitation (MR). This is a frequent finding on echocardiographic assessment of RA patients as well as autopsy though rarely clinically significant(135).

1.5.2. Pathogenesis of CVD in RA

RA is proposed to exhibit cardiovascular abnormalities through a variety of biological mechanisms relating to both the disease itself and, in some instances, treatments used to control patients' symptoms.

1.5.2.1. Abnormalities in lipid profile in RA

Abnormalities in lipid profile have been demonstrated in RA patients. During periods of high levels of inflammation, RA is associated with reduced total and low density lipoprotein levels (LDL), combined with increased high density lipoprotein (HDL) levels(136). A 'lipid paradox' was described by the authors of a large RA cohort study where, paradoxically, lower total cholesterol (<4mmol/L) was associated with a 3.3-fold increase in CV events(137). Furthermore, insulin resistance in established RA is reported(138). Whether any changes in lipid profile beyond total cholesterol values are associated with increased CVD risk in RA is an area of active investigation.

1.5.2.2. Deleterious CV effects due to RA therapies

Treatment for RA has been revolutionised in the past 30 years; where debilitating disease with profound morbidity was once the norm, with early diagnosis and the introduction of newer therapies this has instead become the exception. Glucocorticoids such as Prednisolone have been prescribed for many years to combat the acute symptoms of pain and inflammation associated with RA. However, use of this class of drug demonstrates a clear link with deleterious effects on the CV system. Glucocorticoid use is associated with insulin resistance, obesity and diabetes(139). Within the RA population, patients with active disease randomised to 7.5mg Prednisolone daily as opposed to placebo had significantly increased systemic blood pressure as well as raised levels of total cholesterol(140). The use of long-term high dose Prednisolone (mean dose >7.5mg daily) has been associated with significantly increased CV mortality in patients with RA in a large observational study(140).

1.5.2.3. Endothelial dysfunction and atherogenesis in RA

In spite of findings of lipid abnormalities and insulin resistance in RA, these alone are insufficient to explain the increased incidence of CVD in RA. Vascular dysfunction mediated raised levels of circulating pro-inflammatory proteins has been proposed as being a major contributing factor to increased CVD risk in RA.

Outside of the heart, the cardiovascular system is divided into its macrovascular (aorta and large arteries) and microvascular component (smaller arteries, arterioles and capillaries). This is lined by the endothelium which regulates circulatory function via the release of vasoactive molecules such as nitric oxide (NO), prostacyclin and endothelin-1(141). It has been suggested that in RA, the release of pro-inflammatory molecules in patients with RA such tumour necrosis factor alpha (TNFα) and Interleukins 1 and 6 leads to a step-wise process of micro and macrovascular endothelial dysfunction, followed by atherosclerotic plaque formation(142). The initial phase of endothelial dysfunction is initiated by reduced bioavailability of NO via downregulation of the enzyme responsible for its production(143, 144). This results in reduced endothelial dependent dilatation of the macro and microcirculation(145) thought to occur due to relaxation of the passive tone provided by the smooth muscle layers within the arterial wall(146). Chronic endothelial dysfunction is followed later by a second stage characterised by accelerated atherosclerosis and eventual atherosclerotic plaque formation(147). The complex process of atherosclerotic plaque development begins with an initial phase of intimal thickening, where there is proliferation of smooth muscle cells

within the tunica intima and overall thickening of this layer(148). This is followed by the accumulation of foam cell macrophages within the intimal layer and 'xanthoma formation' (figure 1-2)(149). Plaque formation eventually occurs due to deposition of lipid rich material and cell debris within the tunica intima by foam cells. Additionally, with plaque formation, the loose connective tissue of the tunica intima becomes replaced by collagen-rich, non-compliant fibrous tissue(148).

Figure 1-2 Atherosclerotic plaque formation

Panel A shows healthy artery in cross section. Panel B shows arterial atherosclerotic plaque formation in cross section.

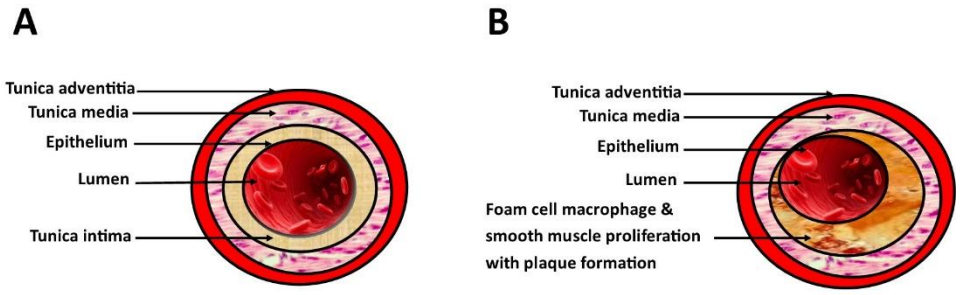

1.5.3. Effects of disease-modifying anti-rheumatic drugs on the cardiovascular system

1.5.3.1. Conventional and biologic DMARD

Methotrexate (MTX) is a conventional synthetic disease-modifying anti-rheumatic drug (csDMARD) used as first line therapy in the treatment of RA(150) which exerts its effects through inhibition of folate metabolism and inhibition of cellular proliferation. A 2012 meta-analysis assessing the effectiveness of Methotrexate across 10 separate clinical trials demonstrated a 21% reduction in total cardiovascular risk. The reason for this apparent benefit and the mechanisms by which it reduces CVD remains unclear, however(136).

Pivotal work in the 1980's led to the appreciation of the central role of pro-inflammatory cytokines in RA pathogenesis, in particular, interleukin-1 (IL-1) and tumour necrosis factor (TNF)(151). TNF and IL-1 are key innate immune system cytokines (152). Levels of TNF have been shown to be raised in areas of active inflammation in RA in patients with RA(153). The tripartite demonstration of raised

TNF levels in synovial tissue(154), in vitro synovial cell culture experiments(155) and the in vivo effects of therapeutic antibodies against TNF in pre-clinical models(156) confirmed TNF's importance(157, 158). Similarly, blockade of IL-1 suggested its therapeutic potential.

This led to the development of targeted biological therapies in the form of anakinra (IL-1 receptor antagonist) and several TNF-inhibitors (TNFi). Whilst anakinra is no longer used in treatment of RA due to poor clinical effectiveness, TNFis are used extensively, when csDMARDs (including MTX) have failed to achieve low disease activity or remission.

1.5.3.2. Biologic DMARD and effect on CVD in patients with RA Endothelial dysfunction

Use of TNFi in RA appears to reduce cardiovascular mortality(159), which is thought to be related the reduction in inflammation rather than by modifying cardiovascular risk factors(136). Treatment with TNFi therapy has been shown to reduce aortic stiffness compared with untreated patients(160), suggesting that improvements in endothelial function and/or disruption of atherogenesis may underpin the apparent improvements in CV mortality seen with TNFi medications in RA.

Over recent years, a great deal of research has been conducted in assessing the role of interleukin-1 (IL-1) in cardiovascular disease as a whole. IL-1 is a pro-inflammatory cytokine and is raised in the presence of CVD risk factors such as hypertension, smoking and diabetes, as well as in RA(161). Raised levels are associated with endothelial dysfunction and resultant atherogenesis(161) as well as adverse LV remodelling in the context of heart failure(162). Direct inhibition of the IL-1 receptor inhibitor with the biological IL-1 inhibitor Anakinra has been shown to result in multiple short and longer term effects on the cardiovascular system. In a small scale study of 23 RA patients randomised to receive a 30-day course of Anakinra, flow mediated dilatation of the brachial artery (a marker of endothelial dysfunction), coronary flow reserve, vascular performance and longitudinal LV S prime by echocardiography were all significantly improved in comparison to RA patients used as controls who did not receive Anakinra(163). The same group randomised 80 RA patients with and without coronary artery disease (CAD) to receive Anakinra or placebo. IL-1 inhibition with Anakinra significantly improve flow-mediated dilatation of the brachial artery, coronary flow reserve, multiple measures of vascular performance and LV global longitudinal function 3 hours after its administration(164). Effects were more marked in patients with RA patients with

coronary artery disease than those without. These two studies highlight the role IL-1 plays in contributing to some of the CV abnormalities seen in RA, as well as suggesting that a subset of patients with CAD may potentially derive more benefit from treatment with Anakinra. However, a trial assessing the efficacy of Anakinra against TNFi therapy failed to demonstrate any benefit over TNFi therapy in terms of RA disease activity, though CV outcomes and surrogate measures were not assessed (165).

These data provide insights into the pathogenesis and treatment effectiveness of CVD in RA. Assessing the efficacy of RA treatments in ameliorating the CVD effects of the disease in clinical trials of RA is inherently challenging; the expected clinical CVD event rate is low and disentangling whether RA or an alternative confounding disease process is the cause of a clinical event or CV abnormality is difficult(166). This highlights the potential role of CMR and other non-invasive imaging modalities in further clarifying CV outcomes in RA, as well as advancing our understanding. In particular, the quantitative, multi-parametric approach of CMR offers the capability to shed further light onto the mechanisms by which RA effects the CV system as a whole and possibly identify potential CVD biomarkers in RA to risk stratify and inform on treatment effectiveness.

1.6. CMR Assessment of RA

A limited number of studies using CMR have sought to characterise the effects of RA on the heart and cardiovascular system. The small number of studies published to date are limited by inclusion of patients with long-established disease treated with a wide range of treatment regimens as well as small sample sizes.

Giles et al(167) compared basic structural CMR findings in 75 patients with established RA (mean disease duration 7 years) with no known cardiovascular disease with 225 age and gender matched healthy controls. RA patients with known risk factors for cardiovascular disease (hypertension, hypercholesterolaemia etc.) were not excluded, however, prevalence of these risk factors was comparable to those in healthy controls. They reported that indexed LV mass was strikingly lower in RA versus controls (mean 63g/m2 versus 76g/m2 p=<0.001). Furthermore, reduced LV mass was significantly and independently associated with use of biological DMARD use and anti-cyclic citrullinated peptide (ACPA) titre (an autoantibody which serves as a marker of RA disease severity(168)).

In the most comprehensive CMR study of RA patients to date, Ntusi et al. (169) assessed 39 RA patients and the same number of age and gender matched healthy controls using a multi-parametric CMR protocol at 1.5T. This protocol included T1 mapping, T2 weighted imaging, extra cellular volume (ECV) imaging and late Gadolinium enhancement imaging in addition to a comprehensive LV function analysis including assessment of circumferential systolic strain values by tagging. RA patients had a mean disease duration of 7 years, no known history of cardiovascular disease and comparable rates of cardiovascular risk factors as healthy controls. Native myocardial T1 values were increased in RA patients versus controls (973 versus 961ms respectively, $p = 0.03$). Global T2 signal intensity values were no different in RA patients versus controls, though in some patients, areas of focal oedema were noted. ECV values were higher in RA patients than controls (30.3 versus 27.9%, $p = <0.001$). 46% of RA patients had evidence of non-ischaemic, focal LGE which tended to be patchy and mid-wall and 5% had evidence of previously undiagnosed prior myocardial infarction. Circumferential strain and strain rate were significantly lower in RA versus healthy controls. Both native T1 values and ECV correlated moderately with disease activity as well as with circumferential strain and strain rate. The authors concluded that CMR is able to detect both diffuse and focal myocardial fibrosis and myocardial inflammation in patients with RA, postulating that myocardial fibrosis in RA is likely to be the final common pathway of contributing factors including microvascular disease, epicardial coronary disease and chronic myocarditis.

Using CMR at 1.5T, Kobyashi et al demonstrated coronary microvascular dysfunction in a pilot study of 18 patients with established RA and no other known cardiovascular disease(170). The cardiac MR protocol included myocardial perfusion at rest and at stress using intravenous adenosine, as well as late Gadolinium enhancement imaging. Presence or absence of perfusion defects was judged visually and classified as being segmental (following the distribution of a coronary artery or arteries) or non-segmental. Two patients (11%) were demonstrated to have perfusion abnormalities at stress but not at rest; one of these being a circumferential subendocardial defect and the other a non-segmental subendocardial defect. Although a small-scale study limited in robustness by the lack of inclusion of a control group or test to exclude the presence or absence of flow-limiting coronary artery disease, this hints at underlying process of coronary microvascular dysfunction in RA given the distribution of perfusion defects demonstrated.

1.6.1. Other key non-invasive imaging studies in RA

Non-invasive imaging techniques other than CMR have been used to investigate the effects of RA on the heart and cardiovascular system.

Myasoedova et al assessed basic LV and RV structure and function in a large transthoracic echocardiography study of 200 established RA patients (mean disease duration 10 years) and 600 age and gender matched healthy controls(171). Similar to the Giles et al. CMR study, the authors reported lower indexed LV mass in RA versus healthy controls (84.6 versus 91.7 g/m^2 respectively, p = <0.001).

There are some conflicting reports of higher LV mass in patients with RA in echocardiography studies(172, 173), however, this probably reflects the relatively low accuracy of echocardiography-derived LV mass measurement in general (not specific to these studies) and the small sample sizes of the currently available reports.

One key echocardiography study using involving asymptomatic RA patients (mean disease duration 14 years) RA with no history of CVD and age and gender-matched controls reported significantly reduced S' values (a measure of LV longitudinal systolic function) and higher E/E' values (indicating increased left ventricular filling pressure) in RA patients versus controls(174). This was a large scale, prospective study of 198 patients with established RA and may indicate asymptomatic progression of diastolic LV impairment in RA patients with simultaneous evolution of subclinical LV systolic impairment.

Recio-Mayoral et al. assessed myocardial blood flow using PET in 12 patients with established RA versus 25 age and gender-matched healthy controls(175). All RA patients underwent CTCA to exclude significant coronary artery disease. This showed abnormalities of hyperaemic myocardial blood flow and coronary flow reserve (difference between resting and maximal coronary blood flow) in patients with RA in the absence of flow-limiting coronary artery disease and cardiovascular risk factors. This again indicates a likely subclinical impairment of coronary microvascular function occurring with established RA.

1.7. Future Directions

The study of subclinical cardiovascular disease using CMR looks set to advance rapidly over the coming years in a number of key areas including faster, more

patient-friendly imaging with diminished reliance on breath-held acquisitions, molecular imaging and flow analysis(176).

Molecular imaging (such as PET) allows visualisation of biological targets within the heart by revealing the location and degree of uptake of specific molecules. Hybrid techniques including PET-CT and PET-MRI which theoretically combine the advantages of both approaches are being assessed(177). Future approaches using molecular imaging may allow the ability to track uptake of radiolabelled therapeutic agents, providing information on disease activity and treatment efficacy(178). Advancements are also being made in the development of 'hyperpolarised' molecules for use in CMR which can be used to assess their intracellular metabolism rather than uptake of the molecules within the tissues of the CV system(179). This could aid diagnosis of specific diseases and improve quantitation of myocardial perfusion.

Lastly, flow analysis using CMR is likely to undergo significant improvements using time-resolved phase contrast (4-D flow) MRI. This could in future offer the potential to fully assess haemodynamics in any desired location within the cardiovascular system as an adjunct to existing multi-parametric assessment provided by CMR(180).

1.8. Summary

The study of subclinical cardiovascular disease offers the opportunity to accurately detect and monitor this disease over time and in response to treatment. This is crucial to patients and offers the potential to initiate treatment before the development of clinical disease as well as the chance to assess the effectiveness of treatments at an individual or population level.

CMR offers a non-invasive CV imaging technique which ideally lends itself to the assessment of subclinical disease and provides an ever expanding range of reproducible, multi-parametric quantitative techniques in a single scan which can be performed safely and in a longitudinal fashion in the same patient if required.

Key areas of research in the context of MI include improving the identification of patients with unrecognised MI, potentially allowing earlier commencement of secondary preventative therapies. Key areas for research in RA include characterisation of the timing in the disease course of cardiovascular involvement,

improved risk stratification and assessing the effect of disease modifying anti-rheumatic drug (DMARD) therapy on the cardiovascular system.

1.9. Thesis hypothesis and aims

1.9.1. Hypothesis

1) The utility of CMR can be expanded to broaden its current repertoire of non-invasive imaging biomarkers to assess subclinical cardiovascular disease according to published frameworks for development of novel CV biomarkers.
2) Existing non-invasive imaging biomarkers as well as those developed within this thesis can be applied to the detection of and effectiveness of treatment in both myocardial infarction and rheumatoid arthritis

1.9.2. Aims

1) To assess the utility of blood bool T1 in the estimation of laboratory haematocrit and the subsequent estimation of extracellular myocardial volume fraction (ECV) a biomarker of subclinical myocardial disease (chapter 3).
2) To assess the reproducibility and feasibility of measuring aortic radial and circumferential strain using CMR feature tracking post-processing software applied to SSFP cine imaging (chapter 4).
3) To investigate the ability of CMR assessment of longitudinal strain parameters assessed using post-processing CMR feature tracking software to correctly identify the presence of prior myocardial infarction (chapter 5).
4) To 1) use CMR measures of aortic stiffness (including those developed in chapter 4) to identify the presence of subclinical cardiovascular involvement in patients at risk and with newly diagnosed, treatment naïve RA and 2) to assess whether these CMR measures of aortic stiffness are able to identify patients likely to be at very high CV risk with carotid atherosclerotic plaque (chapter 6).
5) To use a multiparametric CMR study to assess the relative ability of 2 differing RA treatment strategies to reverse aortic stiffness and other markers of CVD in newly diagnosed, treatment naïve RA (chapter 7).

2. Methods

Methodology common to all results chapters is detailed in this section. The methods described herein are established, validated CMR techniques described in the literature. The development of two novel techniques using CMR, synthetic ECV and aortic strain by CMR-FT are described in subsequent chapters- chapters 3 and 4 respectively. Methodology for these techniques as well as any other techniques specific to individual results chapters is included within the methods section of those relevant chapters.

2.1. Scanner Hardware

All scans at 3.0T were conducted using the same 3.0T system (Achieva, Philips, Best, The Netherlands) using the same 32-channel coil, vectorcardiographic triggering and multi-transmit technology (Philips, Best, The Netherlands).

All scans at 1.5T were conducted using the same 1.5T system (Ingenia, Philips, Best, The Netherlands) using the same 32-channel coil, vectorcardiographic triggering and multi-transmit technology (Philips, Best, The Netherlands).

2.2. CMR Protocols

The components of the basic CMR protocol performed in all patients in subsequent results chapters (chapters 3-7 inclusive) are outlined in the sections below. Any additions to this basic protocol specific to individual results chapters are detailed within each relevant chapter.

Each CMR study was typically performed within 60 minutes in the order illustrated in figure 2-1.

Figure 2-1 Study protocol

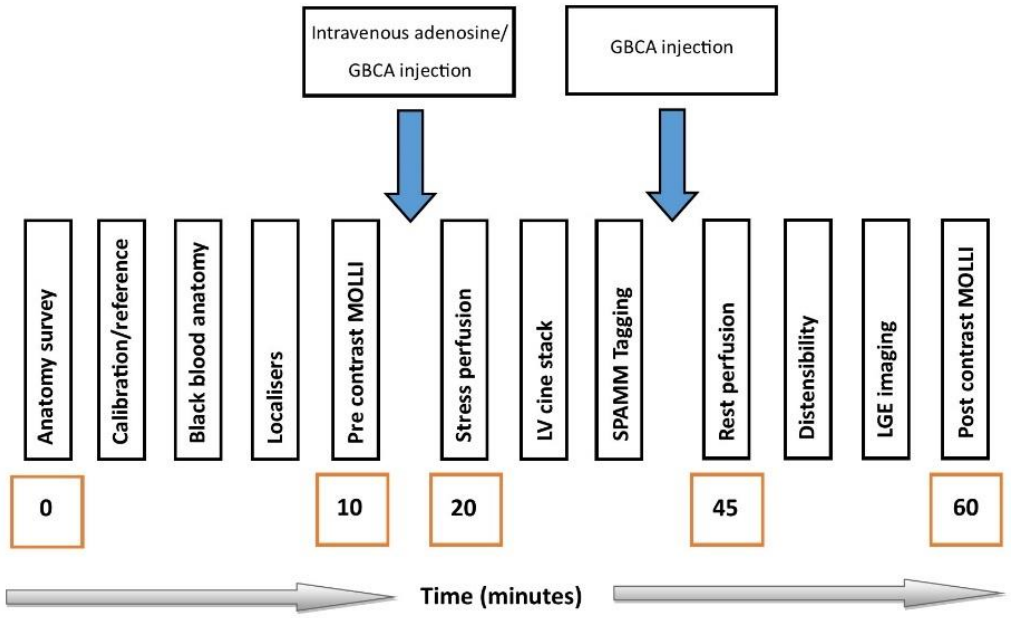

2.3. Cine Imaging

Multi-slice, multi-phase SSFP sequence cine imaging was obtained breath-held at end expiration and included 2 chamber (2Ch) (single slice), 4 chamber (4Ch) (single slice) and left ventricular short axis stack (10-14 slices to ensure full LV coverage) acquisitions. Scan parameters for these cine acquisitions were as follows: echo time (TE) 1.48ms, repetition time (TR) 3.0ms, flip angle 45°, field of view 320 to 420mm depending of patient size, slice thickness 10mm, 30 phases.

A further SSFP axial cine acquisition was obtained of the thoracic aorta at the level of the PA bifurcation to enable calculation of aortic stiffness parameters. Survey images and a sagittal oblique view of the thoracic aorta were used to plan the axial cine acquisition perpendicular to the descending and ascending aorta as described by Lee et al(181). Scan parameters for this were: TE 1.48ms, TR 3.0ms, flip angle 45°, field of view 320 to 420mm depending of patient size, spatial resolution 2.0 x 1.71 x 8mm, 50 cardiac phases. Each patient's blood pressure was taken non-invasively at the same time as this axial cine acquisition.

2.4. Tissue Tagging

Tissue tagging images were obtained for myocardial strain analysis. A spatial modulation of magnetization pulse sequence was used and obtained in the same short axis planes as the stress and rest perfusion sequences, planned using a '3 of 5 approach' from the long axis cine acquisitions. Scan parameters were: spatial resolution 1.51 x 1.57 x 10mm, tag separation 7mm ≥ cardiac phases, typical TR 5.8, TE 3.5ms and flip angle 10°.

2.5. First Pass Perfusion Imaging

First past perfusion imaging was carried out during pharmacological stress (using the intravenous vasodilator adenosine) and at rest. Scan parameters for this aspect of the protocol were as follows: spoiled Turbo Gradient Echo, 5 x k-t Broad-use Linear Acquisition Speed-up Technique 11 training profiles, 1.31 x 1.32 x 10mm, pre-pulse delay 100ms, acquisition shot 123ms/slice, three short axis slices planned using a '3 out of 5' technique from long axis cine images (figure 2-2).

Figure 2-2 3 out of 5 technique for CMR perfusion

Panel A shows VLA (vertical long axis) (upper) and 4Ch (4-chamber) (lower) at end systole with 5 short axis slices. Panel B shoes 5 short axis slices planned parallel to the MV (mitral valve) annulus with slice gap altered ensuring most basal slice is positioned on the MV annulus and the most apical slice at the LV apex. Panel C shows resulting short axis slice positions after reducing number of slices to 3.

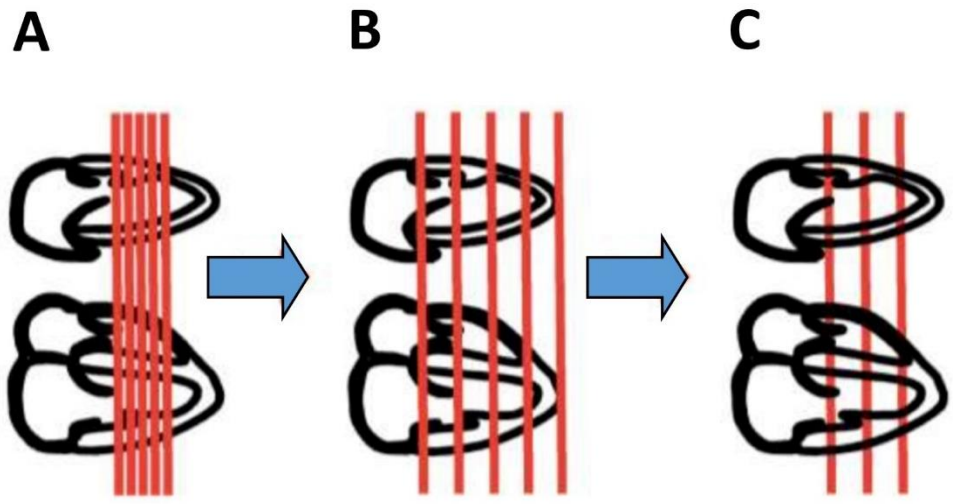

Intravenous adenosine was infused via a cannula in the antecubital fossa at an initial rate of 140µg/kg min with continuous ECG monitoring for 3 minutes and non-invasive blood pressure monitoring every 2 minutes. Adequate haemodynamic response was assumed when any one of the following was achieved: 1) Rise in heart rate ≥10% above baseline heart rate, 2) systolic blood pressure decrease ≥10mmHg or, 3) symptoms consistent with adequate adenosine response including shortness of breath, chest tightness etc. If this was not achieved at 140µg/kg min, the dose was increased to 170 and then 210µg/kg min (maximum dose) at 2 minute intervals until an adequate response was achieved.

Contrast injection of intravenous Gadolinium-DTPA (Gadopentate dimeglumine; Magnevist, Bayer, Berlin, Germany) was performed using a dual bolus technique via a cannula in the antecubital fossa. The initial (dilute) bolus concentration was 0.01mmol/kg followed by the main bolus of 0.1mmol/kg, both infused at a rate of 4.0ml/s using a saline flush injected via power injector (Spectris, Solaris, Pennsylvania, USA).

2.6. Late Gadolinium Enhancement Imaging

Late Gadolinium enhancement imaging was performed 10-15 minutes after the rest perfusion acquisition using inversion recovery prepared gradient echo. A modified Look-Locker (MOLLI) approach was used to determine the optimal inversion time (ms) required to adequately null the LV myocardium. Typical parameters were: TE 2.0ms, TR 3.5ms, flip angle 25°, spatial resolution 1.54 x 1.76 x 10mm. This was performed in 10-14 short axis slices (identical to the LV cine stack) with additional 2Ch/4Ch ± phase swap slices acquired when required.

2.7. T1 Mapping

A single short axis slice at mid LV level was used for pre and post contrast T1 mapping using an electrocardiogram-triggered MOLLI scheme. The pre-contrast scheme used was a 3-3-5 acquisition with 3 R-R interval recovery epochs) acquired at end-expiration (single breath hold) with a trigger delay at end-diastole. Scan parameters were: voxel size 1.7 x 2.14 x 10, flip angle 35° and field of view 320-420mm depending on patient size.

The same mid LV slice was used for post contrast T1 maps. These were acquired 15 minutes after the rest perfusion acquisition using the identical MOLLI scheme detailed above.

2.8. Post processing CMR analysis

CMR analysis in chapter 5 was conducted by 2 operators (GF and PS), each with 2 or more years' experience in CMR analysis. CMR analysis in chapters 6 and 7 was conducted by 2 operators (GF and BE) each with 2 or more years' experience in CMR analysis. All post-processing CMR analysis was carried out using the same software (CVI[42], Circle Cardiovascular Imaging, Calgary, Canada) with the exception of tissue tagging analysis which used separate software (inTag version 1.0, Creatis, Lyon, France).

2.9. Assessment of left ventricular function

Left ventricular endocardial and epicardial borders were manually contoured from the short axis LV cine stack at both end systole and end diastole in order to generate LV end systolic and end diastolic volumes according to the summation of discs methodology(182). LV ejection fraction was derived from the equation:

Equation 2 LV ejection fraction

$$LVEF\,(\%) = ((LVEDV - LVESV) / LVEDV) * 100$$

Where EDV= end diastolic volume(ml), ESV= end systolic volume

Both trabeculation and papillary muscles were excluded. LV mass values were calculated from the end diastolic myocardial volume according to established methods(183).

2.10. Assessment of right ventricular function

Right ventricular volumes and RVEF were calculated from the short axis LV cine stack in a similar fashion to LV volumes and LVEF(184). RV endocardial borders were manually contoured at both end systole and end diastole generating RV end systolic and end diastolic volumes excluding trabeculation from these values. RV ejection fraction was derived from the equation:

Equation 3 RV Ejection fraction

$$RVEF\,(\%) = ((RVEDV - RVESV) / RVEDV) * 100$$

Where EDV= end diastolic volume(ml), ESV= end systolic volume

2.11. Assessment of aortic distensibility and other measures of aortic stiffness

The dedicated axial short axis cine of the descending aorta was used to calculated aortic distensibility (fig 2-3). The endovascular: blood pool interface of the descending aorta was manually traced at its minimum volume in diastole as well as its maximal volume during systole to generate maximal and minimal cross sectional volumes.

Figure 2-3 Calculation of cross-sectional descending aortic area for measures of artic stiffness

The blue ROI traces the endovascular: blood pool interface to calculate cross sectional area

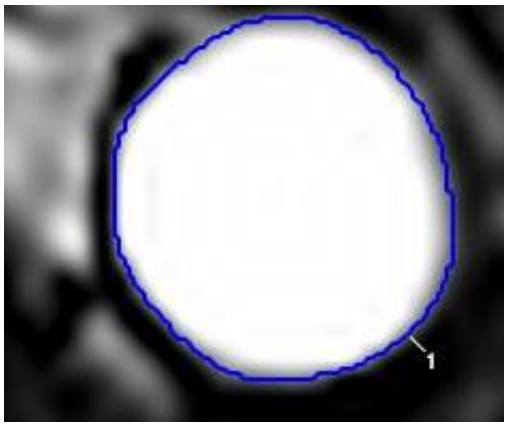

Measures of aortic stiffness including aortic distensibility, aortic compliance and aortic stiffness (β) were calculated according to established methods(185) using the following equations:

Aortic distensibility:

Δ relative aortic cross sectional area CSA / Δ systolic and diastolic blood pressure

Equation 4 Aortic distensibility

$$((CSA\max - CSA\min)/CSA\max))/(SBP - DBP)$$

Where CSAmax= maximum cross sectional area (cm), CSAmin= minimum cross sectional area (cm), SBP = systolic blood pressure (mmHg) and DBP= diastolic blood pressure (mmHg)

Aortic compliance:

Δ absolute aortic cross sectional area / Δ systolic and diastolic blood pressure

Equation 5 Aortic compliance

$$(CSA\max - CSA\min)/(SBP - DBP)$$

Where CSAmax= maximum cross sectional area (cm), CSAmin= minimum cross sectional area (cm), SBP = systolic blood pressure (mmHg) and DBP= diastolic blood pressure (mmHg)

Aortic stiffness index (β):

Ratio of the natural logarithm of systolic BP/diastolic BP to the relative change in aortic cross sectional area

Equation 6 Aortic stiffness index

$$\ln(SBP/DBP)/((CSA\max - CSA\min)/CSA\max)$$

Where: CSA_{max} = maximum aortic cross sectional area, CSA_{min} = minimum aortic cross sectional area, SBP = systolic BP, DBP = diastolic BP, ln = natural logarithm

Intraobserver reproducibility for both maximum and minimum cross sectional area of the descending aorta at 3.0T was assessed between two observers (GF and BE) by calculating coefficient of variation (CoV). Maximum and minimum values were calculated from a total of 12 randomly selected scans. CoV for maximum cross sectional area of the descending aorta was 1.92% while CoV for minimum area was 1.72%.

2.12. Assessment of tissue tagging parameters

Tissue tagging analysis was performed on each of the 3 short axis acquisitions of the left ventricle (LV base, mid and apical slices). Endocardial and epicardial borders were drawn using a semi-automated process using dedicated software (inTag version 1.0, Creatis, Lyon, France). The software then tracked grid tags for each acquired slice throughout systole and diastole. Peak circumferential strain and rotation were calculated for each of the 3 acquired slices. LV twist was calculated by subtracting basal from apical rotation. LV torsion was calculated using the following equation(186):

Equation 7 LV torsion

$$TSA = ((APICALrotation - BASALrotation)x(APICALradius + BASALradius))/(LVlengthx2)$$

Where TSA= torsion sheer angle

Apical radius and basal radius were calculated from the area of the apical and basal slices at end diastole. Length was calculated by subtracting the slice locations of the apical and basal slices and converting to centimetres. Other definitions for LV torsion exist(187), however, when torsion is referred to in this thesis, it is defined as per the above equation,

2.13. Assessment of T1 relaxation times and myocardial extracellular volume fraction

Precontrast 'native' as well as 15 minutes post contrast myocardial and blood pool T1 values were recorded from the mid ventricular slice. Care was taken when selecting the region of interest in the interventricular septum to avoid including adjoining areas of tissue or blood pool which may have given erroneous values due to partial volume effect. Care was also taken when selecting the blood pool region of interest to avoid inclusion of any papillary muscle which may again have generated spurious values (figure 2-4). The septum was chosen as this is arguably the most reproducible area of the LV to assess. A potential disadvantage of this method (as opposed to alternatives such as taking numerous values throughout the LV is that localised areas of high or low T1 may be missed.

Figure 2-4 Calculation of T1 values

The pink circular ROI provides the blood pool T1 value whereas the blue ROI provides the myocardial T1 value. Corresponding values are shown at the foot of the image.

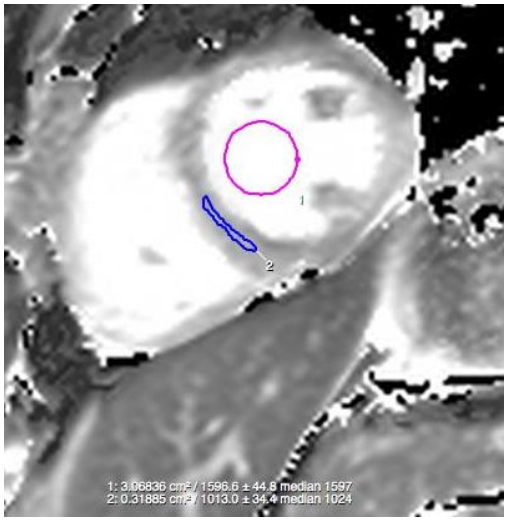

Both native and post contrast myocardial and blood T1 values were combined with a venous haematocrit (Hct) value to calculate estimated myocardial ECV fraction according to the following equation:

Equation 8 ECV calculation

$$ECV = (1 - Hct) \times \frac{(1/\text{myocardial post contrast T1(ms)}) - (1/\text{myocardial native T1(ms)})}{((1/\text{blood post contrast T1(ms)}) - (1/\text{blood pre contrast T1(ms)})}$$

Intraobserver reproducibility for both native and post contrast T1 values was assessed between two observers (GF and BE) by calculating coefficient of variation (CoV). T1 values were assessed on 12 randomly selected scans by each observer. CoV for native T1 was 2.49% and for 2.38% for post contrast T1 values. Intraobserver reproducibility for ECV was also assessed by the same observers by calculating COV for ECV from 12 randomly selected scans. CoV for ECV was 6.46%.

3. Methodology for the development of 'synthetic' extracellular volume fraction at 1.5T and 3.0T

3.1. Background

Myocardial extracellular volume fraction assessed by cardiovascular magnetic resonance estimates the proportion of myocardial extracellular space relative to its cellular component. This may be beneficial in the diagnosis and prognostication of cardiomyopathic processes. Conventionally, ECV calculation requires knowledge of the patient's haematocrit. Treibel et al.(188) recently demonstrated a '*synthetic* ECV' can be calculated by estimating Hct from the longitudinal relaxivity (R1 = 1/T1) of blood. This eliminates the time and cost of obtaining a venous Hct sample, as well as automated generation of in-line ECV maps akin to T1 and T2 maps. So far, *synthetic* ECV has only been described for data acquired with a single vendor (Siemens) and field strength (1.5 Tesla). As such this study applies this novel technique for the first time at 3.0 Tesla field strength and for the first time on a Philips platform.

3.1.1. Hypothesis and aims

We hypothesised *synthetic* ECV can also be derived on a Philips CMR platform and at 3.0 Tesla, potentially broadening applicability of this method.

This study aimed to derive linear regression equations for the correlation of blood pool T1 value with laboratory and test these equations in the estimation of synthetic ECV in a validation cohort as well as against a previously published equation.

3.2. Methods

The patient population for chapter 3 'Methodology for the development of a synthetic extracellular volume fraction' included a total of 421 patients scanned for clinical or research purposes at Leeds General Infirmary, UK between February 2012 and July 2016. These patients were retrospectively recruited and 203 were scanned at 1.5T (Philips, Ingenia, Best, The Netherlands) and 218 were scanned at 3.0T (Philips, Achieva, Best, The Netherlands). The 1.5T cohort comprised 47 patients with valvular heart disease (either aortic stenosis or mitral regurgitation) and 44 with ST-segment elevation myocardial infarction and 112 patients undergoing CMR for acute clinical reasons. The 3.0T cohort comprised 26 healthy

controls, 159 rheumatoid arthritis and 33 hypertrophic cardiomyopathy patients. The sample size was based on similar population sizes in a previous study. The

Patients on both scanners were randomly split into equally-sized derivation and validation subgroups. Derivation groups served to enable derivation of linear regression equations for the relationship of Hct and R1 of blood. This equation was used to calculate *synthetic* ECV and assess its correlation with conventionally calculated ECV in the validation groups.

Bland Altman analyses were conducted to assess bias between laboratory and synthetic Hct and ECV values at both field strengths. Further Bland Altman analysis of bias between Siemens and Philips 1.5T synthetic ECV regression equations was also conducted.

Modified Look-Locker Inversion Recovery acquisition schemes were used to acquire T1 maps produced using vendor software prior to and 15 minutes after administration of either 0.2 mmol/kg Gadopentate Dimeglucide (Magnevist, Bayer Schering) or 0.15 mmol/kg Gadobutrol (Gadovist, Bayer Schering). For all 1.5T patients, a pre-contrast 5s(3s)3s and post-contrast 4s(1s)3s(1s)2s scheme was used to reduce heart rate dependence of T1 values. For all 3.0T patients the same 3(3s)3(3s)5 scheme was used pre and post-contrast. T1 values were derived by drawing a region of interest (ROI) within the interventricular septum and blood pool at mid-ventricular level using post-processing software (CVI 42, Circle Cardiovascular Imaging Calgary, Canada). Scar was included within the interventricular septum ROI when present. Analysis was blinded. ECV was calculated as has previously been reported(188). Statistical analyses were performed using SPSS version 22 (IBM Corporation, Armonk, New York, USA). All results are presented as mean ± standard deviation.

3.2.1. Ethical approval:

All patients gave written informed consent and the study was conducted according to the declaration of Helsinki. The patients included in the study were recruited from a number of different studies covered by the following National Research Ethics Committee approvals: 10/H1307/138, 12/YH/0169, 08/H1307, 14/SC0190 & 12/YH/0551.

3.3. Results

Patient baseline demographics are summarised in table 3-1 for 1.5T patients and table 3-2 for 3.0T patients respectively. There was a broad range of Hct in both 1.5T and 3.0T derivation groups (0.41±0.05, range 0.27 to 0.53 at 1.5T and 0.42±0.04, range 0.31 to 0.54 at 3.0T). There was also a broad range of blood pre-contrast T1 in 1.5T and 3.0T derivation groups (1608±105 ms, range 1402 to 1912 ms at 1.5T and 1780±99ms, range 1457 to 1993 ms at 3.0T). The conventionally calculated ECV in the validation groups was 32±9 % (range 19 to 77%) for 1.5T and 29±5 % (range 20 to 53%) for 3.0T.

Table 3-1 Baseline Demographics for 1.5T patients

Variable	Derivation Group (n=102)	Validation Group (n=101)	Combined groups (n=203)
Male gender	66/102 (65%)	70/101 (69%)	136/203 (67%)
Age (years)	65±17	58±18	61±18
Systolic BP (mmHg)	140±25	129±25	134±25
Diastolic BP (mmHg)	76±29	77±19	77±20
LVEF (%)	52±13	48±15	50±14
Creatinine (mmol/L)	80±23	87±35	83±30
Haemoglobin	133±18	132±21	132±20
Haematocrit	0.41±0.05	0.40±0.06	0.41±0.06
Myocardial native T1 (ms)	1038±95	1052±82	1045±88

Table 3-2 Baseline demographics for 3.0T patients

Variable	Derivation Group (n=109)	Validation Group (n=109)	Combined groups (n=218)
Male gender	47/109 (43%)	54/109 (50%)	101/215 (46%)
Age (years)	49±14	48±18	48±16
BMI (kg/m2)	26±4	26±5	26±4
Systolic BP (mmHg)	123±16	119±14	121±15
Diastolic BP (mmHg)	71±12	67±12	69±12
LVEF (%)	61±6	60±5	60±6
Creatinine (mmol/L)	69±16	66±14	68±15
Haemoglobin	140±13	135±12	138±13
Haematocrit	0.42±0.04	0.42±0.04	0.42±0.04
Myocardial native T1 (ms)	1190±53	1185±58	1187±56

The regression lines between Hct and R1 blood were linear at both field strengths (1.5T: R^2= 0.50, p = <0.001; 3T: R^2= 0.46, p= <0.001), with the following regression equations (Figure 2-2):

Equation 9 Synthetic ECV regression equation at 1.5T

$$\text{Synthetic Hct MOLLI} = (922.6 \cdot [1/\text{T1blood}]) - 0.1668$$

Equation 10 Synthetic ECV regression equation at 3.0T

$$\text{Synthetic Hct MOLLI} = (869.7 \cdot [1/\text{T1blood}]) - 0.071$$

Where Hct is haematocrit (between 0 and 1) and R1blood is 1/T1blood in milliseconds

Using these equations to calculate *synthetic* ECV in both validation cohorts, conventional and *synthetic* ECV were highly correlated (Figure 3-1) (R^2= 0.95, p= <0.001 at 1.5T and R^2= 0.92, p= <0.01 at 3.0T).

Figure 3-1 Linear correlation and regression equations between blood Hct and Blood R1 at 1.5T and linear correlation between blood and synthetic ECV

Panel A: linear correlation and regression equations between blood Hct and blood R1 at 1.5T and 3.0T (Panel B). Linear correlation between conventional and synthetic ECV at 1.5T (Panel C) and 3.0T (Panel D).

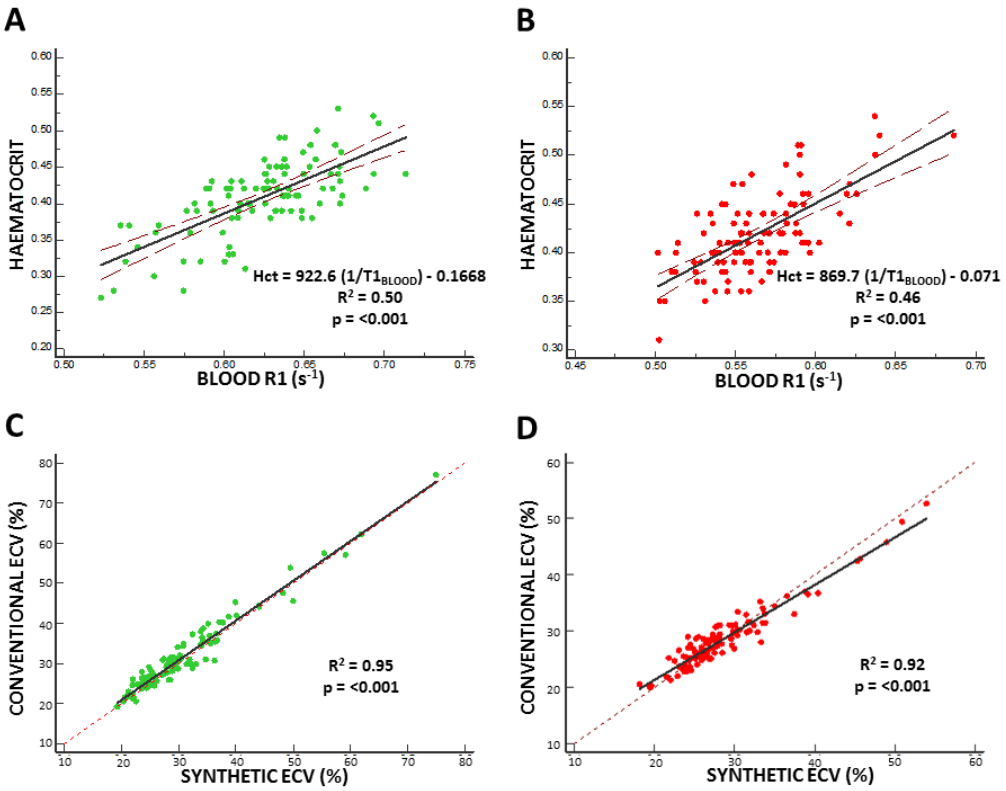

On Bland-Altman analysis (figure 3-2), *synthetic* ECV demonstrated minimal bias at both 1.5T (bias= -0.81%, 95% C.I.-4.97–3.35%) and 3.0T (bias= -0.30%, 95% C.I.-3.92–3.33%) i.e. synthetic ECV was lower than laboratory ECV.

Figure 3-2 Bland Altman analysis of bias between conventional and synthetic ECV

Panel A: 1.5T and panel B: 3.0T

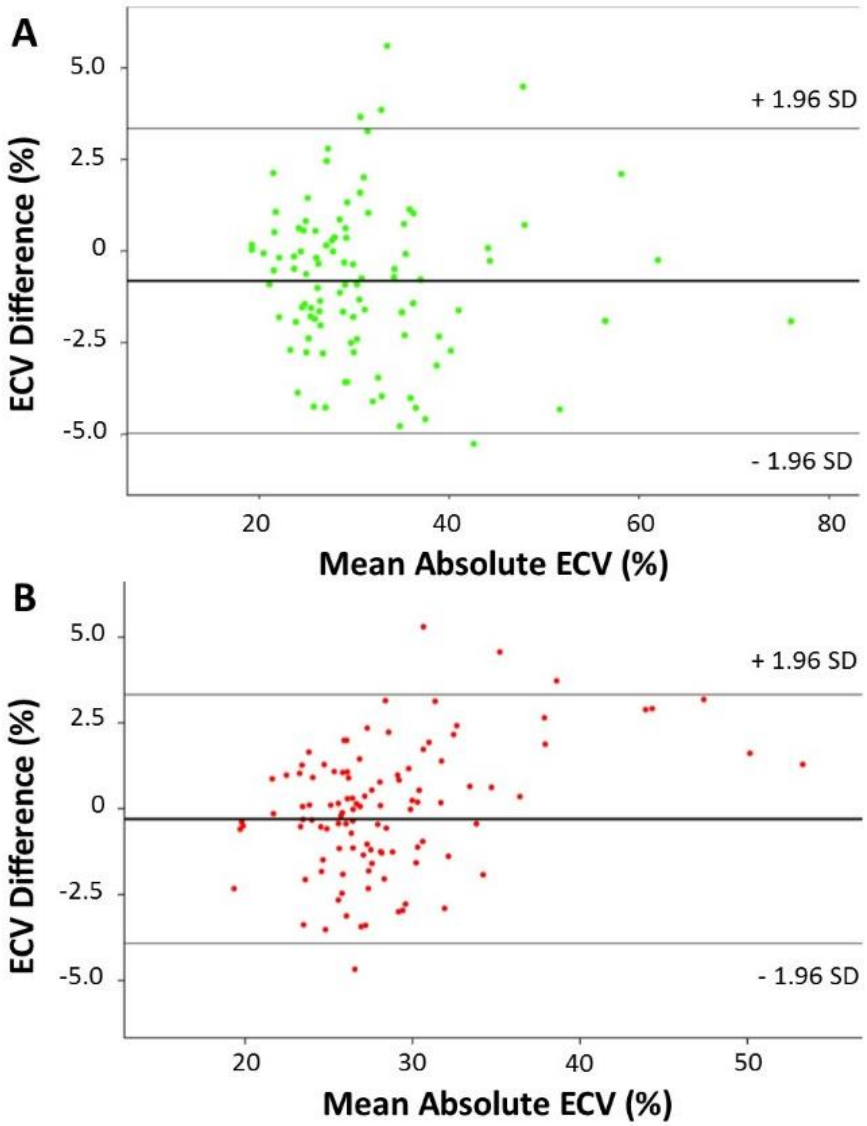

Bland Altman analysis of *synthetic* haematocrit versus laboratory haematocrit showed a slight negative bias (i.e. values were lower for synthetic versus laboratory ECV) at 1.5T and minimal bias at 3.0% (figure 3-3). Mean bias at 1.5T was -0.017, 95% C.I. -0.10 – 0.061) and mean bias at 3.0T was -0.003, 95% C.I. -0.075 – 0.068).

Figure 3-3 Bland Altman analysis of bias between laboratory and synthetic Hct

Panel A shows bias between laboratory and synthetic Hct at 1.5T and panel B shows bias between bias between laboratory and synthetic Hct at 3.0T

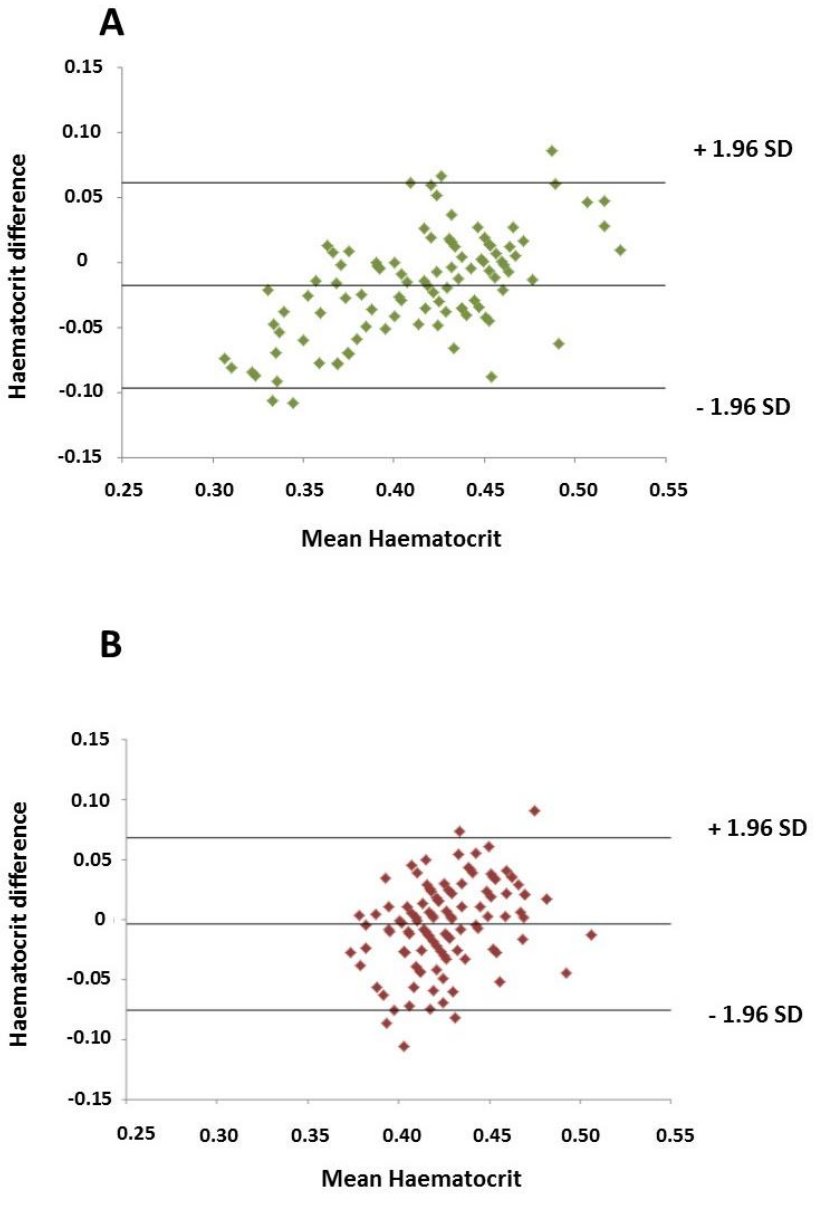

Correlation between conventional ECV and *synthetic* ECV calculated using both the regression equation from the 1.5T derivation cohort and the 1.5T MOLLI synthetic ECV equation reported by Treibel et al.(188) is shown in figure 3-4.

Figure 3-4 Correlation between conventional and synthetic ECV at 1.5T using alternative regression equation

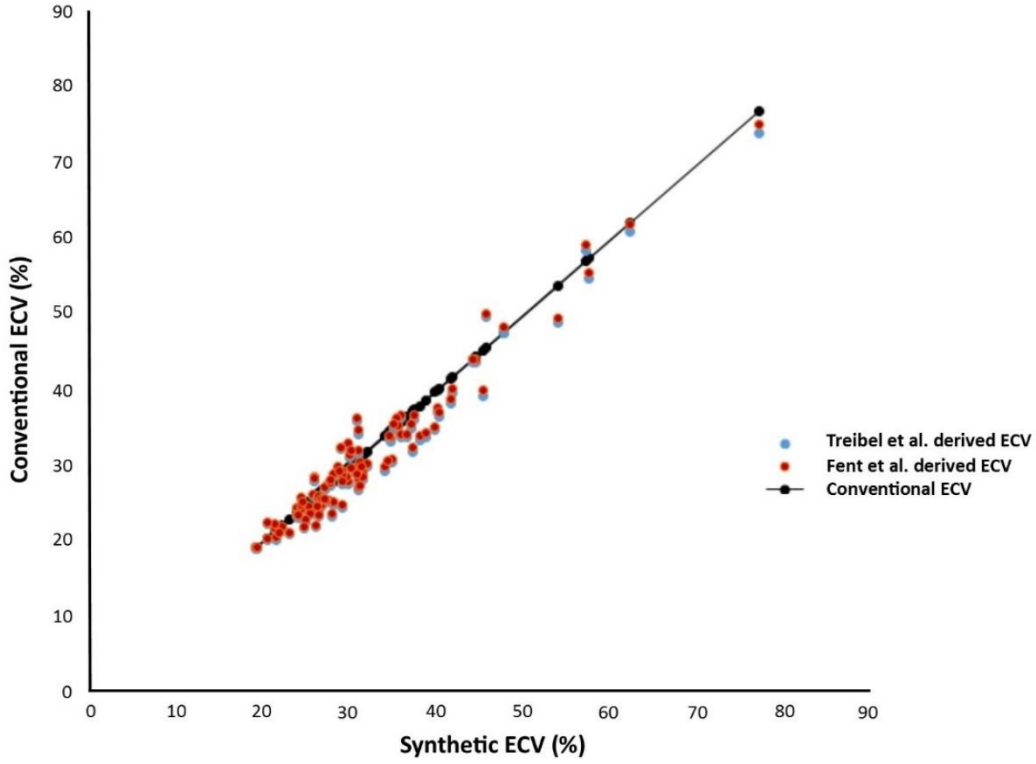

On Bland-Altman analysis, ECV values calculated in the validation cohort using Treibel's 1.5T MOLLI synthetic ECV equation showed minimal negative bias of 0.4%, 95% C.I. 0.06- 0.73% in comparison to ECV calculated the synthetic ECV equation from this study.

3.4. Discussion

We have demonstrated that *synthetic* ECV, derived by estimating Hct from pre-contrast blood T1 values acquired with a MOLLI method on 1.5 and 3T Philips systems, strongly correlates with conventionally calculated ECV. The correlation values demonstrated between Hct and R1 blood in the derivation cohort and

between conventional and *synthetic* ECV in the validation cohort are similar to those reported in the Treibel et al. on a Siemens platform using both MOLLI and shortened MOLLI (ShMOLLI) pulse sequences.

Correlation between between laboratory and *synthetic* Hct was moderate at both field strengths with a negative bias of -0.017 at 1.5T and very minimal bias of 0.003 at 1.5T. There have been early reports of poor agreement of laboratory and synthetic Hct values, particularly with very low or very high Hct as are seen in conditions such as iron deficiency anaemia and dehydration respectively(189). Known factors which may contribute to this include variability in the laboratory Hct measurement in itself, as well as blood flow and body temperature(188). This was apparent to some degree in the 1.5T derivation cohort in this study, who had a wide range of Hct values, but less apparent in the 3.0T derivation cohort who had a narrower range of Hct values which were predominantly within the normal range. However, overall this did not lead to significant accuracies in *synthetic* ECV calculation and the technique appears to offer robust and accurate ECV estimation across a wide range of ECV values.

These findings and synthetic ECV equations could be applied to other Philips 1.5 and 3.0T identical to those used in this study, although ideally local regression equations using similar sized derivation and validation populations to ensure accuracy of synthetic ECV. We have demonstrated that our own 1.5T *synthetic* ECV equation showed excellent agreement with the corresponding equation derived on an alternative vendor platform using a comparable MOLLI pulse sequence. Although ideally such equations should be locally calibrated (as T1 values are dependent on vendor platform), the apparent small differences and minimal bias between *synthetic* ECV values generated by the two equations this gives an indication that universal adoption of the equations we have produced in this study would be unlikely to lead to significant imprecision in *synthetic* ECV calculation. Nevertheless, in this study we have not assessed whether our 3.0T synthetic ECV equation is valid on an alternative vendor platform.

Key areas for future work in the area of *synthetic* ECV should focus on three key areas. Firstly, there appears to some discrepancy between laboratory and *synthetic* Hct values at the lower and higher range. Further work is required to determine why this occurs and, importantly whether any steps can be taken to control any responsible factors and thereby improve accuracy of Hct estimation. Secondly, it remains unclear as to the applicability of the synthetic ECV equations produced in this study across alternative vendor platforms. A future study may

validate this equation on an alternative vendor platform at 3.0T. Finally, the clinical impact of synthetic ECV, particularly the generation of in-line ECV maps in improving the diagnosis and prognostication of cardiomyopathy as well as improvements in clinical workflow has yet to be studied.

3.5. Conclusion

This study underscores the accuracy of synthetic ECV and highlights its applicability across platforms and both 1.5 and 3.0T field strengths. It offers the potential for use on a routine clinical CMR list, eliminating the need for a venous Hct sample, enabling rapid clinical decision-making.

4. Methodology for the development of aortic and circumferential strain analysis using CMR feature tracking

4.1. Background

Aortic stiffness has been proposed as a surrogate marker of generalised atherosclerosis with the potential to identify patients at increased risk of CVD, potentially offering improved CVD risk estimation than standard clinical scoring calculators. Aortic strain analysis has emerged as a promising technique which appears more sensitive than traditional methods in detecting age-related changes in vascular performance(190) and may therefore offer enhanced and more accurate CVD risk estimation than existing techniques. Aortic strain has never been described using CMR, thus this study aims to develop this promising and novel technique for assessment of aortic stiffness.

Studies using echocardiographic speckle tracking have measured circumferential and radial strain in vivo, providing normal values(191, 192) and demonstration of lower values in atherosclerotic disease(193). Circumferential values in particular show promise in identifying patients with significant atherosclerotic disease, who are likely to be the patients at the very highest risk of CV events. Kim et al. demonstrated a correlation between carotid circumferential strain values and the presence or absence of coronary artery atherosclerotic disease on coronary angiography(194). In the same study, carotid intima-media thickness showed no significant correlation with coronary artery disease. Similarly, Podgorski et al. demonstrated a significant negative correlation between carotid circumferential strain values and calcium score, not seen with carotid distensibility or β1 stiffness index(195). These studies highlight the attractiveness of assessing strain values in large arteries and their potential to offer more clinically relevant information than other measures of vascular performance.

CMR-FT is a post-processing technique which works by recognising patterns of features or regularities within a specified region of interest on a series of cine imaging(32). The software tracks and follows these irregularities through time and space, thereby producing deformation parameters. This technique is very similar conceptually to echocardiography speckle tracking, hence CMR-FT has the potential to calculate the same arterial strain indices assessed using echocardiography speckle tracking with the added advantage of unlimited imaging

planes inherent to CMR cine imaging and without the need for additional acquisitions.

4.1.1. Hypothesis and aims

No study to date has demonstrated aortic strain analysis using cardiovascular magnetic resonance imaging. We hypothesised that CMR-FT post-processing software can be used to determine ascending and descending aortic strain from SSFP cine acquisitions.

This study aimed to assess the feasibility and reproducibility of assessing aortic strain parameters using CMR-FT in a group of healthy volunteers with no prior history of cardiovascular disease.

4.2. Methods

The patient population for chapter 4 'Methodology for the development of aortic radial and circumferential strain analysis using CMR feature tracking' included 10 consecutive healthy volunteers recruited between March 2016 and February 2017. All volunteers were scanned at 3.0T (Philips, Achieva, Best, The Netherlands) at Leeds General Infirmary, UK and had no history of CV disease (cardiac, peripheral or cerebral) and no significant past medical history were recruited to undergo CMR examination.

Interobserver, intraobserver and interstudy reproducibility values were calculated by analysing CoV for ascending and descending aorta radial and circumferential strain. For interstudy reproducibility, separate CMR studies were carried out on the same healthy controls 7 days apart. To test reproducibility values at lower and higher temporal resolutions, standard 50-phase cine and higher temporal resolution 100-phase acquisitions for the descending aorta were obtained. The sample size of 10 was chosen on the basis of this representing the minimum acceptable number of samples from which to provide an indication of reproducibility(196).

Mean time taken to analyse both ascending and descending aortic strain as well as mean breath hold time for cine acquisitions was assessed.

In each patient, an axial bSSFP cine acquisition (bSSFP, multiphase, single imaging slice, spatial resolution 2.0 x 1.71 x 8mm, 50 cardiac phases) was acquired of the ascending and descending thoracic aorta at the level of the main pulmonary artery. An additional axial bSSFP cine acquisition was obtained in an identical imaging plane at higher temporal resolution using parallel imaging to maintain an

identical resolution and breath hold time (bSSFP, multiphase, single imaging slice, spatial resolution 2.0 x 1.71 x 8mm, 100 cardiac phases).

The endothelial border and outer wall of the descending and ascending was contoured at end diastole (figure 4-1 on following page) using dedicated post-processing software (CVI 42, Circle Cardiovascular Imaging Calgary, Canada). The software then tracked movement of the aortic endothelial border and aortic wall through time and space to produce radial and circumferential strain values.

Figure 4-1 Descending aortic strain values generated by CMR FT

Panel A shows contouring of the outer aortic wall and endothelial borders at end diastole. Panel B shows the automated generation of strain values. Panel C shows the resultant circumferential strain curve (y axis =strain (%) and x axis = time (ms).

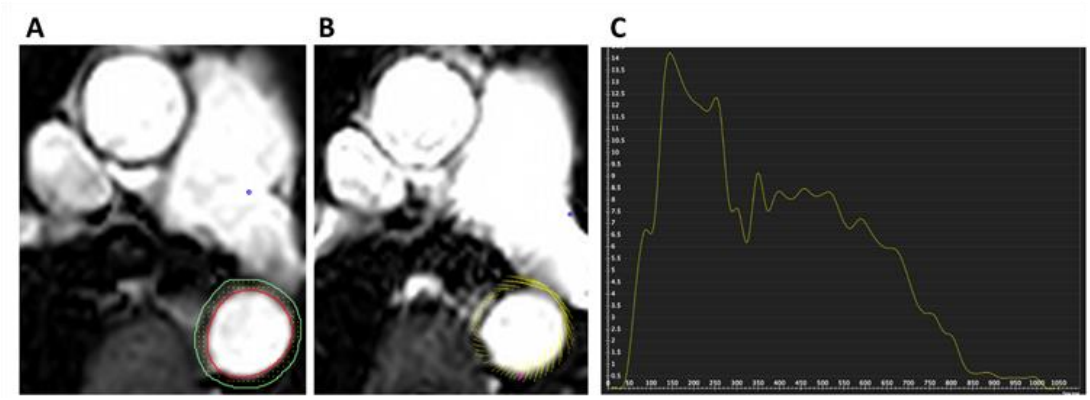

4.2.1. Ethical approval:

All patients gave written, informed consent to take part in the study and the study was conducted according to the declaration of Helsinki. The study was approved by the National Research Ethics Committee (12/YH/0551).

4.3. Results

Demographics of all study participants and results of strain analysis for both the ascending and descending aorta as well as for both radial and circumferential strain by CMR-FT are presented in table 4-1 (following page). Reproducibility values (coefficient of variation) for both ascending and descending aorta and both radial and circumferential strain are summarised in table 4-2 (following page).

4.3.1. Reproducibility of ascending and descending aortic strain

Both radial and circumferential values for the descending aorta were most consistent in terms of intraobserver, interobserver and interstudy with similar coefficient of variation values in the region of 10% obtained at lower (50 phase cine acquisition) and higher temporal resolution (100 phase cine acquisition). For these acquisitions, the same amount of data was acquired as for 50 phase acquisitions, and was split into 100 rather than 50 ‘bins’.

Similarly, intraobserver, interobserver and interstudy reproducibility values for radial and circumferential strain of the ascending were excellent at lower temporal resolution (coefficient of variation <10% for all values).

However, reproducibility at higher temporal resolution gave a coefficient of variation of 14.5 and 17.6 for radial and circumferential strain respectively.

Table 4-1 Baseline demographic data for healthy volunteers

Baseline Characteristics	
	Healthy volunteers
Number (men)	10 (6)
Age	40 ± 10
Systolic blood pressure (mmHg)	119 ± 11
Diastolic blood pressure (mmHg)	63 ± 7

Table 4-2 Reproducibility measurements for aortic strain in healthy volunteers

Reproducibility Measurements				
	Intraobserver Coefficient of Variability (%)	Interobserver Coefficient of Variability (%)	Interstudy Coefficient of Variability (%)	50 versus 100 phase acquisition Coefficient of variability (%)
Ascending aorta				
Radial strain	4.8	8.0	8.3	14.5
Circumferential strain	6.5	9.4	8.3	17.6
Descending aorta				
Radial strain	7.1	8.6	9.5	10.3
Circumferential strain	8.5	10.7	12.3	12.3

4.3.1. Feasiblity of aortic strain by CMR-FT

Mean breath hold time (± standard deviation) for cine acquisitions (50 and 100 phase cine acquisitions) was 12 ± 2 seconds.

Mean time to taken to calculate circumferential and radial strain using post-processing software (± standard deviation) was 58 ± 12 seconds.

4.4. Discussion

In this first study assessing the measurement of novel radial and circumferential strain values using CMR-FT, we have demonstrated two key findings. Firstly, measurement of strain values using CMR-FT is feasible, requiring a short breath-held cine acquisition and a simple and short analysis time using post-processing software. Secondly, the technique used to assess strain values is highly reproducible for both circumferential and radial strain values, with the most reproducible values obtained in the descending aorta as opposed to the ascending aorta.

Our finding of a mean breath-hold time for all cine acquisitions (both 50 and 100 phase bSSFP) of 12 ± 2 seconds compares favourably with other CMR acquisitions and should be achievable for most patients undergoing CMR examination. Although not used in this study, a 'respiratory navigator' allowing free-breathing of the patient during the acquisition could be used in patients unable to breath-hold for the required period of time. This is a standard feature on most built-in scanner software where data is only acquired when the patient's diaphragm is within a pre-defined image location, although overall scan time increases markedly. The mean post-processing analysis time of 58 ± 12 seconds we report was short and compares favourably with other CMR post-processing applications. This, coupled with the short mean breath hold time for the cine acquisition of the descending aorta, indicate assessment of aortic strain using CMR-FT requires straightforward analysis and adds very little time to any CMR protocol. This consideration is important for any emerging imaging parameter, particularly is it is to be adopted into routine clinical use. Although other validated techniques for the assessment of aortic stiffness using modalities other than CMR, CMR involves no ionising radiation and offers the opportunity to combine numerous other quantitative indices (which may further aid assessment of subclinical CVD) in one scan taking less than 1 hour.

Reproducibility for both radial and circumferential strain was comprehensively assessed in this study using coefficient of variation for Intraobserver, interobserver and interstudy reproducibility, as well as reproducibility between lower and higher temporal resolution cine acquisitions. This demonstrated good reproducibility for both radial and circumferential strain which was most consistent within the descending aorta. Reproducibility in the ascending aorta was less consistent, particularly between lower and higher temporal resolution acquisitions.

The reason for this discrepancy may relate to one or both of two factors. There is a higher degree of through-plane motion of the ascending aorta compared with the descending aorta as it shortens and lengthens along its long axis in systole and diastole respectively. This may have led to difficulties in the software tracking the correct features within the specified region of interest at the endothelial border.

A second potential explanation for the discrepancy of ascending aorta strain values obtained from higher and lower temporal resolution images could be the concept of 'flow artefact' due to dephasing of magnetisation in areas of high velocity blood flow which was more prominent within the ascending versus descending aorta. Areas of dephasing within the ascending aorta may have been erroneously tracked by the post-processing software in preference to the endothelial border of the aorta leading to inaccuracy in the strain values obtained.

Flow artefact is increased at higher field strengths and can be reduced (although frequently not eliminated) by changing the phase-encoding direction of image acquisition and careful 'shimming' of images to ensure homogeneity of magnetisation within the desired imaging plane. Although in this study we elected to use a 3.0T field strength to scan patients, it is possible that reproducibility for aortic strain using CMR-FT may be improved at 1.5T given the likelihood that the potential source of inaccuracy relating to flow artefact would be reduced.

Future studies should assess the feasibility and reproducibility of aortic strain using CMR-FT at 1.5T, which may provide improved reproducibility, particularly within the ascending aorta. Furthermore, the utility of aortic strain in assessing vascular performance should be assessed in pathologic disease states associated with increased risk of developing CVD to assess its performance against other established measures of vascular performance.

4.5. Conclusion

We have demonstrated that CMR-FT of the ascending and descending aorta is feasible with good interobserver, intraobserver and interstudy reproducibility. Reproducibility for strain values excellent and is most consistent in the descending aorta with good reproducibility between standard and higher temporal resolution cine acquisitions.

Further study is required to assess the technique in a larger population size and to assess its ability to detect changes in arterial stiffness in populations at increased CVD risk as well as against established alternative measures of aortic stiffness.

5. The Utility of Global Longitudinal Strain in the Identification of Prior Myocardial Infarction in Patients with Preserved Left Ventricular Ejection Fraction

5.1. Background

Prior myocardial infarction is defined as either the presence of pathological Q waves on an ECG, regional loss of myocardium on CV imaging in the absence of a non-ischaemic cause or pathological findings supportive of prior MI(95). Myocardial infarction is frequently unrecognised at the time of its occurrence, accounting for 20-40% of all prior MI in high risk populations diagnosed on ECG criteria(197, 198). Cardiovascular magnetic resonance LGE imaging offers a more sensitive means of diagnosis than ECG and is considered the reference standard non-invasive imaging technique for the detection of prior MI(10, 13). Studies using this approach have suggested that unrecognised MI is more common than recognised prior MI in certain populations, with a prevalence of 18% in an elderly, community-based cohort(199).

The presence of unrecognised MI detected by LGE is associated with a ten-fold increase in risk of CV mortality, which appears to be incremental to conventional clinical and imaging risk factors(115). Recognition of the condition is therefore important and secondary prevention therapy aimed at reducing long-term CV risk is recommended when prior MI is diagnosed(124).

In patients undergoing echocardiography as opposed to CMR or patients with kidney disease precluding the use of Gadolinium based contrast agents, diagnosis of prior MI traditionally relies on the assessment of radial measures of LV systolic function. Indicators suggestive of prior MI include regional wall motion abnormality (hypokinesis, akinesis or dyskinesis of 2 or more contiguous LV segments) with or without reduction in LVEF. However, the relative diagnostic accuracy of both regional wall motion abnormality and LVEF in correctly identifying prior MI are not known.

Longitudinal strain parameters theoretically have the potential to detect prior MI. Myocardial fibres situated in the LV subendocardium contribute significantly to longitudinal LV contraction in systole(200). These fibres are susceptible to ischaemia and increased wall stress(201) and hence, prior MI affecting these fibres may lead to reductions in longitudinal strain values(202). GLS is a summation of myocardial deformation in the longitudinal plane during systole(22). It is proposed

to detect subclinical LV systolic function in a number of cardiomyopathies where LV ejection fraction (LVEF) is preserved(24). Global longitudinal strain rate (GLSR) and early diastolic longitudinal strain rate (GLSRe) represent the rate of longitudinal systolic and early diastolic deformation(22) and are comparable to tissue Doppler derived S prime and E prime measurements(203). CMR feature tracking is an alternative method of measuring these and other myocardial strain indices and uses post-processing software to rapidly obtain measurements from SSFP cine imaging.

GLS has been demonstrated to be reduced in patients with HF-REF due to chronic ischaemic heart disease(204) and in the setting of acute MI(25). However, GLS in patients with MI but preserved LVEF has not yet been investigated.

5.1.1. Hypothesis and Aims

This chapter aimed to assess the performance of 3 longitudinal strain parameters (GLS, global longitudinal strain rate and early diastolic strain rate) measured by CMR-FT in correctly diagnosing the presence of prior myocardial infarction in a group of patients with this condition and a group of healthy controls.

We hypothesised that patients with prior MI detected by LGE but preserved LVEF would have impaired GLS and longitudinal strain rates compared to matched normal controls. Furthermore we hypothesised that these strain parameters would be more accurate than the standard non-invasive imaging parameter, presence of regional wall motion abnormality, in correctly identifying prior MI.

5.2. Methods

5.2.1. Study population

The patient population for Chapter 5 “The Utility of Global Longitudinal Strain in the Identification of Prior Myocardial Infarction in Patients with Preserved Left Ventricular Ejection Fraction” included 40 consecutive clinical patients undergoing CMR examination recruited from and scanned at Leeds General Infirmary, UK between November 2012 and January 2016. Inclusion criteria were 1) evidence of prior MI (defined as hyperenhancement on late Gadolinium enhancement imaging in a typical subendocardial distribution) and preserved LVEF (LVEF ≥55% on cine imaging). Exclusion criteria included MI having occurred in the past 3 months as this could have affected scar burden and/or LV systolic function.

The healthy control population included 40 healthy controls prospectively recruited between September 2014 and January 2016 and matched for age and gender with the prior MI patient population. These patients had no history of CV disease (cardiac, peripheral or cerebral). All participants (patients and healthy volunteers) were screened for CV risk factors by completion of a health questionnaire and from medical records.

This was a single centre case control study involving 40 clinical patients with prior MI occurring > 3 months previously and preserved LVEF (≥55%) and 40 controls matched for age and sex with LVEF (≥55%). Prior MI patients were retrospectively recruited from consecutive patients undergoing CMR for clinical reasons and selecting those with MI and preserved LVEF. Although ideally patients without CVD risk factors would have been chosen so as to minimise the potential for these to act as confounding factors, this would have left an unacceptably small sample size given the low prevalence of prior MI in patients without these risk factors. Healthy controls were prospectively recruited volunteers with no history of cardiac disease. All participants were screened for CV risk factors by completion of a health questionnaire and from medical records.

CMR Acquisition

All patients underwent CMR at either 1.5T (Philips Ingenia) or 3.0T (Philips Achieva) and controls at 3.0T (Philips Achieva). Images were acquired with breath holding on end-expiration prior to contrast administration and prospectively gated using a 3-lead vector ECG.

Cine images were planned from the scout images and for every patient a 2Ch, 4Ch and an LV short axis cine stack were acquired to ensure full coverage of the left ventricle.

LGE imaging was performed in all patients with acquisitions of a short axis LV stack, 2Ch and 4Ch obtained 10 minutes after administration of 0.2mmol/kg Gadolinium DTPA contrast (Gadovist, Bayer Schering) using inversion recovery-prepared T1 weighted echo.

The optimal inversion time (TI) to null normal myocardial signal ascertained by the Look Locker approach. Between 10 and 12 short axis LV, 2Ch and 4Ch images were acquired for every patient. Further imaging with altered phase-encoding direction or systolic imaging were acquired when prior MI was suspected after initial imaging.

5.2.1. CMR analysis

All post processing analysis of CMR scans was performed using the same software (CVI 42, Circle Cardiovascular Imaging Calgary, Canada). LV contours were drawn manually at both end diastole and end systole on the LV short axis SSFP cine stack. LV papillary muscles were considered part of the LV cavity.

Percentage myocardial systolic wall thickening (SWT) was calculated from the end diastolic and end systolic contours as previously reported (205). SWT was calculated for each LV segment based on the 16 segment AHA model. A cut-off value of 30% was used to define the presence of wall motion abnormality (WMA) in an individual LV segment(206). The minimum value for each of the 16 LV segments in each patient was taken and used for comparison between prior MI patients and controls.

The presence of LGE in a subendocardial pattern suggestive of prior MI was determined independently by two physicians with over 4 years' experience in CMR. Quantitative assessment of myocardial scar burden was performed using a threshold of 50% of the maximum intensity within the scar (full width half max method) which has been proposed as the most reproducible method for this purpose(207).

After optimisation of brightness and contrast settings, manual delineation of two separate user-defined ROIs were made on an LGE short axis slice where infarcted myocardium was present. One ROI was an area of hyperintense infarcted myocardium and a second ROI was drawn in remote myocardium containing no infarcted myocardium. Automated calculations for the remaining LV short axis LGE stack based on these two ROIs were then performed.

The strain parameters GLS, GLSR and GLSRe were calculated using feature tracking software from 4Ch and 2Ch SSFP cine acquisitions (figure 5-1).

Prior to analysis, brightness and contrast settings were adjusted to allow optimisation of endocardial and blood pool differentiation. The epicardial and endocardial borders were traced manually. The software then tracked the voxel features of the myocardium to quantify the motion of myocardium and compute strain values(32). This process results in generation of values of percentage deformation in the longitudinal plane throughout the cardiac cycle (providing a value for GLS) as well as deformation rate throughout the cardiac cycle (providing values for GLSR and GLSRe).

Figure 5-1 Calculation of GLS using CMR feature tracking in a healthy control

Panel A: 4Ch cine acquisition with manually contoured epicardial and endocardial borders. Panel B: 2Ch cine acquisition with manually contoured epicardial and endocardial border. Panel C: Feature tracking of 4Ch cine acquisition. Panel D: Feature tracking of the 2Ch cine acquisition. Panel E: Graph showing GLS (x axis shows time (ms) and y axis shows deformation (%) in longitudinal plane). Panel F: Graph showing longitudinal strain rate (x axis shows time (m/s) and y axis shows deformation rate (%/s)).

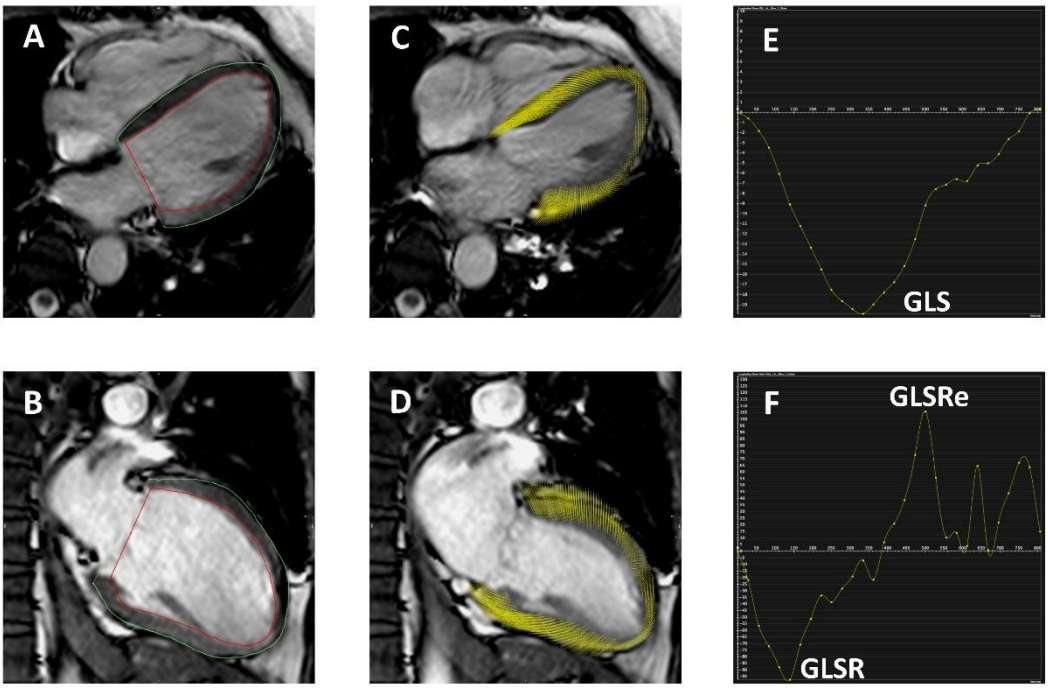

5.2.2. Statistical analysis and power calculation

Normality of data was tested using a Shapiro-Wilk test. Mean values ± SD are reported. Unpaired Student t-test and Mann-Whitney U test were used as appropriate to compare continuous variables. Cut-off values to identify prior MI were derived from receiver-operating characteristic (ROC) curve analysis using Youden index giving maximum sensitivity and specificity.

Area under the curve values (AUCs) were compared by using validated methods described by DeLong et al(208). Multivariable linear regression was used for variables with a statistical significance of < 0.1 on univariable linear regression.

Intra and interobserver variability for GLS were tested on 10 randomly selected healthy controls using coefficient of variation. All tests were two-sided and $p<0.05$ was considered statistically significant.

Based on the pooled standard deviation of 2.8% 31 subjects are needed in each group to detect an absolute reduction of GLS by 2% in those with chronic MI (α=0.8, significance=0.05).

5.2.3. Ethical approval:

All patients gave written, informed consent to take part in the study. The study was completed according to the declaration of Helsinki. The study protocol was approved by the National Research Ethics Committee (12/YH/0169).

5.3. Results

A total of 40 prior MI and 40 healthy controls were recruited. Analysis was completed in all 40 patients in both groups, thus all were included in the final study sample.

The prior MI patients were well-matched with controls for age and sex. Other variables including blood pressure, body mass index, LV mass, LVEDV and LV systolic function were comparable across both groups. There were no statistically significant differences between any of these variables (table 5-1 on following page).

Table 5-1 Patient characteristics in patient and prior MI groups

Clinical Variable	**Prior MI (n=40)**	**Controls (n=40)**	**p Value**
Age	60 ± 11	57 ± 10	0.29
Females	9/40 (23%)	9/40 (23%)	-
LVEF (%)	62.3 ± 3.9	62.1 ± 3.8	0.82
LV mass (g)	107.9 ± 24.6	100.7 ± 23.8	0.18
LVEDV(ml)	159.8 ± 34.3	161.3 ± 30.2	0.84
Systolic blood pressure (mmHg)	133 ± 25.6	130.0 ± 12.3	0.61
Diastolic blood pressure (mmHg)	78 ± 19.5	73.0 ± 9.8	0.19
Body mass index (kg/m2)	27.9 ± 3.4	27.8 ± 3.9	0.82
Haemoglobin (g/L)	146 ± 11.5	142 ± 14.5	0.27
Creatinine (micromol/L)	77 ± 13.4	75 ± 13.6	0.52
Estimated GFR (ml/min/1.73m^2)	81 ± 8.5	83 ± 9.1	0.83
Hypertension	13/40 (33%)	4/40 (9%)	**0.008**
Hypercholesterolemia	10/40 (25%)	1/40 (3%)	**0.004**
Diabetes Mellitus	6/40 (15%)	0/40	**0.02**
Smoking	18/40 (45%)	2/40 (6%)	**<0.001**

5.3.1. Feature tracking parameters of myocardial strain

Feature tracking analysis was successfully performed in all prior MI patients and controls. Global longitudinal strain (figure 5-2 and figure 5-3) was significantly lower in prior MI patients than controls (-17.3 ± 3.7% versus -19.3 ± 1.9%, p=0.012). Global longitudinal strain rate was significantly lower in prior MI patients versus controls (-88.0 ± 33.7%s^{-1} versus -103.3 ± 26.5%s^{-1} p=0.005). Early diastolic longitudinal strain rate was also significantly lower in prior MI patients versus controls (76.4 ± 28.4%s^{-1} versus 95.5 ± 26.0%s^{-1}, p=0.001).

GLS was not significantly different in prior MI patients scanned at 1.5 and 3.0T (mean GLS at 1.5T -18.0 ± 1.8 versus -17.2 ± 4.0 at 3.0T, p = 0.61).

Figure 5-2 Example of GLS in prior myocardial infarction

Panel A shows short axis cine acquisition of LV at end diastole. Panel B shows short axis cine acquisition of LV at end systole with no appreciable RWMA. Panel C shows LGE acquisition with subendocardial MI of basal inferolateral LV segment. Panel D shows resultant GLS of 14%.

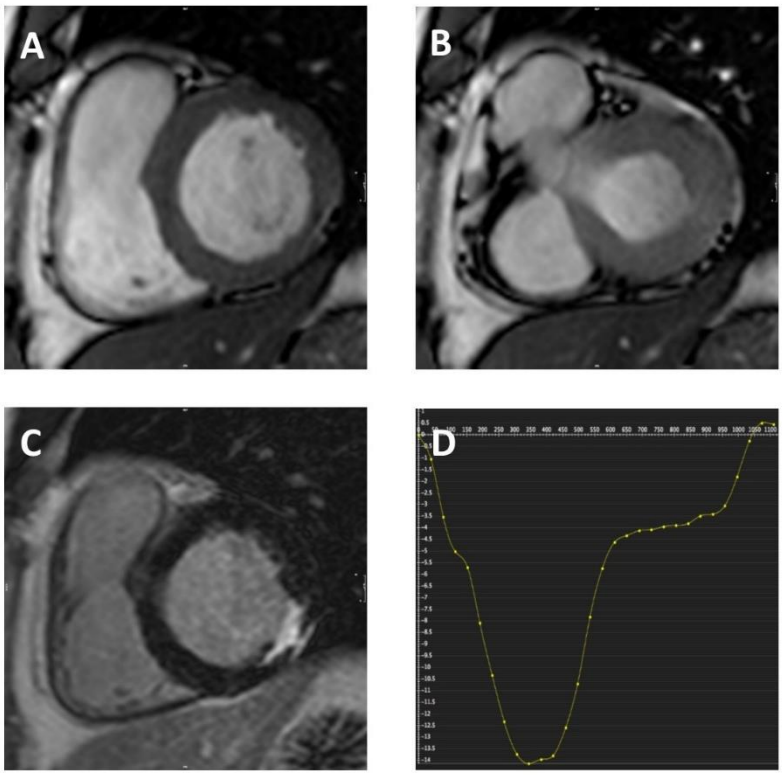

Figure 5-3 Box and whisker plots for GLS in healthy controls and prior MI patients

The horizontal line within the box represents the median value, the bottom line of the box represents the 25th centile and the top of the box the 75th centile. The narrower 'whiskers' above and below the box represent the 95% confidence interval.

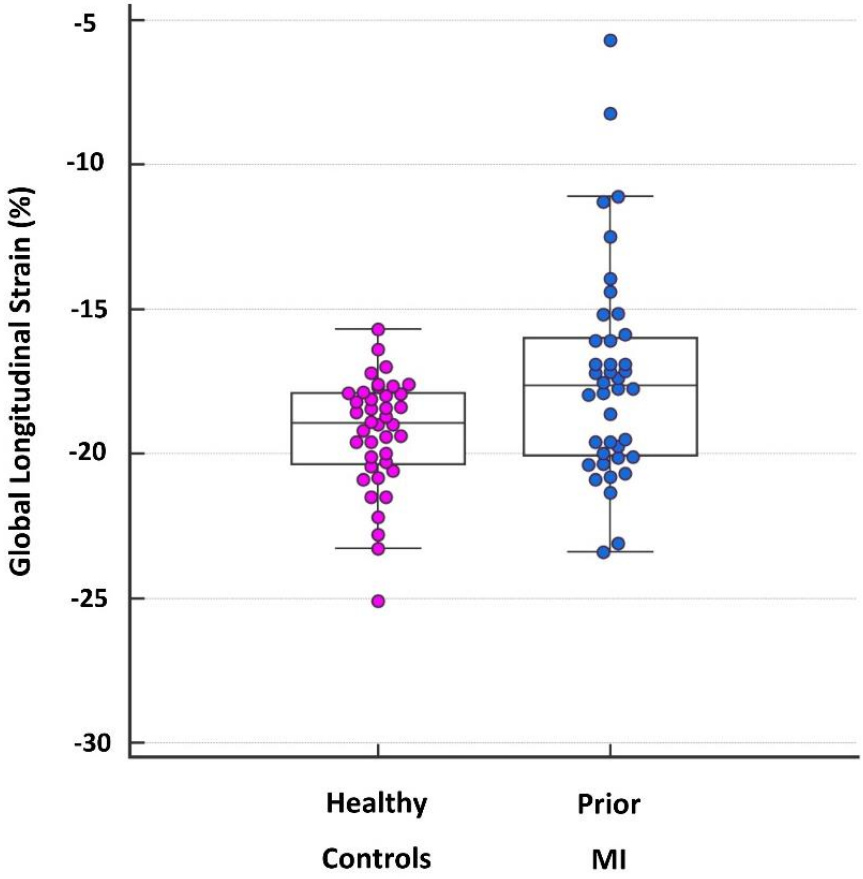

5.3.2. Quantitative systolic wall thickening

Quantitative systolic wall thickening analysis was possible in all prior MI patients and controls. There was no significant difference in minimum SWT in those with prior MI compared to controls (46.0 ± 18.3% versus 42.0 ± 14.1%, p=0.093). There was no significant difference in the proportion of subjects with WMA defined as a segment with SWT<30% (6/40 (15%) prior MI patients and 6/40 (15%) controls.

5.3.3. Receiver operator characteristic analysis

AUC for the ability of each longitudinal strain parameter to correctly identify prior MI were as follows (figure 3-3): GLS 0.662 (95% C.I. 0.540-0.785), p=0.01, GLSR 0.684 (95% C.I. 0.566-0.802), p=0.005 and for GLSRe 0.707 (95% C.I. 0.592-0.821), p=0.001. By comparison, AUC for the ability of both presence of WMA and minimum SWT to correctly identify prior MI were lower at 0.500 (95% C.I. 0.386 – 0.614), p=1.0 and 0.609 (95% C.I. 0.483-0.735), p=0.09 respectively.

Comparison of AUC values for all longitudinal strain parameters assessed showed significantly higher diagnostic accuracy for the detection of prior MI than WMA (GLS p= 0.02, GLSR p=0.01 and GLSRe p=0.001). Comparison of AUC values between longitudinal strain parameters and minimum SWT showed no statistical significance (GLS p= 0.59, GLSR p=0.39 and GLSRe p=0.29).

Figure 5-4 ROC curves for the accuracy of longitudinal strain parameters (GLS, GLSR and GLSRe) and presence of WMA in the prediction of prior MI

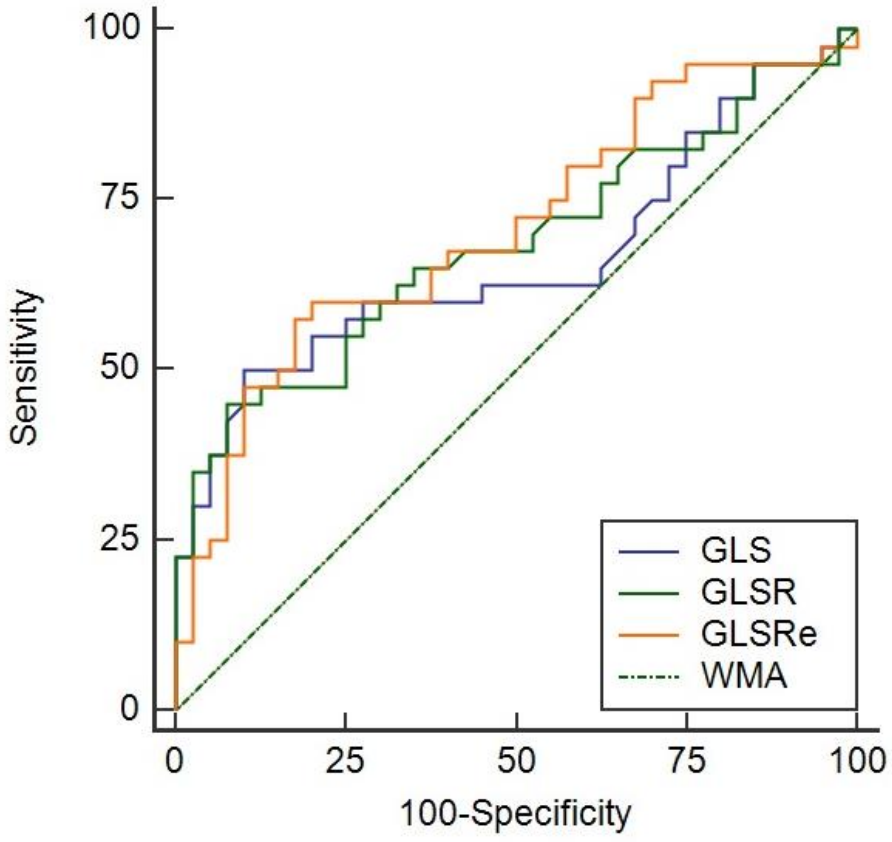

5.3.4. Scar quantitation

Scar quantitation was successfully performed in all prior MI patients. The range of absolute scar mass was wide at between 0.7g and 21.4g. The overall mean absolute scar mass was 5.5 ± 4.3g, equating to a relative percentage of LV mass of 4.9 ± 3.3 %.

5.3.5. Sensitivity and specificity of feature tracking derived strain values

Two approaches were used in determining sensitivity and specificity for the correct identification of prior MI by the different longitudinal strain values assessed. Firstly, the cut-off value giving maximum area under the curve was determined for each variable. Secondly, the value giving maximum specificity was determined. Results are summarised in table 5-2.

Table 5-2 Identification of prior MI with longitudinal strain parameters optimised for sensitivity and specificity

Variable	Sensitivity (%)	Specificity (%)	MI correctly identified	MI Incorrectly identified
GLS cut-off >-18%	60	72.5	24/40	11/40
cut-off >-15.7%	22.5	100	9/40	0/40
GLSR cut-off >-93.5%s^{-1}	65	60	26/40	16/40
cut-off >-66.4%s^{-1}	22.5	100	9/40	0/40
GLSRe cut-off <86%s^{-1}	67.5	60	27/40	16/40
cut-off <44.81%s^{-}	10	100	4/40	0/40

5.3.6. Univariable and multivariable regression analysis for GLS

Variables including patient demographics, risk factors for CVD and presence of prior MI were analysed to determine univariable predictors of GLS (table 5-3). Multivariable regression analysis revealed only prior MI to be an independent predictor of change in GLS.

Table 5-3 Univariable and multivariable regression analysis for global longitudinal strain

Variable	**Beta**	**95% CI**	p value
Age	0.04	-0.03 – 0.10	0.29
Hypertension	1.26	-0.48 – 3.00	0.15
Hypercholesterolemia	1.84	-0.17 – 3.84	0.07
Diabetes	0.77	-1.96 – 3.49	0.58
Smoking (ever)	0.47	-1.16 – 2.10	0.57
Prior MI	-1.97	-3.29 - -0.65	**0.004**
Systolic BP	-0.01	-0.05 – 0.03	0.76
Diastolic BP	0.02	-0.03 – 0.07	0.49
Multivariable regression for Global Longitudinal Strain			
Variable	**Beta**	**95% CI**	**p value**
Hypercholesterolemia	0.93	-1.11 – 2.97	0.37
Prior MI	-1.94	-3.41 - -0.47	**0.01**

5.3.7. Observer variability

On intraobserver analysis, mean GLS values by CMR feature tracking were similar at -20.3% and -19.6% (p= 0.60) and CoV 3.9%. On interobserver analysis, mean GLS values CMR feature tracking were again similar at -20.3% and -19.6 (p= 0.62) and CoV% 4.0%.

5.4. Discussion

We have found that in patients with preserved LVEF and prior MI there is impairment of GLS, GLSR and GLSRe. Furthermore, impairment of GLSR and GLSRe had superior diagnostic accuracy than the quantitative assessment of WMA in the detection of prior MI. These results demonstrate that prior MI may be detected when GLS is impaired when LVEF is preserved, although its ability to detect prior MI in this context is moderate.

Impairment of longitudinal measures of strain in prior MI may relate to myocardial fibre arrangement within the left ventricle. Subendocardial myofibres contribute predominantly to contraction in the longitudinal plane with subepicardial fibres providing a lesser contribution. Conversely, both circumferential and radial motion of the myocardium are generated by fibres predominantly located in the midwall(200). Longitudinal function is particularly vulnerable to any disease process affecting the subendocardium. It is therefore possible that in limited subendocardial MI, longitudinal myocardial deformation is reduced whereas radial function, which results from contraction of LV midwall fibres, may be relatively preserved. Given that LVEF and systolic wall thickening are predominantly measures of radial contraction, this would explain the findings in this study that minimum SWT, presence of WMA and LVEF were all poor predictors of prior MI in patients with preserved LV function. Delgado et al. demonstrated that although GLS was reduced in patients with HF-REF due to chronic ischaemic heart disease, the relationship between LVEF and GLS was only weakly linear (r=0.62, p= <0.001)(204) which would again potentially support the concept of impaired GLS being largely attributable to loss of subendocardial myocardial fibre contraction.

There was no significant difference in the proportion of patients with WMA (>30% minimum SWT in any LV segments) between the prior MI and control groups. Our finding of WMA in asymptomatic controls was not unexpected and has previously been reported elsewhere in the literature(205, 209).

The importance of LVEF and regional LV systolic function as indicators of prior MI is stressed in international guidelines(95). Our results demonstrate the potential additive value of longitudinal strain parameters and in particular GLS in looking beyond traditional means of assessing LV systolic function in the detection of prior MI.

Of the longitudinal strain parameters assessed, GLS was moderately useful in terms of specificity and sensitivity with a cut-off value of >-18% giving a sensitivity of 60% and specificity of 72.5% and was the most useful of the 3 strain values assessed. These findings broadly correlate with those of Nucifora et al. who demonstrated a correlation between reduced GLS measured by echocardiography and the presence of significant coronary artery disease on CT coronary angiography in patients with symptoms suggestive of stable angina with normal LVEF(210). In that study, the authors proposed a cut off value ≥-17.4% predicting significant coronary artery disease with a sensitivity of 83% and specificity of 77%. It is unclear why our own values for the sensitivity and specificity of GLS in identifying prior MI were lower, though one reason could be that ischaemia has a more profound effect on GLS than infarction, possibly due to the influence of LV remodelling in the context of chronic infarction.

GLS has good inter and intra-observer variability when measured by CMR feature tracking as demonstrated in both this and another study(211). Similar values have also been demonstrated using echocardiography(212). The findings of this study adds to the growing evidence base supporting the use of GLS in clinical practice. It has shown potential in terms of prognostication and has been demonstrated to be superior to LVEF in predicting morbidity and mortality in patients with IHD (213). Additionally, it shows promise as a potential screening tool for silent MI(214).

Several studies have demonstrated impairment of GLS, predominantly by speckle tracking echocardiography, in a range of disease states including diabetes(215), heart failure with preserved ejection fraction (HFPEF)(216) and aortic stenosis(217). In these studies, impairment of longitudinal function was attributed to a direct cardiomyopathic process. However, LGE imaging was not performed in these patients and it is therefore possible that impairment of GLS may have related to unrecognised MI. Thus, future studies of the prognostic importance of GLS should include LGE imaging to exclude MI as the mechanism of impairment of longitudinal function.

Our findings support the potential utility of GLS as a screening tool for identifying prior MI in patients with preserved LV ejection fraction, although when used alone,

its ability to correctly identify prior MI in this context is only moderate. Further prospective studies are needed to identify whether combining it with other imaging and/or clinical parameters lead to improvement in its specificity and sensitivity. As GLS has been shown to be impaired independently of LVEF in aortic stenosis(217), hypertrophic cardiomyopathy(218) and heart failure with preserved ejection fraction (HFPEF) (216), it must be interpreted with caution where these conditions are present or are suspected.

5.4.1. Limitations of the study

The values for the strain parameters measured in this study were calculated using feature tracking post-processing software. This remains a research application and currently lacks the clinical validation to enable its adoption into routine clinical practice. Nevertheless, both GLS and GLSR can be readily measured using modern echocardiographic speckle tracking (22) which have been validated against CMR strain measurements(219) .

CMR tagging has traditionally been considered the reference standard technique for calculation of strain values and was not used in this study. We have elected to use feature tracking preferentially for this study because tagging techniques suffer from both lower temporal resolution and fading of the tag overlay as the cardiac cycle progresses(211). Furthermore agreement between feature tracking and CMR tagging is excellent(220) and can be easily performed without the need for acquisition of additional sequences.

We have not carried out invasive assessment of coronary anatomy in all patients and it is possible that undiagnosed ischaemia may have contributed to impairment of longitudinal strain parameters. However, performing coronary angiography on patients in whom it is not clinically indicated would not be ethically appropriate.

Finally, there were higher rates of CV risk factors in our prior MI population compared with healthy volunteers, thus it is unclear as to their relative contribution (if any) to the observed decrease in GLS seen in prior MI patients. Nevertheless, in our multivariable analysis, only prior MI was an independent predictor of change in GLS and CV risk factors including hypertension, smoking, hypercholesterolemia and diabetes were not. These CV risk factors were all potential confounding factors in the observation of lower GLS in the prior MI patients, although no studies to date have assessed their individual relative impact on GLS. A future study may seek to address this by including additional control groups with no prior MI including hypertensive patients, diabetic patients and active smokers in addition to healthy

controls. Pre-test probability of prior MI was not calculated in this study due to its retrospective selection of patients, however, this could also be performed in a future study, to assess whether longitudinal strain parameters provide incremental benefit above the use of standard clinical and non-invasive imaging tests.

5.5. Conclusions

The strain parameters GLS, GLSR and GLSRe are reduced in patients with prior MI in the context of normal LVEF. A normal LVEF and lack of WMA is insufficient to exclude prior MI. Prior MI may be suspected when impaired GLS, GLSR or GLSRe are detected by non-invasive imaging.

6. Assessment of Large Artery Involvement in Rheumatoid Arthritis Over Time: Prior to Diagnosis, at Diagnosis and in Established Disease

6.1. Background

Rheumatoid Arthritis (RA) is associated with an increase in cardiovascular mortality, approximately twice that of the general population(117). Traditional risk factors alone are insufficient to explain this increase and inflammation is thought to be a major contributory factor. Inflammation is thought to affect the vascular system of patients with RA through progressive endothelial dysfunction, arterial hardening (arteriosclerosis) and, eventually, largely irreversible atherosclerotic plaque formation in larger arteries(147).

Demonstrating the time in the disease course of RA at which endothelial dysfunction first becomes evident may improve long-term CV outcomes in RA through earlier initiation of disease-modifying medication. Furthermore, greater understanding of how measures of arterial performance relate to CV outcomes may improve CV risk assessment in RA patients(125).

Aortic stiffness can be assessed using non-invasive imaging as an indicator of function of the larger arteries and is a useful surrogate marker of increased risk of CV events(221). Aortic stiffness is defined as resistance to deformation (lengthening or shortening) of the aortic wall(222). The thoracic aorta, aside from its role as a conduit vessel, serves to dampen the high systemic pressures generated by the left ventricle in systole, protecting distal vascular beds of organs including the kidneys and brain(223). This elastic recoil of the aorta diminishes naturally with ageing, resulting in damage to distal vascular beds and raised systemic blood pressure. RA is thought to accelerate this process of vascular ageing and dysfunction. Aortic stiffness has been reported to be increased in newly diagnosed(224) as well as established disease(225), but may begin even before a formal diagnosis of RA. A ‘systemic autoimmune phase’ lasting months or even years is recognised, where the patient is largely asymptomatic, yet anti-cyclic-citrullinated peptide (ACPA), a highly specific serological marker for RA, is raised(226). Progression of such ‘at risk’ individuals can be predicted with the use of risk scoring models incorporating radiological parameters(227). Measurement of radial and circumferential strain has been validated using speckle tracking echocardiography(191), showing promise in demonstrating the presence or

absence of atherosclerotic disease(228). The presence of carotid plaque using ultrasound is a well-established marker of increased CVD risk in RA(229). It is therefore likely that patients with plaque disease are furthest along the continuum of endothelial dysfunction, arteriosclerosis and eventual atherosclerosis. For this reason, identifying a non-invasive imaging technique able to detect atherosclerotic plaque either directly or indirectly may strengthen its utility in CVD risk estimation. Circumferential carotid strain has been shown to be superior to carotid intima media thickness in predicting the presence and severity of coronary artery disease(194). Furthermore, carotid circumferential strain has also been shown to have a significant negative correlation with coronary calcium score ($r= -0.4$, $p <0.01$) which was not apparent with conventional measures of arterial performance(195).

Aortic distensibility is a more established technique recognised as a surrogate marker of increased CV mortality with evidence of abnormalities in treatment-naïve, early RA(230) and established RA(231). Limitations of assessing distensibility include its significant correlation with age and systolic BP(231).

6.1.1. Hypothesis and Aims

We hypothesised the following:

1) Both aortic distensibility and aortic strain would be lower at all time points of RA (prior to diagnosis, at diagnosis and in established disease).
2) Aortic circumferential strain would more accurately differentiate patients with established disease with and without CMR evidence of carotid plaque disease than aortic distensibility.

The aim of this study was twofold:

1) To assess the ability of an existing, established measure of aortic stiffness (aortic distensibility) and the novel measures of aortic stiffness (aortic radial and circumferential strain) to detect subclinical aortic stiffness in individuals at risk of RA as well as patients with newly diagnosed RA versus healthy controls.
2) To assess the ability of an existing, established measure of aortic stiffness (aortic distensibility) and the novel measures of aortic stiffness (aortic radial and circumferential strain) to correctly identify atherosclerotic carotid plaque disease in a group of patients with established RA.

6.2. Methods

The patient population for Chapter 6 “Assessment of Large Artery Involvement in Rheumatoid Arthritis Over Time: Prior to Diagnosis, at Diagnosis and in Established Disease” included healthy controls (n=30) and 3 RA populations (individuals at risk of RA (n=18), newly diagnosed, treatment naïve RA patients (n=83) and RA patients with established disease (n=40).

At risk’ RA individuals were recruited between January 2016 and September 2016. This population included 18 consecutive patients with symptoms of arthralgia and detectable ACPA under active monitoring for the development of RA. These patients were recruited from the outpatient clinic service at a tertiary centre (Chapel Allerton Hospital, UK) and underwent CMR at 3.0T (Philips, Achieva, Best, The Netherlands). All patients had no history of previous CV disease (cardiac, peripheral or cerebral). Positive ACPA was considered to be a serum level ≥2.99U/ml (anti-CCP2; immunocap assay, Phadia, Uppsala, Sweden) at the time of recruitment. Arthralgia was defined as pain in any joint, without clinical evidence of synovitis. All participants were screened for CV risk factors by completion of a health questionnaire and from medical records.

Newly diagnosed, treatment naïve RA patients were recruited between February 2012 and November 2015. This population consisted of 82 consecutive patients fulfilling the 2010 American College of Rheumatology/European League Against Rheumatism diagnostic criteria for RA who were recruited from the outpatient clinic service at a tertiary centre (Chapel Allerton Hospital, UK) as part of the CADERA study (Coronary Artery Disease in Early Rheumatoid Arthritis). These patients were already recruited into the Very Early versus Delayed Etanercept in Rheumatoid Arthritis randomised drug trial (VEDERA). All patients had a recent diagnosis of RA (less than 1 year), displayed signs of active disease (clinical or imaging evidence of synovitis and Disease Activity Score in 28 joints with Erythrocyte Sedimentation Rate (DAS28-ESR) ≥3.2 and had not previously received any DMARD therapy. Patients had no previous history of CV disease. As part of the VEDERA trial patients were randomised to either the tumour necrosis factor inhibitor (TNFi) Etanercept combined with Methotrexate as first line therapy, or optimal standard therapy including Methotrexate as first line therapy, only escalating to Etanercept in combination with Methotrexate if a patient failed to achieve clinical remission from RA 24 weeks or more after enrolment(166).

Following a baseline scan immediately after recruitment, 71 of these patients underwent a repeat year one scan between 51 and 53 weeks after their baseline scan.

Established RA patients were recruited between February 2011 and August 2014. This population consisted of 40 consecutively recruited patients fulfilling the 1980 American College of Rheumatology diagnostic criteria for RA were recruited from the outpatient clinic service at a tertiary centre (Chapel Allerton Hospital, UK) and scanned at 3.0T (Philips, Achieva, Best, The Netherlands) as part of the IACON (Inflammatory Arthritis disease CONtinuum) study. At the same time as the CMR scan, these patients also underwent a series of Time of Flight, proton-density, T1 and T2-weighted acquisitions of both carotid arteries, deemed to be of diagnostic quality for both the right and left carotid arteries. All patients had been diagnosed with RA for > 5 years. Patients had no previous history of CV disease (cardiac, peripheral or cerebral) or diabetes.

Healthy volunteers for this study were recruited between September 2014 and March 2015 and scanned at 3.0T at Leeds General Infirmary, UK. The population included 30 volunteers with no prior history of RA or prior CV disease (cardiac, peripheral or cerebral) who were consecutively recruited on a volunteer basis to undergo CMR examination. These were matched in age and gender to the treatment naïve, newly diagnosed RA patients.

Exclusion criteria in all groups included known CVD (including ischaemic heart disease heart failure or cardiac arrhythmia), renal failure (estimated glomerular filtration rate <30ml/min^{-1}) and inability to undergo CMR due to obesity.

Cardiovascular risk factors such as hypertension, diabetes, hypercholesterolaemia and smoking status were assessed by history and medical records. Hypertension was defined as blood pressure >140/90mmHg or the use of anti-hypertensive medications. Diabetes was defined as fasting glucose ≥7mmol/L^{-1}, HbA1C ≥48mmol/mol, or the use of oral anti-hyperglycaemia medication or subcutaneous insulin. Hypercholesterolaemia was defined as total cholesterol <5mmol/L^{-1} or the use of statin medication.

The sample sizes were based on the maximum available number of patients within each cohort during the recruitment periods, accepting that the sample size for individuals at risk of RA (n=18) is relatively low owing to difficulty in recruitment of this cohort.

6.2.1. CMR protocol

All patients underwent CMR at 3.0T (Philips Achieva). Images were acquired with breath holding on end-expiration prior to contrast administration and prospectively gated using a 3-lead vector ECG. The CMR protocol for all patients included a cine LV short axis covering the long axis of the LV in its entirety, with one slice acquired per breath hold in end-expiration, parallel to the mitral valve annulus (bSSFP, multiphase, 10-12 contiguous slices, spatial resolution 2.0 x 1.63 x 10mm, 30 cardiac phases). Additionally, 50-phase cine acquisitions of the ascending and descending aorta were acquired as described in the methods chapter.

Patients in the established RA patient cohort also underwent a series of non-contrast, non-breath held MR images at 3.0T (Philips Achieva, Philips, Best, The Netherlands) which were acquired using a 10cm phased array coil (Philips dStream Flex, Best, The Netherlands). Survey images were used to locate the point of bifurcation of the common carotid into the internal and external carotid artery. Perpendicular, axial slices were then planned form the survey images. Time of flight (ToF), proton density-weighted (PD), T1 and T2-weighted slices were then acquired (10 slices in total; 5 above and 5 below the carotid bifurcation). Spatial resolution for ToF acquisitions was 0.89 x 0.89 x 3mm, PD 0.7 x 0.7 x 2mm, T1 0.7 x 0.7 x 2mm and T2 0.7 x 0.7 x 2mm.

6.2.2. CMR analysis

All post processing analysis of CMR scans was performed using the same software (CVI 42, Circle Cardiovascular Imaging Calgary, Canada). Analysis of scans was performed by a single assessor with 2 years' experience in CMR reporting blinded to all patient details. Left ventricular contours were drawn manually at both end diastole and end systole on the LV short axis SSFP cine stack. LV papillary muscles were considered part of the LV cavity. Aortic distensibility was calculated according to previously described methods(181). Radial and circumferential aortic strain were calculated using post-processing CMR-FT analysis as described in detail within chapter 4.

Carotid T1/T2/TOF and PD acquisitions were visually assessed for the presence or absence of carotid atherosclerotic plaque, graded according to previously described methods(232). Patients were only included in the analysis if image quality of both carotid arteries was of diagnostic quality. Carotid atherosclerotic plaque was

considered present when either artery showed either diffuse intimal thickening, evidence of small eccentric plaque within the vessel lumen or more obvious larger eccentric plaque with clear narrowing of the vessel lumen (see figure 6-1).

Figure 6-1 Example of CMR carotid imaging

Panel A shows PD acquisition of right carotid artery in patient with no evidence of atherosclerotic plaque. Panel B shows PD acquisition of left carotid artery with evidence of eccentric atherosclerotic plaque formation (see red asterisk).

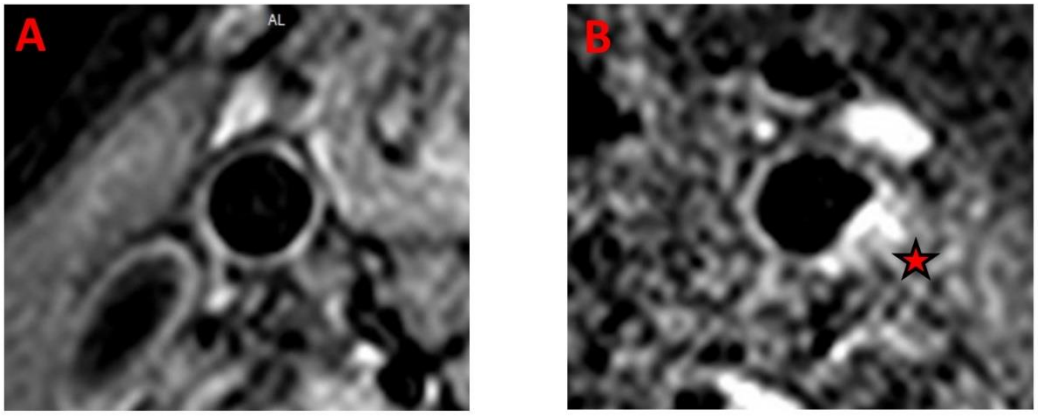

6.2.3. Statistical analysis

Normality of data was tested using a Shapiro-Wilk test. Mean values ± SD are reported. Unpaired Student t-test and Mann-Whitney U test were used as appropriate to compare continuous variables.

Cut-off values to identify presence of carotid atherosclerotic plaque were derived from ROC curve analysis using Youden index giving maximum sensitivity and specificity. AUCs were compared by using validated methods described by DeLong

et al(208). All tests were two-sided and $p<0.05$ was considered statistically significant.

6.2.4. Ethical approval:

The study was conducted according to the declaration of Helsinki. All patients gave their written, informed consent to take part in the study. Patients were recruited from a number of different studies covered by the following National Research Ethics Committee approvals 09/1-11307/98, 10/H1307/138 & 12/YH/0551.

6.3. Results

6.3.1. Feasibility of vascular performance measurements

Analysis of descending aortic radial and circumferential strain was possible in 162/169 (96%) of all patients included in the study and was not possible in 1/18 (3%) at risk of RA, 6/81 (7%) newly diagnosed RA patients all due to degradation of image quality due to flow artefact. Assessment of aortic distensibility was possible in all 169 patients.

6.3.2. Patient characteristics (healthy controls, at risk RA and newly diagnosed RA)

Patient characteristics of healthy controls, at risk RA and newly diagnosed patients are shown in table 6-1 on following page. Healthy controls were well matched with at risk RA and newly diagnosed RA patients for age and gender. There were also no statistically significant differences between these groups for systolic or diastolic blood pressure (BP), hypertension and hypercholesterolaemia and proportion of active smokers. There were significant differences between groups for body mass index (BMI), diabetes, proportion of ex-smokers and mean pack years of smoking.

Table 6-1 Patient demographics (healthy controls, at risk RA and newly diagnosed RA)

Characteristic*	Healthy controls (n=30)	At risk RA (n=18)	Newly diagnosed RA (n=81)	p value (between groups)
Age (yrs)	49±16	53±12	49±13	0.52
Females (%)	19/30 (63%)	14/18 (78%)	55/81 (68%)	0.59
BMI	25.3±4.6	28.7±5.4	25.7±4.6	**0.03**
Systolic BP	119±12	122±16	121±15	0.70
Diastolic BP	65±13	65±11	70±11	0.05
Hypertension (%)	0/30	1/18 (6%)	6/81 (7%)	0.32
Hypercholesterolaemia(%)	0/30	0/18	2/81 (2%)	0.55
Diabetes (%)	0/30	2/18 (11%)	0/81	**0.002**
Active smoker (%)	3/30 (10%)	2/18 (11%)	17/81 (21%)	0.31
Ex-smoker (%)	5/30 (17%)	10/18 (56%)	25/81 (31%)	**0.02**
Pack years	1±4	10±14	6.8±12	**0.01**
CRP ≥5 (%)	-	5/18 (28%)	50/81 (62%)	-
ESR	-	12.9±13.3	36.8±27.2	-
RF positive (%)	-	8/18 (44%)	60/81 (74%)	-
CCP positive (%)	-	18/18 (100%)	68/81 (84%)	-
DAS28-ESR	-	-	5.6±1.1	-
Predicted risk of RA (%)	-	49±17	-	-

*Mean ± SD unless stated otherwise

6.3.3. Patient demographics (established RA)

CMR evidence of carotid atherosclerotic plaque disease was evident in 22/40 (55%) patients with established RA. There were no statistically significant differences in demographic data between patients with and without carotid plaque (table 6-2), although there was a trend towards higher BMI, active smoker status and higher systolic BP in those with plaque versus those without.

Table 6-2 Patient demographic data (established RA)

Characteristic*	Established RA (n=40)	Carotid plaque present (n= 22)	Carotid plaque absent (n=18)	p value (carotid plaque present vs. absent)
Age (yrs)	58.6±8.7	59.4±8.9	57.7±8.6	0.54
Females (%)	30/42 (71%)	73%	70%	0.97
BMI	25.4±3.0	26.1±3.1	24.6±2.7	0.10
Systolic BP	134±19	137±23	131±14	0.36
Diastolic BP	80±11	80±14	81±7	0.64
Hypertension (%)	13/42 (31%)	36%	28%	0.58
Hypercholesterolaemia (%)	11/42 (26%)	23%	33%	0.47
Diabetes (%)	0/42	0%	0%	-
Active smoker (%)	5/42 (12%)	18%	6%	0.24
Disease durations (yrs)	-	17±11	19±9	0.45
CRP ≥5 (%)	16/42 (38%)	36%	39%	0.87
ESR	24±27	22±25	28±31	0.53
RF positive (%)	29/42 (69%)	68%	67%	0.92
CCP value	151±134	122±138	181±124	0.21
DAS28-ESR	3.2±1.6	3.3±1.7	3.0±1.6	0.81

*Mean ± SD unless stated otherwise

6.3.4. CMR findings in at risk RA and newly diagnosed RA patients versus healthy controls

CMR results are shown in table 6-3. There were no statistically significant differences between groups for left ventricular ejection fraction (LVEF), left ventricular end diastolic volume (LVEDV), LVEDV indexed to body surface area (BSA), right ventricular ejection fraction (RVEF) or left ventricular (LV) mass. LV mass indexed to BSA was significantly reduced between groups (p=0.03).

Table 6-3 CMR findings (healthy controls, at risk RA and newly diagnosed RA patients)

Variable*	**Healthy controls (n=30)**	**At risk RA (n=18)**	**Newly diagnosed RA (n=81)**	**p value (between groups)**
LVEF (%)	62±5	62±4	61±6	0.42
LVEDV (ml)	146±25	155±23	148±33	0.61
LVEDVi (ml/m^2)	78±10	83±12	80±13	0.47
RVEF (%)	54±7	55±6	54±5	0.76
LV Mass (g)	91±18	87±24	81±23	0.10
LVMi (g/m^2)	49±8	46±10	44±9	**0.03**
Distensibility ($10^{-3}mmHg^{-1}$)	4.9±2.1	3.6±1.4	3.4±1.5	**<0.001**
Radial strain (%)	-8.1±3.6	-6.4±2.9	-6.4±2.8	**0.04**
Circumferential strain (%)	10.3±5.4	7.7±3.9	7.2±4.8	**0.01**
Ratio of radial to circumferential strain	-0.81±0.07	-0.86±0.05	-0.84±0.19	0.61

*Mean ± SD unless stated otherwise

Mean (SD) aortic distensibility (figure 6-2 on following page) was 4.9±2.1 in healthy controls, 3.6±1.4 in at risk RA individuals and 3.4±1.5 x 10^{-3}mmHg^{-1} in newly diagnosed RA. Aortic distensibility in at risk RA individuals (p= 0.02) as well as early RA patients (p=<0.001) was significantly lower than in healthy controls, with no significant difference between at risk RA individuals and early RA patients (p=0.54).

Radial strain (figure 6-2 on following page) was -8.1±3.6 in healthy controls, -6.4±2.9 in at risk RA individuals and -6.4±2.9% in early RA patients. Radial strain was significantly lower in early RA versus healthy controls (p= 0.01) with no significant difference between at risk RA individuals and early RA patients (p=0.91).

Circumferential strain (figure 6-2 on following page) was 10.3±5.4 in healthy controls, 7.7±3.9 in at risk RA individuals and 7.2±4.8% in early RA. Circumferential strain was significantly reduced in early RA versus healthy controls (p=0.004) with no significant difference between at risk RA individuals and early RA patients (p=0.75).

Figure 6-2 Measures of aortic stiffness in controls, at risk RA and early RA

Panel A: aortic distensibility. Panel B: radial strain. Panel C: circumferential strain. p values shown in legend below box and whisker charts.

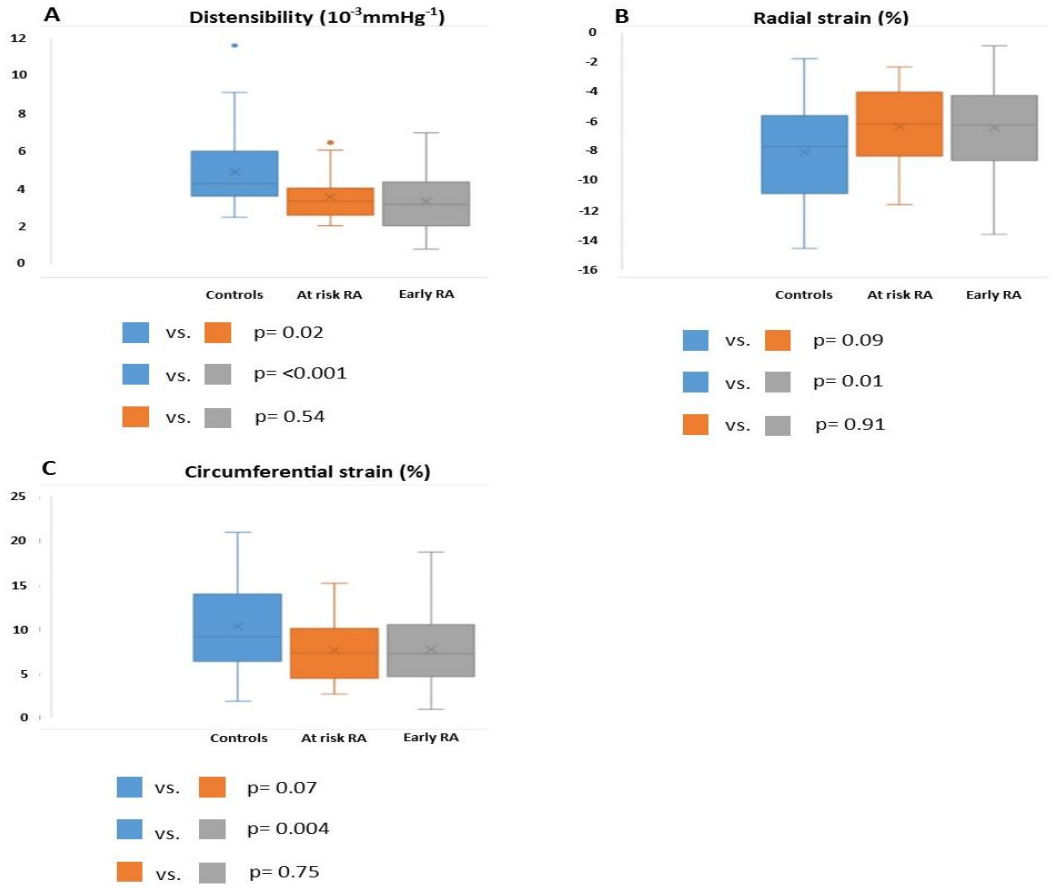

6.3.5. CMR findings in Established RA

CMR findings in established RA are summarised in table 6-4. Circumferential strain (5.7±3.0 vs. 6.7±2.6% p=0.29), radial strain (-4.9±2.4 vs. -5.7±2.0%,p= 0.27) and ratio of radial to circumferential strain (-0.89±0.05 vs. -0.87±0.04, p=0.22) were all lower in patients with carotid plaque versus those without, however, this was not statistically significant (table 6-4). Aortic distensibility was similar in patients with and without carotid plaque (2.6±1.4 vs. 2.7±1.2 x 10^{-3}mmHg^{-1}, p=0.89).

The ability of aortic distensibility, radial and circumferential strain and ratio of radial to circumferential strain to correctly identify the presence of atherosclerotic carotid plaque disease was assessed with ROC analysis (table 6-5 on following page). All strain parameters were mildly effective in correctly identifying plaque, however, no single variable or a combination of 3 strain variables reached statistical significance.

Table 6-4 CMR Findings in Established RA

Variable*	**All established RA patients (n=40)**	**Carotid plaque present (n= 22)**	**Carotid plaque absent (n=18)**	**p value**
LVEF (%)	60±5	-	-	-
LVEDV (ml)	143±30	-	-	-
LVEDVi (ml/m2)	80±15	-	-	-
RVEF (%)	58±6	-	-	-
LV Mass (g)	64±22	-	-	-
LVMi (g/m2)	36±12	-	-	-
Distensibility	2.6±1.3	2.6±1.4	2.7±1.2	0.89
Radial strain	-5.1±2.4	-4.9±2.4	-5.7±2.0	0.27
Circumferential strain	6.1±2.9	5.7±3.0	6.7±2.6	0.29
Ratio of radial to circumferential strain	-0.88±0.04	-0.89±0.05	-0.87±0.04	0.22

*Mean ± SD unless stated otherwise

Table 6-5 Accuracy of CMR measures of vascular performance in identifying presence of carotid atherosclerotic plaque

Vascular performance measure	AUC median (95% C.I.)	p value
Distensibility	0.530 (0.349-0.712)	0.74
Radial strain	0.601 (0.288-0.778)	0.28
Circumferential strain	0.604 (0.427-0.780)	0.27
Ratio of radial to circumferential strain	0.601 (0.423-0.779)	0.28
Combination of 3 strain variables	0.611 (0.434-0.788)	0.23

6.4. Discussion

In this study, we assessed the use of a novel, CMR-FT derived measure of aortic radial and circumferential strain, as well as aortic distensibility in healthy controls, individuals at risk of RA, newly diagnosed, treatment naive RA and established RA patients with and without carotid atherosclerotic plaque.

We have demonstrated 3 key findings. Firstly, measurement of aortic radial and circumferential strain by CMR-FT is both technically feasible and is able to detect abnormalities in arterial stiffness at different time points in the RA disease continuum. Secondly, perhaps most significantly, we have demonstrated increased arterial stiffness in individuals at risk of developing RA compared with controls, which is similar in magnitude to that seen in newly diagnosed, treatment naïve RA. Thirdly, we have shown a weak association between reduced aortic strain values by CMR and the presence of atherosclerotic carotid plaque.

Measurement of aortic radial and circumferential strain by CMR-FT was technically feasible in a high proportion of patients; 162/169 (96%) of all patients included in this study. In the small number of patients where this was not possible, this was due to flow artefact on the cine acquisition. This meant that the endothelial border of the aorta was obscured throughout the systolic phase and the computer software tracked image artefact in preference, leading to abnormal appearances of the strain curve and erroneously high strain values. Flow artefact is relatively common on CMR cine acquisitions where high velocity blood flow occurs within the imaging slice and is more prevalent at 3.0T(19). Image degradation from flow artefact can

almost always be overcome, by altering the phase-encoding direction of the acquisition and by carefully ‘shimming’ over the area of interest to ensure homogeneity of the magnetic field.

To our knowledge this is the first study showing subclinical aortic stiffness amongst individuals with raised ACPA and non-specific musculoskeletal symptoms deemed ‘at risk’ of developing RA. Although our sample size was small, aortic distensibility was significantly reduced versus healthy controls and close to the values seen in newly diagnosed, treatment naïve RA. This was somewhat surprising given mean predicted absolute risk of at risk patients developing RA was 46% and may imply a role of ACPA-mediated arteriosclerosis predating synovitis and a clinical diagnosis of RA. One previous study has shown both the presence of ACPAs within atherosclerotic plaque, as well as an association between some ACPAs and computerised tomography detected atherosclerotic plaque burden in female patients with RA(233).

The apparent aortic stiffness in at risk RA individuals we have demonstrated may represent the earliest indication of a process culminating in accelerated atherosclerotic plaque formation, though our findings need to be confirmed in larger and, ideally, longitudinal studies to assess changes in aortic stiffness of time in these individuals. Specifically, such studies should include appropriate negative controls (i.e. proven ACPA negative controls as well as ACPA positive but no musculoskeletal symptom controls) and evaluate and compare CV changes in patients ultimately progressing (or not progressing) to a clinical diagnosis of RA.

The finding of a high proportion of patients with evidence of atherosclerotic plaque formation in the cohort of established RA patients (55%) was in line with previous ultrasound studies (234, 235). Although CMR-FT measures of radial and circumferential strain as well as the ratio of these two values showed a weak predictive accuracy in assessing the presence of atherosclerotic carotid plaque, this did not reach statistical significance. Furthermore, aortic distensibility showed an even lower predictive accuracy in assessing the presence of atherosclerotic carotid plaque. A limited ability of both aortic strain and distensibility in distinguishing between patients with and without carotid plaque may reflect that aortic stiffness increases and plateaus due to endothelial dysfunction and arteriosclerosis and subsequently does not increase further once atherosclerotic plaque forms. Translating this to its potential utility in CVD risk assessment in RA, this may mean that measures of aortic stiffness are most useful in identifying patients at

heightened CVD risk earlier in the disease course, but may not separate out those at the very highest risk much later in the disease.

6.4.1. Study limitations

Our sample size of individuals at risk of RA was low (n=18). As such, the study should really be considered as a pilot study suggesting evidence of increased aortic stiffness prior to a clinical diagnosis of rheumatoid arthritis, but not definitively proving this is the case. The same cohort included two patients with type 2 diabetes which may have been a confounding factor, although the measures of aortic stiffness aligned numerically with those of individuals without diabetes and the confidence intervals of all 3 measures of aortic stiffness were narrow in this cohort. There were high rates of smoking in both the at risk RA and early RA groups in comparison to the healthy control group. Smoking itself may be associated with raised ACPA(236), thus high rates of smoking in at risk RA individuals is unsurprising. The extent, if any, to which smoking in at risk RA individuals affected measures of aortic stiffness in this study is unclear, however, previous studies have not demonstrated any effect of chronic smoking on aortic stiffness(237).

Although the ability of descending aortic circumferential strains to correctly predict the presence of carotid atherosclerotic plaque was better than that of aortic distensibility (AUC 0.604 vs. 0.530 respectively) this predictive accuracy was weak and not statistically significant. Ideally atherosclerotic plaque imaging and strain values would also have been assessed in the same large artery (carotid or descending aorta), cine imaging of the carotid artery was not available in this study. Nevertheless our findings suggest that measures of aortic strain (as well as aortic distensibility) by CMR feature tracking is limited in its ability to correctly identify carotid artery atherosclerotic plaque.

6.5. Conclusion

CMR assessment of aortic strain is feasible and demonstrates reduced arterial stiffness in new onset RA. Aortic stiffness appears to be increased in individuals at risk of developing RA with symptoms of arthralgia and detectable ACPA, though larger scale studies are required to confirm this finding. The presence of atherosclerotic plaque in patients with established RA is a common finding

associated with current smoking status. The ability of both CMR-FT aortic strain and aortic distensibility to identify patients with carotid plaque is limited.

7. CMR Assessment of Newly Diagnosed Treatment Naïve RA Patients at Baseline and 1 Year After Randomisation to Either Etanercept & Methotrexate or Standard Therapy

7.1. Background

The pathogenesis of CVD in RA is incompletely understood and the small number of previous studies evaluating this have focussed almost exclusively on heterogeneous patient populations with established disease. It is therefore unclear as to the nature and extent of CVD in RA at the time of diagnosis, prior to treatment initiation. Furthermore, the impact of both conventional synthetic DMARD therapy (csDMARD) and modern biological disease modifying anti-rheumatic drugs (bDMARD) on the structure and function of the CV system in RA remains unknown.

Evidence from the literature supports treatment as early as possible in the course of RA. Although the rate of CV events is low in the early stages of RA, delayed diagnosis is associated with higher rates of CV events, with hypertension being the strongest independent predictor of CV events(238).

Current European League Against Rheumatism guidelines recommend that patients with newly diagnosed RA are commenced on a csDMARD therapy in combination with glucocorticoids(239). bDMARD therapy, including TNFi therapy, is recommended only if csDMARDs (usually at least 2 are tried, including methotrexate, MTX) fail to confer adequate disease control, with escalation to bDMARD particularly advised in poorer prognostic groups(239). Strategy studies comparing first-line csDMARD in a treat to target approach versus TNFi show variable results, demonstrating equivalence or superiority of first-line TNFi. Improvements in radiographic evidence of joint disease and higher rates of drug free remission have been demonstrated with bDMARD therapy as well as similar or slightly greater remission induction rates (240–242).

In addition to the role of DMARD strategies in improving the traditional aspects of RA, there is significant focus on the extent to which effective RA disease control can also improve co-morbidity, especially CVD. Long-term registry data have demonstrated a significant reduction in the incidence of acute myocardial infarction in patients receiving TNFi versus sDMARD therapy(243). For this reason, such considerations are becoming increasingly relevant in determining optimal treatment strategies in RA.

Here we report the findings of CADERA study, to our knowledge the first study to assess the extent of subclinical CVD in treatment naïve, newly diagnosed patients with no known cardiovascular disease and establish the degree of improvement following initiation of RA. This study was conducted as a bolt-on study to a phase IV, pragmatic, single-centre, open-label, randomised control trial, VEDERA. The purpose of CADERA was to assess CVD using multi-parametric CMR assessment in patients with new onset, treatment naïve RA before and 12 months after initiation of either (i) immediate TNFi (etanercept, ETN) and MTX or (ii) MTX +/- additional csDMARD in a treat to target approach with switch to delayed ETN and MTX in the event of failure to achieve clinical remission at 6 months.

7.1.1. Hypothesis and aims

We hypothesised that treatment with initial ETN-MTX would lead to improved aortic stiffness in comparison to standard RA treatment comparing aortic distensibility by CMR at baseline (pre treatment) and 1 year after commencement of treatment. We also hypothesised that other markers of subclinical disease in RA would improve following initiation of treatment for RA.

The aims were as follows:

Primary objective

- To establish whether (any) RA DMARD strategy is associated with improvement in AD over a 1 year period

Secondary objectives

To explore whether the following factors affect AD change over 1 year:

- DAS28 control (DAS28 defined clinical response/non-response)
- Therapeutic intervention (TNFi/MTX and conventional DMARD including MTX)

Aortic distensibility was chosen as the primary outcome for the study due to its dynamic nature, high reproducibility and ability to predict major CV events independently of traditional clinical risk scoring models in patients with no known CVD(244). The alternative methods for assessing vascular performance developed in Chapter 4 and tested on patient populations in Chapter 6 (aortic radial and circumferential strain) were not used on the basis they 1) offered no statistically significant benefit over AD in correctly identifying the presence of atherosclerotic plaque disease and 2) currently lack longitudinal prognostic outcome data to validate their utility as a biomarker for increased risk of CVD.

7.2. Methods

The methods used in VEDERA(245) and CADERA(166) have been published previously. Patients were recruited between February 2012 and November 2015 from a single tertiary centre, early RA Rheumatology outpatient clinic (Chapel Allerton Hospital, Leeds, UK).

The patients included in this chapter were the same treatment naïve, newly diagnosed RA patients included in chapter 6; baseline and year 1 scans were used for this chapter.

Consecutive patients diagnosed with new onset RA according to ACR/EULAR 2010 criteria(240) were invited to enrol into the VEDERA randomised control trial and parallel CADERA CVD sub-study. Inclusion criteria included no previous use of DMARD therapy, symptom duration ≤ 1 year, DAS28-ESR ≥3.2 and at least one poor prognostic factor (positive anti-citrullinated protein antibody (ACPA) +/- abnormal power Doppler in any joint). Exclusion criteria included prior DMARD therapy, contra-indications to TNFi therapy or patients considered clinically unsuitable for TNFi therapy by the treating physician. Additional exclusion criteria for CADERA included renal failure (estimated glomerular filtration rate (e-GFR) <30ml/min/1.73m^2), contra-indications to intravenous adenosine (asthma or high degree AV block), known allergy to Gadolinium-based contrast agent (GBCA), claustrophobia, weight ≥ 120kg and metallic implant/foreign body deemed unsafe to for CMR.

All patients were randomised on a 1:1 basis either to immediate Etanercept in combination with Methotrexate (ETN-MTX) or Methotrexate with or without additional csDMARD with escalation to Etanercept in patients not achieving clinical remission at week 24 T2T (treatment to target) (MTX-T2T ± ETN-MTX). Clinical remission was defined as DAS28-ESR ≥2.6(246). Clinical response was imputed using baseline DAS28 score for patients whose responder status at 24 weeks was unknown.

CMR scans were conducted at baseline (prior to the commencement of RA treatment) and 1 year after enrolment. Scans were performed on the same 3.0T system (Philips Achieva, Best, The Netherlands). The CMR protocol included left and right ventricular volumes, left ventricular mass, CMR-tagging, aortic distensibility, adenosine stress and rest first pass perfusion imaging using a dual bolus technique with intravenous infusion of 0.01 and 0.1mmol/kg Gadopentate

Dimeglumine (Magnevist, Bayer, Berlin, Germany), T1 mapping pre and post GBCA and late Gadolinium enhancement (LGE) imaging.

All post processing analysis of CMR scans was performed using the same software (CVI 42, Circle Cardiovascular Imaging Calgary, Canada). Analysis of scans was performed by two assessors (GF,BE) both with 2 years' experience in CMR reporting blinded to all patient details. LV contours were drawn manually at both end diastole and end systole on the LV short axis SSFP cine stack. LV papillary muscles were considered part of the LV cavity. Aortic distensibility was calculated according to previously described methods(181).

Statistical analysis was performed using IBM SPSS® Statistics 22.0 (IBM Corp., Armonk, New York, USA) and R version 2.14.1 (The R Foundation for Statistical Computing, Vienna, Austria).

The sample-size estimation for the primary endpoint aortic distensibility was based on previous work by Ikanomidis et al showing improved aortic distensibility in RA patients in response to interleukin-1 therapy(247). We calculated that 33 patients in each treatment group would equate to an 80% power to detect a difference in aortic distensibility between the two treatment groups at a 5% significance level. Normality of data was tested using a Shapiro-Wilk test. Mean values ± SD are reported where data are normally distributed and as median values with interquartile range where data were non-normally distributed. The primary outcome aortic distensibility was analysed using an intention-to-treat (ITT) analysis with assistance from a biostatistician (EH). The methodology for this ITT analysis is summarised in the appendix (page 158-159). Distensibility values were natural log-transformed prior to analysis. Missing data were imputed using an imputation model including numerous clinical and demographic data, allowing adjusted analyses to be performed via multiple regression (see appendix). Exploratory analyses were compared using paired t tests and Wilcoxon signed rank tests as appropriate.

7.2.1. Ethical approval:

The study was conducted according to the declaration of Helsinki with approval from the local ethics committee (National Research Ethics Committee reference: 10/H1307/138). All participants gave written informed consent to take part in the study.

7.3. Results:

A total of 81 patients were enrolled into CADERA and underwent baseline CMR scan, with 71 undergoing a 1 year CMR scan (figure 7-1). A total of 4 of the patients were withdrawn from the study; one due to treatment non-compliance and the other 3 all due to serious adverse events relating to treatment. The reasons for the remaining 7 patients not undergoing a 1 year CMR scan included refusal or claustrophobia (6 patients) and 1 patient who moved away and was not able to attend a repeat scan.

Figure 7-1 Study recruitment flowchart

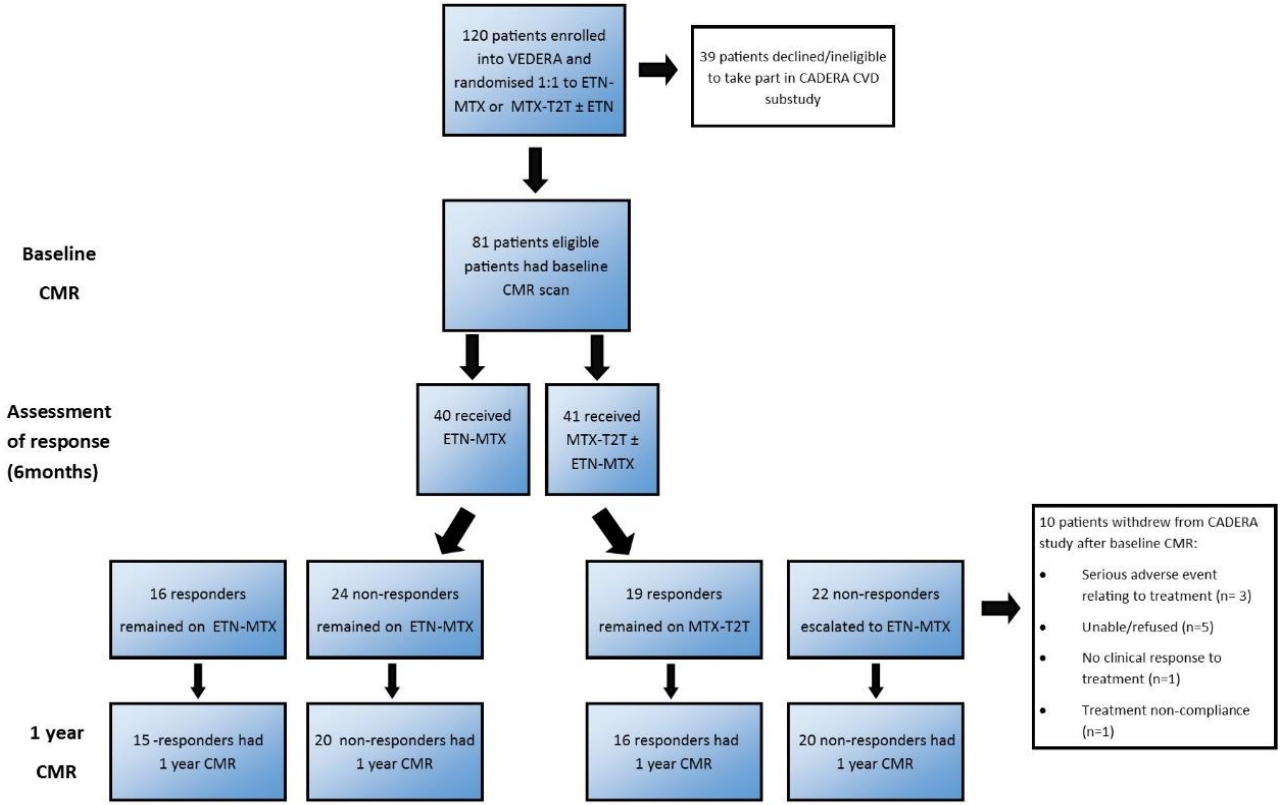

Median age of the 81 patients scanned at baseline was 51 years (IQR 39-61), 26/81 (32%) were male and mean baseline DAS28-ESR score was 5.6±1.1. All CMR studies were of diagnostic quality with interpretable data for all 81 baseline scans and 71 one year follow up scans. Patient demographics at study baseline are summarised in table 7-1 for both the whole CADERA study population and within each treatment arm. Baseline demographic data were similar across both treatment arms for all variables with the exception of median pack years of smoking.

Table 7-1 Baseline demographic data

Variable*	**All baseline CADERA (n=81)**	**ETN-MTX group (n=40)**	**MTX-T2T ±ETN-MTX group (n=41)**	**p value ETN-MTX vs. MTX-T2T ±ETN-MTX**
Male gender	26/81 (32%)	16/40 (40%)	10/41 (24%)	0.14
Age (years)	51 (39-61)	51 (39-61)	54 (38-61)	0.45
BMI (kg/m^2)	25 (23-28)	25 (23-28)	25 (23-28)	0.84
ESR	30 (18-49)	30 (18-49)	30 (20-50)	0.38
CRP	8 (0-25)	8 (0-49)	8 (1-20)	0.90
CCP positive	67/81 (83%)	32/40 (80%)	35/41 (85%)	0.53
RF positive	57/81 (70%)	26/40 (65%)	31/41 (76%)	0.30
Baseline DAS28 score	5.6±1.1	5.7±1.2	5.6±1.0	0.61
6-month DAS28 score	3.3±1.5	3.1±1.6	3.5±1.4	0.34
Hypertension	6/81 (7%)	1/40 (3%)	5/41 (12%)	0.10
Hypercholesterolaemia	2/81 (3%)	0/40	2/41 (5%)	0.16
Diabetes	0/81	0/40	0/41	-
Family history IHD	7/81 (9%)	2/40 (5%)	5/41 (12%)	0.26
Current smoker	17/81 (21%)	6/40 (15%)	11/41 (27%)	0.20
Ex smoker	28/81 (35%)	12/40 (30%)	16/41 (39%)	0.40
Pack years smoking	2 (0-11)	0 (0-6)	4 (0-20)	**0.03**

*Mean ± SD or median (IQR) unless stated otherwise

7.3.1. Primary objective (aortic distensibility)

At 1 year in the combined treatment groups (n=81) there was an increase in aortic distensibility of 19.6% (geometric mean ratio 1.196 CI 1.08, 1.324) which was highly statistically significant; p<0.001.

An intention-to-treat analysis was performed to assess change in aortic distensibility between baseline and 1-year CMR which is displayed in table 7-2 and figure 7-2 on the following pages.

Treatment groups were defined as follows:

- Group 1: First line ETN-MTX
- Group 2: First-line MTX-T2T ± ETN-MTX

Treatment subgroups were defined as follows:

- Group 1a: First line ETN-MTX responders (24-wk DAS28-ESR ≥2.6)
- Group 1b: First line ETN-MTX non-responders (24-wk DAS-ESR <2.6)
- Group 2a: First line MTX-T2T responders remaining on MTX-T2T (24-wk DAS28-ESR ≥2.6)
- Group 2b: First line MTX-T2T non-responders escalating to ETN-MTX (24-wk DAS-ESR <2.6)

Table 7-2 Differences between treatment groups and subgroups, either adjusted for 24-week DAS28-ESR or additionally adjusted for age/sex

Comparison		Geometric mean (unadjusted)		Ratio (95% CI), *P* value		
				Unadjusted	Adjusted 1 *	Adjusted 2 **
Group 1 (n=40)	Group 2 (n=41)	3.77	3.40	0.90 (0.69, 1.17), p=0.436	n/a	0.89 (0.71, 1.12), p=0.311
Group 1a (n=16)	Group 2a (n=19)	3.31	2.91	0.88 (0.58, 1.34), p=0.537	n/a	0.82 (0.58, 1.15), p=0.234
Combined groups 1b + 2b (n=46)	Combined groups 1a + 2a (n=35)	4.00	3.09	0.77 (0.59, 1.00), p=0.050	0.69 (0.48, 0.98), p=0.040	0.76 (0.55, 1.05), p=0.095
Group 2b (n=22)	Group 2a (n=19)	3.88	2.91	0.75 (0.51, 1.10), p=0.138	0.67 (0.40, 1.10), p=0.106	0.76 (0.48, 1.21), p=0.239
Combined Group 1 + 2b (all ETN-MTX patients) (n=62)	Group 2a (n=19)	3.81	2.91	0.76 (0.56, 1.04), p=0.086	0.76 (0.55, 1.06), p=0.106	0.78 (0.59, 1.03), p=0.075

*Adjusted 1: Adjusted for 24-week DAS28-ESR

*Adjusted 2: Adjusted for age and sex (±DAS28-ESR as appropriate)

The results were unchanged when adjusted for baseline aortic distensibility

Figure 7-2 1 year aortic distensibility in responders and non-responders to first-line ETN and to standard therapy +/- delayed ETN

Box and whisker plot of aortic distensibility across treatment groups. The horizontal line within the box represents the median value, the bottom line of the box represents the 25th centile and the top of the box the 75th centile. The narrower 'whiskers' above and below the box represent the 95% confidence interval.

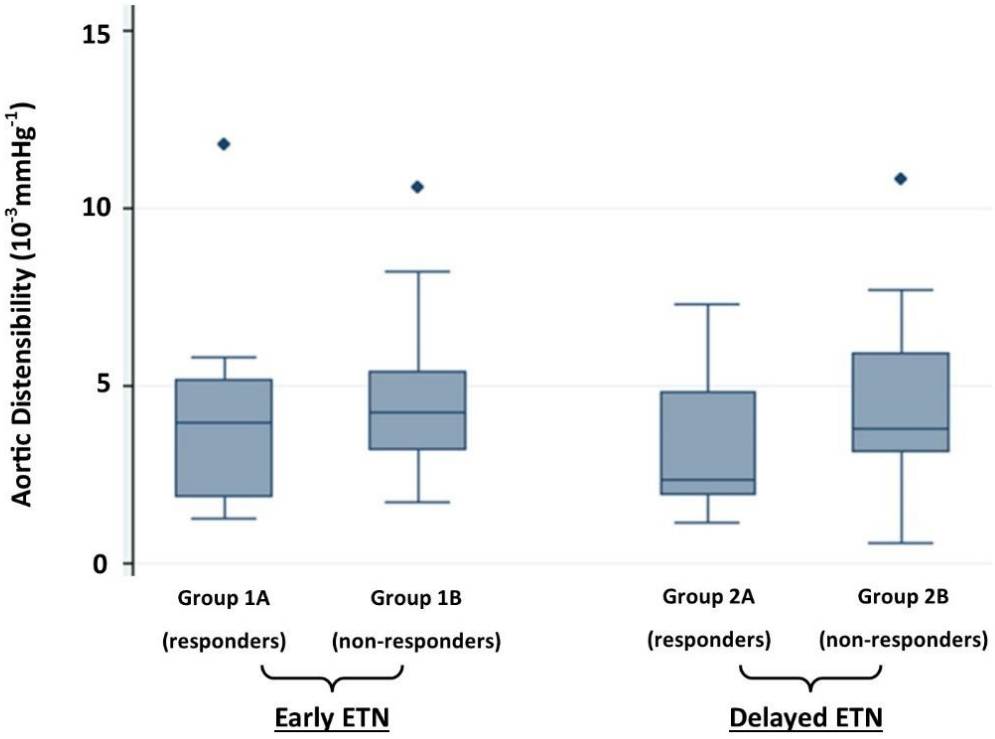

7.3.2. Secondary outcome measures

A number of other exploratory CMR markers of subclinical CVD were assessed in patients before and after initiating RA treatment (table 7-3 on following page) . These parameters included LV and RV volumes, ejection fraction and mass, LV deformation indices (S', torsion and twist), myocardial native T1, myocardial extra cellular volume fraction and late Gadolinium enhancement (LGE). Myocardial perfusion will findings will be presented elsewhere.

Absolute LV mass (74 (IQR 63-96g) pre-treatment versus 79 (IQR 66-98g) post treatment, p =<0.001) as well as LV mass indexed to body surface area (42 (IQR 38-48g/m^2) pre-treatment versus 44 (IQR 38-50g/m^2) , p = 0.002) increased 1 year after commencing treatment in all patients, but did not differ significantly between treatment groups.

No other parameters showed any statistically significant differences either in all patients following treatment, or between the 2 treatment arms. LV S' (a measure of longitudinal LV systolic function) at 1 year was numerically higher in patients who received immediate Etanercept (1.15 (IQR 1.08-1.24) versus 1.12 (IQR 1.04-1.23) respectively, p= 0.18. Native myocardial T1 (a measure of myocardial composition) was numerically lower in patients who received immediate Etanercept (1178 ± 69 versus 1198 ± 55 respectively, p= 0.18).

Table 7-3 Secondary Outcomes Before and After Treatment

Parameter*	All patients baseline (n=71)	All patients 1 year (n=71)	p value (baseline vs. 1 year)	Immediate Etanercept at 1 year (n=35)	Delayed Etanercept at 1 year (n=36)	p value (Immediate vs. delayed)
LVEDV	148 ± 31	149 ± 31	0.46	149 ± 28	149 ± 34	0.96
LVEDV (indexed to BSA)	80 ± 12	80 ± 12	0.66	80 ± 12	81 ± 12	0.70
LVEF (%)	60 (58-65)	61 (58-64)	0.47	61 (55-63)	62 (59-65)	0.13
LV Mass (g)	74 (63-96)	79 (66-98)	**0.001**	77 (69-96)	82 (62-104)	0.99
LV Mass indexed to BSA	42 (38-48)	44 (38-50)	**0.002**	43 (38-49)	44 (38-54)	0.67
RVEF (%)	54 ± 5	55 ± 6	0.37	54 ± 6	55 ± 6	0.48
S' (s^{-1})	1.16 (1.06-1.25)	1.13 (1.07-1.23)	0.61	1.15 (1.08-1.24)	1.12 (1.04-1.23)	0.18
Peak twist (degrees)	15.4 ± 3.5	15.4 ± 3.8	0.85	15.5 ± 4.0	15.3 ± 3.7	0.80
Peak torsion (degrees)	13.7 ± 3.1	13.2 ± 3.2	0.26	13.4 ± 3.3	13.1 ± 3.2	0.67
Native myocardial T1 (ms)	1183 ± 42	1188 ± 62	0.46	1178 ± 69	1198 ± 55	0.18
Myocardial ECV (%)	27 ± 4	27 ± 3	0.06	26 ± 3	27 ± 3	0.74

*Mean ± SD or median (IQR) unless stated otherwise

7.3.3. Patterns of late gadolinium enhancement

A total of 10/71 patients (14%) showed evidence of abnormal hyperenhancement on LGE imaging either at baseline, 1 year CMR or both (patterns of LGE are shown in figure 7-3). All were non-infarct patterns. The majority (8/10) affected the mid-wall mid inferior RV insertion point and were either focal (7/8) or patchy (1/8). The remaining patterns seen were linear, mid wall hyperenhancement of the mid antero/inferoseptum (1/10) and patchy midwall hyperenhancement of basal inferolateral segment (1/10).

Figure 7-3 Patterns of LGE in RA

Panel A shows the most common inferior RV insertion point pattern, panel B shows linear septal LGE and panel C shows patchy lateral midwall LGE

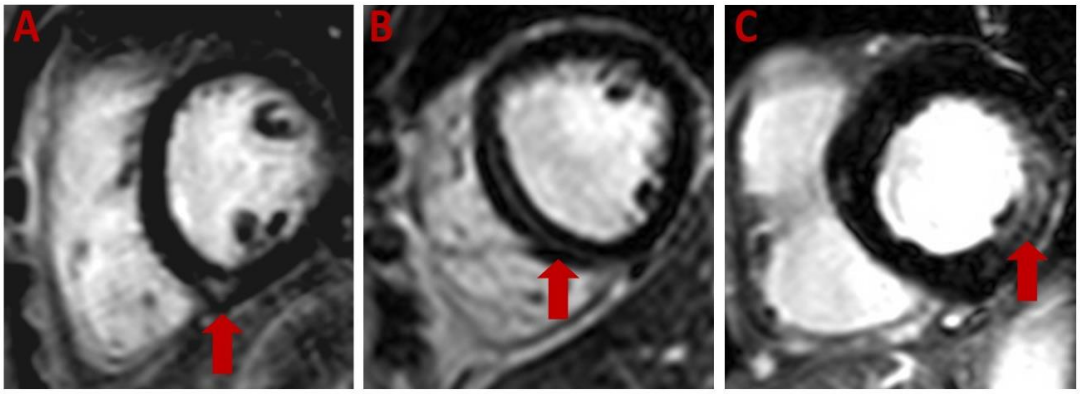

7.4. Discussion

This prospectively conducted single-centre randomised control trial is, to our knowledge, the first to assess the impact of modern DMARD therapy on CMR markers of subclinical CVD in patients with newly-diagnosed, treatment naïve RA and no prior history of CVD. Unlike previous non-invasive imaging studies of RA patients which have been limited by their inclusion of heterogeneous patient populations with established RA and/or patients with known cardiovascular disease,

this study excluded patients with established RA, those previously treated with DMARDs as well as known cardiovascular disease.

We have demonstrated that aortic distensibility, a measure of aortic stiffness and surrogate marker for increased risk of CVD, improves markedly after initiation of RA treatment in those treated with either first-line ETN-MTX or first line MTX-T2T ± ETN-MTX. We have also shown a clear signal that ETN-MTX provides additional benefit over and above standard therapy with evidence of greater improvements in aortic stiffness which persist after adjustment for disease activity score. Of note, 25% difference was observed between first-line standard therapy non-responders (that received delayed ETN) to responders and similarly between all receiving ETN (first-line and delayed) and first-line standard therapy responders.

Lastly, we have demonstrated an increase in LV mass following treatment for RA in those treated with either first-line ETN-MTX or first line MTX-T2T ± ETN-MTX. Other markers of subclinical CVD including LV strain indices, ECV and native myocardial T1 relaxation time do not differ significantly after with treatment.

7.4.1. Aortic stiffness in RA

In recent years, greater understanding has been gained of the contribution of age-related stiffening of larger arteries to the development of heart disease, CV events and microvascular disease of the major organs; collectively termed the ageing vascular continuum(223). RA is thought to accelerate this process, initially through increased vascular tone and subsequently via development of atherosclerotic plaque(147).

A number of previous studies have demonstrated reduced aortic stiffness using a variety of non-invasive imaging techniques in patients with established RA. Provan et al. showed in a cross-sectional study that RA patients in clinical remission had lower augmentation index values than patients with active RA(225). More recently, Ikdahl et al. demonstrated that high augmentation index and aortic pulse wave velocity values were predictive of CV events in 138 patients over a 6-year follow-up period(248). Our own results are the first to demonstrate improvements in aortic stiffness following treatment initiation in a treatment naïve RA cohort. Importantly, treatment with ETN-MTX (whether as first or second line therapy) appears to provide additional benefit over standard therapy. This was evidenced by comparison of all first-line ETN-MTX (group 1) and all first line MTX-T2T ± ETN-MTX (group 2) which showed a numerical improvement in favour of first line ETN-

MTX. Comparison of first-line MTX-T2T non-responders who received ETN-MTX (group 2b) versus first line MTX-T2T responders (group 2a) who did not, showed a substantial (25%) improvement in aortic distensibility in favour of ETN-MTX. Lastly, comparison of all patients receiving ETN-MTX at any stage (groups 1+2b) with first-line MTX-T2T responders (group 2a) showed a similar 24% improvement in aortic distensibility in favour of ETN-MTX.

7.4.2. LV mass and LGE in RA

We have demonstrated in this study an apparent increase in LV mass and LV mass indexed to body surface area following RA treatment (irrespective of treatment arm). Table 6-3 in the preceding chapter demonstrates that LV mass was reduced in at the time of diagnosis in patients with early RA, thus this increase actually reflects a shift towards normalisation of LV mass in response to RA treatment initiation. As such, this normalisation of LV mass is likely to indicate a degree of recovery and positive LV remodelling in response to RA treatment rather than an indication of deleterious effects of RA treatment.

Reduced LV mass when comparing RA patients to healthy controls has been reported in other studies assessing established RA (167, 171) although its cause is unclear. Experimental animal models have shown LV dilatation and systolic impairment, coupled with LV wall thinning(249) and myocardial collagen deposition in response to elevated TNF-α(250) thus LV remodelling may be a direct effect of TNF-α. A second plausible explanation could be that reduced LV myocardial mass relates to the phenomenon of ‘rheumatoid cachexia’ which is linked to a combination of inflammation and reduced physical activity in RA patients. A high proportion of RA patients exhibit rheumatoid cachexia, which manifests as reduced skeletal muscle mass in combination with increased fat mass(251) and such individuals may have poorer CV outcomes. It is possible that the reduction in muscle mass extends beyond skeletal muscle to involve the myocardium in patients with rheumatoid cachexia.

Our finding of a sizeable proportion of RA patients (14%) with non-ischaemic abnormal LGE corresponds broadly to those of Ntusi et al. who assessed 39 established RA patients using multi-parametric CMR and found focal, predominantly non-ischaemic LGE in 46% of RA patients. The lower rates we have reported are likely related to the much shorter disease duration in our study population. The cause of LGE in RA possibly reflects active or previous myocarditis which is a widely reported finding in RA(125).

7.4.3. Study Limitations

It is important to acknowledge that our analyses of aortic distensibility across treatment group and subgroups are exploratory in nature, in line with the study design and the absence of comparable previous study data. Therefore, although aortic distensibility values across these groups and subgroups have been assigned 'p values' (that did not reach conventional statistical significance levels), we would highlight that p-values are in reality not suitable in an exploratory analysis of pilot study data such as these(252), thus we feel the appropriate interpretation is of a signal whereby ETN-MTX *appears* to confer a benefit over standard therapy. We did not detect any significant differences in measures of LV systolic function (LVEF, LV S', LV twist and LV torsion) following treatment in all patients and between treatment groups. Similarly we did not detect any differences in myocardial T1 and ECV. Possible reasons for this include our sample size and, secondly, that our study population involved patients with newly diagnosed RA. Significant changes in these parameters may occur later in the course of the disease, a factor which should be addressed in part by the planned 2-year follow up scan which will be conducted and reported as part of the CADERA study protocol.

7.5. Conclusion

Aortic distensibility, a measure of aortic stiffness and surrogate marker of increased risk of CV disease is decreased in treatment naïve, newly diagnosed RA and improves markedly with initiation of RA therapy. Treatment with Etanercept in combination with Methotrexate (whether first or second-line) appears to confer additional benefit in terms of improvement in aortic stiffness above standard therapy.

8. Discussion

Cardiovascular disease remains a major cause of morbidity and mortality in the 21st century and improving its diagnosis in treatments constitutes a worldwide health priority. As non-invasive cardiovascular imaging improves and evolves, this allows insights to be gained into mechanisms by which cardiovascular diseases occur and progress. Furthermore, this offers the opportunity to detect disease before symptoms occur, potentially mitigating serious late complications of that disease.

The overarching aim of this thesis was to explore and refine the utility of both existing and emerging cardiovascular magnetic resonance imaging techniques in the context of subclinical cardiovascular disease, with a particular emphasis on both prior myocardial infarction and rheumatoid arthritis. Cardiovascular magnetic resonance imaging is ideally suited to this aspect of exploratory cardiovascular research on the basis of its lack of use of non-ionising radiation and inherently quantitative nature which vastly reduces subjectivity of assessment and allows reproducible comparison of studies across patient groups.

Chapters 3 and 4 were CMR methods development chapters aiming to improve upon and refine existing techniques in CMR suitable in the assessment of subclinical CV disease in cardiomyopathy evaluation (chapter 3) and assessment of aortic stiffness (a potential biomarker of heightened cardiovascular risk) in chapter 4.

Chapters 5 and 6 aimed to apply quantitative CMR parameters to subclinical disease states (myocardial infarction and across a spectrum of time points in the disease course of rheumatoid arthritis respectively) and assess their usefulness in the detection of these disease states.

Lastly, chapter 7 assessed the relative impact of two different rheumatoid arthritis treatment strategies on subclinical CMR markers of subclinical cardiovascular disease.

8.1. Discussion, study limitations and future directions relating to chapter 3

Chapter 3 “Methodology for the development of ‘synthetic’ extracellular volume fraction at 1.5T and 3.0T” aimed to assess whether a patient’s blood pool native T1 value could be used to approximate blood haematocrit and thereby used to derive their ‘synthetic’ myocardial ECV value. The potential benefit in doing so was to

remove the time, cost and inconvenience associated with obtaining a venous haematocrit value which has clear benefits in terms of workflow in both the research and clinical setting. This was the first study to demonstrate a high correlation of synthetic and laboratory ECV at 3.0T and also validated the technique for the first time on a 1.5T Philips system. This finding potentially broadens the applicability of the technique across vendors and field strengths and may be of particular benefit in the research arena in the generation of immediate 'in-line' ECV maps and, in the clinical setting, of reducing the expense and time associated with obtaining a haematocrit sample. Furthermore, the study showed good correlation between 1.5T laboratory and synthetic ECV values derived using our own equation and values derived using an equation from a previous study using a Siemens MOLLI pulse sequence(188). The potential significance of this finding is that the equations generated in this study may be interchangeable across vendors- potentially meaning that they could be used by other centres without the need for them to derive their own linear regression equations using a derivation cohort on their own scanner, though some negative bias in ECV was demonstrated.

There were some limitations in the study; primarily that the native blood bool T1 and venous haematocrit was only moderately correlated at both field strengths, with a suggestion that values at both low and high extreme values were more prone to inaccuracy than those closer to the mean. Nevertheless, this did not appear to affect overall laboratory and synthetic ECV correlation- likely in part due to the relatively low contribution of haematocrit component of the ECV equation and the relatively low proportion of patients with these extreme values in our study. Although this study showed a good correlation between alternative vendor synthetic ECV equations with laboratory derived ECV at 1.5T, this was not assessed at 3.0T and therefore it is not known whether the 3.0T synthetic ECV equation reported in this study could be used across an alternative vendor.

We speculate that this technique will prove useful in the clinical and research arena as a valid alternative to obtaining laboratory venous haematocrit. Key future directions for this technique include the assessment of influences such as pulse sequence (MOLLI, ShMOLLI, SASHA) on the accuracy of blood pool derived haematocrit estimation. In order to refine the technique further, future studies in this area may also assess the influence of taking the native T1 blood pool measurement from alternative sites such as the left or right atrium, as well as the influence of heart rate, age and patient gender. Lastly, the issue of whether these equations are suitable to be used in other centres on alternative vendor platforms,

or whether equations should be derived independently on each scanner should be explored.

8.2. Discussion, study limitations and future directions relating to chapter 4

Chapter 4 “Methodology for the development of aortic and circumferential strain analysis using CMR feature tracking” was another methods development chapter aimed at improving upon existing CMR assessment of aortic stiffness in subclinical cardiovascular disease. This sought to assess the feasibility and reproducibility of measuring radial and circumferential aortic strain (as an indicator of aortic stiffness) in healthy volunteers by applying CMR feature tracking as a post-processing software technique to short axis cine acquisitions of the ascending and descending aorta. This study was the first to develop and assess this technique for measuring aortic stiffness using CMR and demonstrated that the technique was feasible- reliably producing systolic strain curves in healthy volunteers with an acceptably short analysis time. Reproducibility (interstudy, interobserver and intraobserver reproducibility were assessed) of descending aortic strain (both radial and circumferential) was excellent and good for ascending aortic strain. The significance of demonstrating this feasibility and reproducibility of aortic radial and circumferential strain was that other studies using speckle tracking echocardiography have shown a correlation of circumferential strain with atherosclerotic plaque in coronary arteries(228). This presents the opportunity of exploring the potential of CMR aortic strain assessment to identify individuals at the highest risk of developing cardiovascular disease and consequently to target preventative therapies at such individuals.

Limitations to this study were primarily its low number of subjects and narrow age range of subjects, such that the values generated could not be considered as a normal reference range for aortic strain values. Other post-processing software for the measurement of CMR-feature tracking is available and the agreement between values across software vendors was not assessed in this study. Furthermore, the strain values generated in this study were not validated against a reference standard technique such as speckle tracking echocardiography to demonstrate their validity.

Future directions in this area of research should include the publication of reference values for aortic strain by CMR feature tracking, as well as validating the technique

against speckle tracking echocardiography. Crucially, the ability of (if any) of aortic strain values to predict the incidence of cardiovascular events as well as their relative performance against conventional risk scores such as Framingham and Q-Risk(125) should also be assessed, particularly as these are based upon incident cardiovascular events amongst general populations and are prone to inaccuracy in specific high risk patient populations such as rheumatoid arthritis where cardiovascular risk is frequently underestimated. The validity of descending aortic strain by CMR feature tracking was partly tested in a later chapter, chapter 6 "Assessment of Large Artery Involvement in Rheumatoid Arthritis Over Time: Prior to Diagnosis, at Diagnosis and in Established Disease" in terms of its ability to detect aortic stiffness in patients with Rheumatoid arthritis versus healthy controls as well as its ability to identify patients at the highest risk of cardiovascular events in a cohort of rheumatoid arthritis patients with proven carotid atherosclerotic plaque disease. This further validation is vital if the technique is to become more widely adopted.

8.3. Discussion, study limitations and future directions relating to chapter 5

Chapter 5 "The utility of global longitudinal strain in the identification of prior myocardial infarction in patients with preserved left ventricular ejection fraction" aimed to assess the ability of longitudinal strain parameters (including global longitudinal strain as well as global longitudinal strain rate and early diastolic strain rate) to predict the presence of prior myocardial infarction in patients with and without CMR evidence of subendocardial late gadolinium enhancement consistent with myocardial infarction. Prior myocardial infarction is prevalent in certain high risk patient populations(197) and associated with worse cardiovascular outcomes. Importantly, prior myocardial infarction may be subclinical i.e. present without a patient having presented with classical symptoms of myocardial infarction and therefore such patients may benefit from secondary prevention medications and/or further investigations or consideration for coronary revascularisation. Conventionally, prior myocardial infarction is suspected on left ventricular assessment by echocardiography (or CMR) when abnormalities in LV radial function are seen; either in terms of reduced LV ejection fraction, hypokinesis or akinesis in 2 or more contiguous LV segments (regional wall motion abnormality) or both. However, reliance on such measures of LV radial function alone is insufficient

to exclude prior myocardial infarction as this may be present went these features are absent.

In this study, we demonstrated that global longitudinal strain (as well as global longitudinal strain rate and early diastolic strain rate) are reduced in individuals with prior myocardial infarction as compared with healthy volunteers. The overall ability of global longitudinal strain to correctly identify prior myocardial infarction was found to be modest (AUC 0.662, sensitivity 60%, specificity 72.5%). The findings of this study highlight the limitations of radial strain assessment in the context of ischaemic heart disease and demonstrate an ability of global longitudinal strain to potentially 'flag up' patients who may have prior myocardial infarction in spite of 'preserved' LV ejection fraction. Although this study used CMR feature tracking to assess global longitudinal strain, this measurement can be made using other modalities such as echocardiography. This is important as not all patients undergo CMR examination in the routine assessment of LV function and not all patients who undergo CMR examination are suitable for gadolinium contrast.

There were a number of limitations to this study. Firstly, GLS is by no means perfect in identifying prior MI in individuals with preserved LV ejection fraction; a normal GLS does not reliably exclude prior MI and a low GLS does not always imply prior MI. Secondly, the contribution of cardiovascular risk factors such as hypertension, hypercholesterolaemia, smoking and diabetes was not assessed in this study, although multivariable analysis showed that none of these variable were independent predictors of GLS whereas prior MI was, suggesting the presence of prior MI rather than these risk factors was responsible for lower GLS in individuals with prior MI.

Future directions in this area of research should seek to build on the findings of this study. Although GLS alone exhibits a modest ability to predict the presence of prior MI, a combination of other quantitative non-invasive imaging parameters such as regional/segmental strain indices or native myocardial T1 values and/or clinical parameters such as presence of cardiovascular risk factors or ECG evidence of Q waves may help to refine and improve upon the detection of prior MI in high risk patient groups. Further areas of research include the validation of GLS by feature tracking across post-processing software vendors as well as across non-invasive imaging vendors. Lastly the validation of GLS in this cohort of patients with prior myocardial infarction in terms of long-term prognostication should be assessed and compared against more established quantitative parameters such as LV ejection fraction to determine with GLS offers improved prognostication.

8.4. Discussion, study limitations and future directions relating to chapter 6

Chapter 6 “Assessment of Large Artery Involvement in Rheumatoid Arthritis Over Time: Prior to Diagnosis, at Diagnosis and in Established Disease” served 2 main purposes. The first was to identify whether subclinical evidence of aortic stiffness (a surrogate marker of increased risk of future cardiovascular disease) assessed by CMR and including descending aortic strain developed in chapter 4 was present in different stages of the rheumatoid arthritis continuum; in newly diagnosed disease as well as patients without clinical evidence but at high risk of developing rheumatoid arthritis. The second purpose was to assess whether CMR measures of aortic stiffness (again including the descending aortic strain method developed in chapter 4) was able to identify the presence of atherosclerotic plaque disease detected by CMR in a cohort of patients with well-established rheumatoid arthritis. Rheumatoid arthritis patients are at high risk of developing CV disease and are three times more likely to have had either an acute MI or unrecognised MI in the two years preceding formal diagnosis than age and sex matched individuals without RA(121). Diagnosis of RA can only made once a patient develops symptoms and presents for assessment by a healthcare professional. Perhaps unsurprisingly then, a subclinical autoimmune phase is described lasting months or in some cases years, where a patient is largely asymptomatic but has autoimmune abnormalities in the form of positive anti-cyclic-citrullinated peptide (ACPA), a highly specific serological marker for RA(226). Having developed and assessed the reproducibility and feasibility of CMR feature tracking assessment of descending aortic radial and circumferential strain in chapter 4, it was validated in this chapter in terms of its ability to detect subclinical aortic stiffness in rheumatoid arthritis and individuals at risk of rheumatoid arthritis versus healthy controls and directly compared with aortic distensibility, a more established method of assessing aortic stiffness using CMR. Carotid artery circumferential strain has been shown to correlate with coronary artery atherosclerotic plaque, thus we hypothesised that circumferential descending aortic strain in particular may demonstrate an ability to correctly identify CMR carotid plaque (a potential marker of high risk for future CV events) in established RA patients.

Our finding of increased arterial stiffness in individuals at risk of developing RA compared with controls, similar in magnitude to that seen in newly diagnosed, treatment naïve RA is, to the best of our knowledge, the first time this has been reported. This may be the first indication that subclinical arterial stiffening occurs

(and is detectable using non-invasive imaging) much earlier than has previously been demonstrated and potentially shifts research and clinical priority further towards an emphasis on much earlier diagnosis and treatment of RA with the intention of reducing cardiovascular events later in the disease course. In this study, we also demonstrated a weak association between reduced aortic strain values by CMR and the presence of CMR detected atherosclerotic carotid plaque in patients with established RA.

The study had a number of limitations. The first of these was that the sample size of individuals at risk of RA (n=18) was low. As such, the study should really be considered as a pilot study suggesting evidence of increased aortic stiffness prior to a clinical diagnosis of rheumatoid arthritis, but not definitively proving this is the case. Additionally, although the ability of descending aortic circumferential strains to correctly predict the presence of carotid atherosclerotic plaque was better than that of aortic distensibility (AUC 0.604 vs. 0.530 respectively) this predictive accuracy was weak and not statistically significant. Although ideally atherosclerotic plaque imaging and strain values would also have been assessed in the same large artery (carotid or descending aorta), cine imaging of the carotid artery was (or T1/T2/PD acquisitions of the descending aorta) were not available in this study. Nevertheless, the findings of the study suggest that aortic strain (as well as aortic distensibility) by CMR feature tracking is limited in its ability to correctly identify carotid artery atherosclerotic plaque (and possibly, therefore, patients at the very highest risk of cardiovascular events).

Future research in this area should investigate larger numbers of ACPA positive patients with musculoskeletal symptoms at high risk of developing RA to confirm the findings of this small scale study with stratification of patients according to their predicted risk of RA to identify whether aortic stiffness increases incrementally with RA risk or whether aortic stiffness is directly mediated by ACPA positive autoimmune status. Using ACPA positive and ACPA negative controls with no musculoskeletal symptoms would further contribute to answering this research question.

8.5. Discussion, study limitations and future directions relating to chapter 7

The final chapter “CMR Assessment of Newly Diagnosed Treatment Naïve RA Patients at Baseline and 1 Year After Randomisation to either Etanercept & Methotrexate or Standard Therapy” utilised a quantitative multiparametric CMR in patients with newly diagnosed, treatment naïve RA before and 1 year after randomisation to either standard therapy or early biological therapy. The primary objective was to establish whether (any) RA DMARD strategy is associated with improvement in aortic distensibility over a 1 year period. The secondary objectives were to explore whether the following factors affect AD change over 1 year:

- DAS28 control (DAS28 defined clinical response/non-response)
- Therapeutic intervention (TNFi/MTX and conventional DMARD including MTX)

The key finding of this study were that aortic distensibility improves markedly after initiation of RA treatment in those treated with either first-line ETN-MTX or first line MTX-T2T ± ETN-MTX. A clear signal was also shown that ETN-MTX provides additional benefit over and above standard therapy with evidence of greater improvements in aortic stiffness which persist after adjustment for disease activity score. Notably, a 25% difference was observed between first-line standard therapy non-responders (that received delayed ETN) to responders and similarly between all receiving ETN (first-line and delayed) and first-line standard therapy responders. LV mass increased following treatment for RA in those treated with either first-line ETN-MTX or first line MTX-T2T ± ETN-MTX. Other markers of subclinical CVD including LV strain indices, ECV and native myocardial T1 relaxation time did not differ significantly after with treatment.

To the best of our knowledge this study was the first to assess effects of modern RA therapy on subclinical cardiovascular disease assessed by non-invasive imaging. Although the no statistically significant benefit in terms of aortic stiffness was shown between the ETN-MTX or first line MTX-T2T ± ETN-MTX groups, sub-analysis of treatment strategies suggested a clear benefit associated with patients receiving ETN-MTX at any stage. Recently published registry data suggests a reduction in incidence of MI among RA patients receiving anti-TNF therapy(243) versus those receiving standard DMARD therapy. The exact mode by which this reduction occurs, but this may link to the reduced aortic stiffness demonstrated in this study.

Limitations of this study were that a larger sample size may have led to a statistically significant difference between the two treatment arms and strengthened the conclusions drawn from the sub-analysis indicating a probable benefit in aortic stiffness reduction from Etanercept therapy.

Future directions in this area are twofold; firstly follow up of patients entered into CADERA is on-going and a later study will report 2 year CMR findings across the two treatment strategies. This may further address the question as to the optimal RA treatment strategy from a cardiovascular standpoint and whether the likely benefit from Etanercept is sustained over the longer term. Secondly, a long-term CADERA patient registry linked to long-term clinical outcomes will shed light onto the prognostic performance of the quantitative CMR parameters included in the protocol for the CADERA study, which may be also be of future benefit in assessment of subclinical cardiovascular diseases other than RA.

8.6. Overall future directions

The perfect non-invasive biomarker would be one which was acceptable to the patient, which poses no short or long-term risk to that patient, providing accurate and reproducible measurements linking precisely to disease activity in a dynamic fashion as well as linking accurately to long-term prognostication in terms of morbidity and mortality. For more widespread adoption of such a non-invasive biomarker to occur, the same biomarker should be cost efficient with rapid acquisition and analysis time. In the context of the conditions assessed in this thesis (prior myocardial infarction and rheumatoid arthritis), future studies should aim to address the following:

<u>Prior myocardial infarction:</u>

A key priority in this condition within non-invasive imaging is to improve the accuracy of diagnosis, ideally without the need for intravenous contrast agent. There may be a single as yet undiscovered (CMR) imaging parameter able to detect prior MI with 100% sensitivity and specificity, or a combination of non-invasive imaging and clinical parameters may be able to achieve this.

Future studies in this area may seek to use CMR LGE to identify prior MI in a high risk patient population (poorly controlled diabetes, established rheumatoid arthritis or elderly population) and identify whether use of CMR and treating patients identified as having prior MI with aggressive secondary prevention therapy

improves outcomes versus standard care i.e. use of clinical risk scoring tools e.g. Framingham or Q-Risk.

Other possible studies would be to assess the long-term prognostic implications of GLS in patients with prior MI yet preserved LVEF.

Rheumatoid arthritis

One of the key findings of this thesis has been an indication that anti-CCP individuals at risk of RA appear to exhibit early subclinical evidence of CVD (in the form of increased vascular stiffness) similar in degree to that of patients with a new clinical diagnosis of RA. As already mentioned, a larger study assessing more of these patients as well as the inclusion of an asymptomatic anti-CCP positive individuals as a control group is needed. Beyond this, a randomised control trial assessing the effect of closer follow up and earlier initiation of RA therapy in the highest risk individuals linked to long-term joint and CVD outcomes would be indicated.

Other key studies in Rheumatoid arthritis include the assessment of the performance of the non-invasive CMR biomarkers used in this study (AD, LV mass, T1, ECV etc.) in terms of predicting long-term treatment response as well as prognostication of CVD and all-cause mortality. Lastly, a randomised control trial is needed to assess if CVD outcomes are improved with non-invasive (CMR) biomarker (or alternative non-invasive imaging modality) guided primary CVD prevention therapy versus clinical risk score guided primary CVD prevention therapy.

8.7. Recently published literature

The following section discusses studies relevant to this thesis published after writing the background chapter.

Relevant to the work detailed in chapter 3, Raucci Jr. et al. recently published a study of the use of synthetic ECV in the paediatric and young adult congenital heart disease population and found that correlation of synthetic ECV with lab ECV was better with the use of a locally derived linear regression equation as opposed to previously published equation on a 1.5T Siemens CMR scanner(253). Additionally, they showed that using a cut-off value to define normal versus abnormal ECV (3 standard deviations above the mean value from a normal reference population) that synthetic ECV ‘misclassified’ ECV as abnormal/normal compared with the laboratory ECV value. They concluded that the strength of synthetic ECV was

therefore was primarily as a research tool (i.e. across populations) rather than in individual clinical patients. Nevertheless, it could be argued that their cut-off value to define normal versus abnormal is somewhat arbitrary given that the primary strength of ECV in a clinical setting is to identify highly abnormal values in infiltrative cardiomyopathies such as amyloid or HCM and that a small error (perhaps up to 5%) is not clinically relevant.

In relation to GLS assessed by CMR-FT, a recent study(254) showed that GLS assessed this way in a large (n=470) cohort of patients with LVEF <50% due to ischaemic or non-ischaemic aetiology showed a strong, independent association with mortality. Although these patients had reduced rather than preserved LVEF, this highlights that GLS by CMR-FT is a robust technique with strong potential as a non-invasive imaging biomarker.

Finally, in the context of anti-citrullinated protein antibody, Hermans et al recently reported raised ACPA in 11% of 275 recent STEMI patients with no history or prior diagnosis of RA with an independent association with long-term CVD mortality rates in ACPA positive patients(255). The authors postulated that ACPA positivity may be an independent CVD risk factor. As detailed in this thesis, it was unclear in our own small cohort of individuals at risk of RA whether ACPA positivity in itself led to impaired AD or whether their intrinsic propensity to develop RA was the cause of this finding. As such this highlights what a key area of future research this is.

8.8. Conclusions

Multiparametric CMR is ideally suited to the furthering our understanding of subclinical cardiovascular disease, providing insights into disease mechanisms, diagnosis of a disease, as well as its progression over time. In this thesis we have demonstrated the ability of synthetic ECV derived from native blood pool T1 to provide robust estimation of myocardial extracellular volume fraction, as well as reporting the development of a highly reproducible, novel aortic strain parameters which was validated in RA patients demonstrating its ability to identify vascular stiffness in RA patients versus controls. We have shown a moderate ability of GLS to correctly identify prior myocardial infarction. For the first time we have demonstrated evidence of subclinical vascular stiffness in individuals at high risk of developing RA. Lastly we have shown that vascular stiffness exhibited at the time of diagnosis of RA reverses with treatment for the condition 1 year after diagnosis

with a suggestion that a greater reversal occurs with Etanercept as compared with standard therapy.

.

References

1. Williams FH. A Method for More Fully Determining the Outline of the Heart by Means of the Fluoroscope Together with Other Uses of This Instrument in Medicine. Bost. Med. Surg. J. 1896;135:335–337. Available at: http://dx.doi.org/10.1056/NEJM189610011351402.

2. Mathers CD, Boerma T, Ma Fat D. Global and regional causes of death. Br. Med. Bull. 2009;92:7–32.

3. Wagner J A. Overview of biomarkers and surrogate endpoints in drug development. Dis. Markers 2002;18:41–6. Available at: http://www.ncbi.nlm.nih.gov/pubmed/12364809.

4. Hunter DJ, Losina E, Guermazi A, Burstein D, Lassere MN, Kraus V. A pathway and approach to biomarker validation and qualification for osteoarthritis clinical trials. Curr. Drug Targets 2010;11:536–45. Available at: http://www.ncbi.nlm.nih.gov/pubmed/20199395%5Cnhttp://www.pubmedcentral.nih.gov/articlerender.fcgi?artid=PMC3261486.

5. Lesko L, Atkinson A. Use of Biomarkers and Surrogate Endpoints in Drug Development and Regulatory Decision Making: Criteria, Validation, Strategies. Annu. Rev. Pharmacol. Toxicol. 2001;41:347–366.

6. Pennell DJ. Cardiovascular Magnetic Resonance. Circulation 2010;121:692–705. Available at: http://circ.ahajournals.org/cgi/doi/10.1161/CIRCULATIONAHA.108.811547.

7. Hundley WG, Bluemke DA, Finn JP, et al. ACCF/ACR/AHA/NASCI/SCMR 2010 Expert Consensus Document on Cardiovascular Magnetic ResonanceA Report of the American College of Cardiology Foundation Task Force on Expert Consensus Documents. J. Am. Coll. Cardiol. 2010;55:2614–2662. Available at: http://dx.doi.org/10.1016/j.jacc.2009.11.011.

8. Fleming TR, Powers JH. Biomarkers and surrogate endpoints in clinical trials. Stat. Med. 2012;31:2973–2984.

9. Eitel I, De Waha S, Wöhrle J, et al. Comprehensive prognosis assessment by CMR imaging after ST-segment elevation myocardial infarction. J. Am. Coll. Cardiol. 2014;64:1217–1226. Available at: http://dx.doi.org/10.1016/j.jacc.2014.06.1194.

10. Motwani M, Kidambi A, Greenwood JP, Plein S, Cardiovascular M. Advances in

cardiovascular magnetic resonance in ischaemic heart disease and non-ischaemic cardiomyopathies. Heart 2014;100:1722–1733. Available at: http://.

11. Hombach V, Merkle N, Torzewski J, et al. Electrocardiographic and cardiac magnetic resonance imaging parameters as predictors of a worse outcome in patients with idiopathic dilated cardiomyopathy. Eur. Heart J. 2009;30:2011–2018.

12. Barison A, Aquaro GD, Pugliese NR, et al. Measurement of myocardial amyloid deposition in systemic amyloidosis: insights from cardiovascular magnetic resonance imaging. J. Intern. Med. 2015;277:605–614.

13. Hendel RC, Patel MR, Kramer CM, et al. ACCF/ACR/SCCT/SCMR/ASNC/NASCI/SCAI/SIR 2006 Appropriateness Criteria for Cardiac Computed Tomography and Cardiac Magnetic Resonance Imaging□A Report of the American College of Cardiology Foundation Quality Strategic Directions Committee Appropriateness Cr. J. Am. Coll. Cardiol. 2006;48:1475–1497. Available at: http://dx.doi.org/10.1016/j.jacc.2006.07.003.

14. Kanal E. Gadolinium based contrast agents (GBCA): Safety overview after 3 decades of clinical experience. Magn. Reson. Imaging 2016.

15. Dawson P, Punwani S. Nephrogenic systemic fibrosis: non-gadolinium options for the imaging of CKD/ESRD patients. Semin. Dial. 2008;21:160–165.

16. Kanda T, Fukusato T, Matsuda M, et al. Gadolinium-based Contrast Agent Accumulates in the Brain Even in Subjects without Severe Renal Dysfunction: Evaluation of Autopsy Brain Specimens with Inductively Coupled Plasma Mass Spectroscopy. Radiology 2015;276:228–232.

17. Kramer CM, Barkhausen J, Flamm SD, Kim RJ, Nagel E. Standardized cardiovascular magnetic resonance (CMR) protocols 2013 update. J. Cardiovasc. Magn. Reson. 2013;15:91. Available at: http://www.pubmedcentral.nih.gov/articlerender.fcgi?artid=3851953&tool=pmcentrez&rendertype=abstract.

18. Alfakih K, Plein S, Thiele H, Jones T, Ridgway JP, Sivananthan MU. Normal human left and right ventricular dimensions for MRI as assessed by turbo gradient echo and steady-state free precession imaging sequences. J. Magn. Reson. Imaging 2003;17:323–329. Available at: http://doi.wiley.com/10.1002/jmri.10262.

19. van der Graaf AWM, Bhagirath P, Ghoerbien S, Götte MJW. Cardiac magnetic resonance imaging: Artefacts for clinicians. Netherlands Hear. J. 2014;22:542–549.

20. Nacif MS, Zavodni A, Kawel N, Choi E-Y, Lima JAC, Bluemke DA. Cardiac

magnetic resonance imaging and its electrocardiographs (ECG): tips and tricks. Int. J. Cardiovasc. Imaging 2012;28:1465–75. Available at: http://www.pubmedcentral.nih.gov/articlerender.fcgi?artid=3476721&tool=pmcentrez&rendertype=abstract.

21. Nayak K, Hu B. The future of real-time cardiac magnetic resonance imaging. Curr. Cardiol. Rep. 2005;7:45–51.

22. Blessberger H, Binder T. NON-invasive imaging: Two dimensional speckle tracking echocardiography: basic principles. Heart 2010;96:716–722.

23. Mizuguchi Y, Oishi Y, Miyoshi H, Iuchi A, Nagase N, Oki T. The Functional Role of Longitudinal, Circumferential, and Radial Myocardial Deformation for Regulating the Early Impairment of Left Ventricular Contraction and Relaxation in Patients With Cardiovascular Risk Factors: A Study With Two-Dimensional Strain Im. J. Am. Soc. Echocardiogr. 2008;21:1138–1144. Available at: http://www.sciencedirect.com/science/article/pii/S0894731708004355.

24. Smiseth OA, Torp H, Opdahl A, Haugaa KH, Urheim S. Myocardial strain imaging: how useful is it in clinical decision making? Eur. Heart J. 2015;37:1196–207. Available at: http://www.pubmedcentral.nih.gov/articlerender.fcgi?artid=4830908&tool=pmcentrez&rendertype=abstract.

25. Ersbøll M, Valeur N, Mogensen UM, et al. Prediction of all-cause mortality and heart failure admissions from global left ventricular longitudinal strain in patients with acute myocardial infarction and preserved left ventricular ejection fraction. J. Am. Coll. Cardiol. 2013;61:2365–2373.

26. Elliott PM, Anastasakis A, Borger MA, et al. 2014 ESC Guidelines on diagnosis and management of hypertrophic cardiomyopathy. Eur. Heart J. 2014;35:2733–2779. Available at: http://eurheartj.oxfordjournals.org/content/35/39/2733.abstract.

27. Thavendiranathan P, Poulin F, Lim K-D, Plana JC, Woo A, Marwick TH. Use of myocardial strain imaging by echocardiography for the early detection of cardiotoxicity in patients during and after cancer chemotherapy: a systematic review. J. Am. Coll. Cardiol. 2014;63:2751–2768.

28. Axel L, Dougherty L. MR imaging of motion with spatial modulation of magnetization. Radiology 1989;171:841–845.

29. Shehata ML, Cheng S, Osman NF, Bluemke DA, Lima JA. Myocardial tissue tagging with cardiovascular magnetic resonance. J. Cardiovasc. Magn. Reson.

2009;11:55. Available at: http://jcmr-online.biomedcentral.com/articles/10.1186/1532-429X-11-55.

30. Ibrahim E-SH. Myocardial tagging by Cardiovascular Magnetic Resonance: evolution of techniques--pulse sequences, analysis algorithms, and applications. J. Cardiovasc. Magn. Reson. 2011;13:36. Available at: http://jcmr-online.biomedcentral.com/articles/10.1186/1532-429X-13-36.

31. Obokata M, Nagata Y, Wu VC-C, et al. Direct comparison of cardiac magnetic resonance feature tracking and 2D/3D echocardiography speckle tracking for evaluation of global left ventricular strain. Eur. Heart J. Cardiovasc. Imaging 2016;17:525–532.

32. Pedrizzetti G, Claus P, Kilner PJ, Nagel E. Principles of cardiovascular magnetic resonance feature tracking and echocardiographic speckle tracking for informed clinical use. J. Cardiovasc. Magn. Reson. 2016:1–12. Available at: http://dx.doi.org/10.1186/s12968-016-0269-7.

33. Wu L, Germans T, Güçlü A, Heymans MW, Allaart CP, Van Rossum AC. Feature tracking compared with tissue tagging measurements of segmental strain by cardiovascular magnetic resonance. J. Cardiovasc. Magn. Reson. 2014;16:1–11. Available at: http://jcmr-online.com/content/16/1/10.

34. Schuster A, Morton G, Hussain ST, et al. The intra-observer reproducibility of cardiovascular magnetic resonance myocardial feature tracking strain assessment is independent of field strength. Eur. J. Radiol. 2013;82:296–301. Available at: http://dx.doi.org/10.1016/j.ejrad.2012.11.012.

35. Salerno M, Beller G a. Noninvasive assessment of myocardial perfusion. Circ. Cardiovasc. Imaging 2009;2:412–424.

36. Layland J, Carrick D, Lee M, Oldroyd K, Berry C. Adenosine: Physiology, pharmacology, and clinical applications. JACC Cardiovasc. Interv. 2014;7:581–591.

37. Foley JR, Plein S, Greenwood JP. Assessment of stable coronary artery disease by cardiovascular magnetic resonance imaging: Current and emerging techniques. World J. Cardiol. 2017;9:92. Available at: http://www.wjgnet.com/1949-8462/full/v9/i2/92.htm.

38. Plein S, Greenwood J, Ridgeway J. Components of CMR Protocols. In: Cardiovascular MR Manual. First. London: Springer Netherlands, 2011:216.

39. Plein S, Ryf S, Schwitter J, Radjenovic A, Boesiger P, Kozerke S. Dynamic contrast-enhanced myocardial perfusion MRI accelerated with k-t sense. Magn

Reson Med 2007;58. Available at: http://dx.doi.org/10.1002/mrm.21381.

40. Jaarsma C, Leiner T, Bekkers SC, et al. Diagnostic performance of noninvasive myocardial perfusion imaging using single-photon emission computed tomography, cardiac magnetic resonance, and positron emission tomography imaging for the detection of obstructive coronary artery disease: a meta-anal. J. Am. Coll. Cardiol. 2012;59:1719–1728.

41. Greenwood JP, Maredia N, Younger JF, et al. Cardiovascular magnetic resonance and single-photon emission computed tomography for diagnosis of coronary heart disease (CE-MARC): A prospective trial. Lancet 2012;379:453–460. Available at: http://dx.doi.org/10.1016/S0140-6736(11)61335-4.

42. Schuster A, Zarinabad N, Ishida M, et al. Quantitative assessment of magnetic resonance derived myocardial perfusion measurements using advanced techniques: microsphere validation in an explanted pig heart system. J. Cardiovasc. Magn. Reson. 2014;16:82. Available at: http://dx.doi.org/10.1186/s12968-014-0082-0.

43. Ishida M, Schuster A, Morton G, et al. Development of a universal dual-bolus injection scheme for the quantitative assessment of myocardial perfusion cardiovascular magnetic resonance. J Cardiovasc Magn Reson 2011;13. Available at: http://dx.doi.org/10.1186/1532-429X-13-28.

44. Crea F, Camici PG, Merz CNB. Coronary microvascular dysfunction: An update. Eur. Heart J. 2014;35:1101–1111.

45. Cecchi F, Olivotto I, Gistri R, Lorenzoni R, Chiriatti G, Camici PG. Coronary microvascular dysfunction and prognosis in hypertrophic cardiomyopathy. N. Engl. J. Med. 2003;349:1027–1035.

46. Neglia D, Parodi O, Gallopin M, et al. Myocardial blood flow response to pacing tachycardia and to dipyridamole infusion in patients with dilated cardiomyopathy without overt heart failure. A quantitative assessment by positron emission tomography. Circulation 1995;92:796–804.

47. Rajappan K, Rimoldi OE, Dutka DP, et al. Mechanisms of coronary microcirculatory dysfunction in patients with aortic stenosis and angiographically normal coronary arteries. Circulation 2002;105:470–476.

48. Chareonthaitawee P, Kaufmann PA, Rimoldi O, Camici PG. Heterogeneity of resting and hyperemic myocardial blood flow in healthy humans. Cardiovasc. Res. 2001;50:151–161.

49. Morton G, Chiribiri A, Ishida M, et al. Quantification of absolute myocardial perfusion in patients with coronary artery disease: comparison between cardiovascular magnetic resonance and positron emission tomography. J. Am. Coll. Cardiol. 2012;60:1546–1555.

50. Lockie T, Ishida M, Perera D, et al. High-resolution magnetic resonance myocardial perfusion imaging at 3.0-Tesla to detect hemodynamically significant coronary stenoses as determined by fractional flow reserve. J. Am. Coll. Cardiol. 2011;57:70–75.

51. Ripley DP, Motwani M, Plein S, Greenwood JP. Established and emerging cardiovascular magnetic resonance techniques for the assessment of stable coronary heart disease and acute coronary syndromes. Quant. Imaging Med. Surg. 2014;4:330–44. Available at: http://www.pubmedcentral.nih.gov/articlerender.fcgi?artid=4213424&tool=pmcentrez&rendertype=abstract.

52. Moon JCC, Reed E, Sheppard MN, et al. The histologic basis of late gadolinium enhancement cardiovascular magnetic resonance in hypertrophic cardiomyopathy. J. Am. Coll. Cardiol. 2004;43:2260–2264. Available at: http://dx.doi.org/10.1016/j.jacc.2004.03.035.

53. Bellin M-F, Van Der Molen AJ. Extracellular gadolinium-based contrast media: an overview. Eur. J. Radiol. 2008;66:160–167.

54. Sugihara N, Genda A, Shimizu M, et al. [Diastolic dysfunction and its relation to myocardial fibrosis in essential hypertension]. J. Cardiol. 1988;18:353–361.

55. Kellman P, Arai AE, McVeigh ER, Aletras AH. Phase-Sensitive Inversion Recovery for Detecting Myocardial Infarction Using Gadolinium-Delayed Hyperenhancement. Magn. Reson. Med. 2002;47:372–383. Available at: http://www.ncbi.nlm.nih.gov/pmc/articles/PMC2041905/.

56. Kuruvilla S, Adenaw N, Katwal AB, Lipinski MJ, Kramer CM, Salerno M. Late gadolinium enhancement on cardiac magnetic resonance predicts adverse cardiovascular outcomes in nonischemic cardiomyopathy: A systematic review and meta-analysis. Circ. Cardiovasc. Imaging 2014;7:250–257.

57. Iles LM, Ellims AH, Llewellyn H, et al. Histological validation of cardiac magnetic resonance analysis of regional and diffuse interstitial myocardial fibrosis. Eur. Heart J. Cardiovasc. Imaging 2015;16:14–22.

58. Mikami Y, Kolman L, Joncas SX, et al. Accuracy and reproducibility of semi-

automated late gadolinium enhancement quantification techniques in patients with hypertrophic cardiomyopathy. J. Cardiovasc. Magn. Reson. 2014;16:85. Available at: http://www.ncbi.nlm.nih.gov/pmc/articles/PMC4189726/.

59. Captur G, Manisty C, Moon JC. Cardiac MRI evaluation of myocardial disease. Heart 2016:heartjnl-2015-309077. Available at: http://heart.bmj.com/lookup/doi/10.1136/heartjnl-2015-309077.

60. Moon JC, Messroghli DR, Kellman P, et al. Myocardial T1 mapping and extracellular volume quantification: a Society for Cardiovascular Magnetic Resonance (SCMR) and CMR Working Group of the European Society of Cardiology consensus statement. J. Cardiovasc. Magn. Reson. 2013;15:1. Available at: Journal of Cardiovascular Magnetic Resonance.

61. Perea RJ, Ortiz-Perez JT, Sole M, et al. T1 mapping: characterisation of myocardial interstitial space. Insights Imaging 2015;6:189–202. Available at: http://dx.doi.org/10.1007/s13244-014-0366-9.

62. Fontana M, White SK, Banypersad SM, et al. Comparison of T1 mapping techniques for ECV quantification. Histological validation and reproducibility of ShMOLLI versus multibreath-hold T1 quantification equilibrium contrast CMR. J. Cardiovasc. Magn. Reson. 2012;14:88. Available at: Journal of Cardiovascular Magnetic Resonance.

63. Everett RJ, Stirrat CG, Semple SIR, Newby DE, Dweck MR, Mirsadraee S. Assessment of myocardial fibrosis with T1 mapping MRI. Clin. Radiol. 2016;71:768–778.

64. Messroghli DR, Radjenovic A, Kozerke S, Higgins DM, Sivananthan MU, Ridgway JP. Modified Look-Locker inversion recovery (MOLLI) for high-resolution T1 mapping of the heart. Magn. Reson. Med. 2004;52:141–146.

65. Piechnik SK, Ferreira VM, Dall'Armellina E, et al. Shortened Modified Look-Locker Inversion recovery (ShMOLLI) for clinical myocardial T1-mapping at 1.5 and 3 T within a 9 heartbeat breathhold. J. Cardiovasc. Magn. Reson. 2010;12:69. Available at: http://jcmr-online.biomedcentral.com/articles/10.1186/1532-429X-12-69.

66. Chow K, Flewitt JA, Green JD, Pagano JJ, Friedrich MG, Thompson RB. Saturation recovery single-shot acquisition (SASHA) for myocardial T(1) mapping. Magn. Reson. Med. 2014;71:2082–2095.

67. Kellman P, Wilson JR, Xue H, Ugander M, Arai AE. Extracellular volume

fraction mapping in the myocardium, part 1: evaluation of an automated method. J. Cardiovasc. Magn. Reson. 2012;14:1. Available at: http://jcmr-online.com/content/pdf/1532-429X-14-63.pdf%5Cnpapers3://publication/doi/10.1186/1532-429X-14-63.

68. Wong TC, Piehler KM, Kang IA, et al. Myocardial extracellular volume fraction quantified by cardiovascular magnetic resonance is increased in diabetes and associated with mortality and incident heart failure admission. Eur. Heart J. 2014;35:657–664.

69. Sado DM, Flett a. S, Banypersad SM, et al. Cardiovascular magnetic resonance measurement of myocardial extracellular volume in health and disease. Heart 2012;98:1436–1441.

70. Barison A, Gargani L, De Marchi D, et al. Early myocardial and skeletal muscle interstitial remodelling in systemic sclerosis: insights from extracellular volume quantification using cardiovascular magnetic resonance. Eur. Heart J. Cardiovasc. Imaging 2015;16:74–80.

71. Miller CA, Naish JH, Bishop P, et al. Comprehensive validation of cardiovascular magnetic resonance techniques for the assessment of myocardial extracellular volume. Circ. Cardiovasc. Imaging 2013;6:373–383.

72. Wong TC, Piehler K, Meier CG, et al. Association between extracellular matrix expansion quantified by cardiovascular magnetic resonance and short-term mortality. Circulation 2012;126:1206–1216.

73. Abdel-Aty H, Simonetti O, Friedrich MG. T2-weighted cardiovascular magnetic resonance imaging. J. Magn. Reson. Imaging 2007;26:452–459.

74. Eitel I, Friedrich MG. T2-weighted cardiovascular magnetic resonance in acute cardiac disease. J. Cardiovasc. Magn. Reson. 2011;13:13. Available at: http://dx.doi.org/10.1186/1532-429X-13-13.

75. Friedrich MG, Abdel-Aty H, Taylor A, Schulz-Menger J, Messroghli D, Dietz R. The salvaged area at risk in reperfused acute myocardial infarction as visualized by cardiovascular magnetic resonance. J Am Coll Cardiol 2008;51. Available at: http://dx.doi.org/10.1016/j.jacc.2008.01.019.

76. Wince WB, Kim RJ. Molecular imaging: T2-weighted CMR of the area at risk--a risky business? Nat Rev Cardiol 2010;7. Available at: http://dx.doi.org/10.1038/nrcardio.2010.124.

77. Giri S, Chung YC, Merchant A, Mihai G, Rajagopalan S, Raman S V. T2

quantification for improved detection of myocardial edema. J Cardiovasc Magn Reson 2009;11. Available at: http://dx.doi.org/10.1186/1532-429X-11-56.

78. Bönner F, Janzarik N, Jacoby C, et al. Myocardial T2 mapping reveals age- and sex-related differences in volunteers. J. Cardiovasc. Magn. Reson. 2015;17:9. Available at: http://jcmr-online.com/content/17/1/9.

79. Bohnen S, Radunski UK, Lund GK, et al. Performance of T1 and T2 Mapping Cardiovascular Magnetic Resonance to Detect Active Myocarditis in Patients with Recent-Onset Heart Failure. Circ. Cardiovasc. Imaging 2015;8.

80. Carpenter JP, He T, Kirk P, et al. On T2* magnetic resonance and cardiac iron. Circulation 2011;123:1519–1528.

81. Nambi V, Brunner G, Ballantyne CM. Ultrasound in cardiovascular risk prediction: don't forget the plaque! J. Am. Heart Assoc. 2013;2:1–4.

82. Westenberg JJM, van Poelgeest EP, Steendijk P, Grotenhuis HB, Jukema JW, de Roos A. Bramwell-Hill modeling for local aortic pulse wave velocity estimation: a validation study with velocity-encoded cardiovascular magnetic resonance and invasive pressure assessment. J. Cardiovasc. Magn. Reson. 2012;14:2. Available at: http://www.pubmedcentral.nih.gov/articlerender.fcgi?artid=3312851&tool=pmcentrez&rendertype=abstract.

83. Mattace-Raso FUS, Van Der Cammen TJM, Hofman A, et al. Arterial stiffness and risk of coronary heart disease and stroke: The Rotterdam Study. Circulation 2006;113:657–663.

84. Sakuragi S, Abhayaratna WP. Arterial stiffness: methods of measurement, physiologic determinants and prediction of cardiovascular outcomes. Int. J. Cardiol. 2010;138:112–118.

85. Laurent S, Cockcroft J, Van Bortel L, et al. Expert consensus document on arterial stiffness: Methodological issues and clinical applications. Eur. Heart J. 2006;27:2588–2605.

86. Dogui A, Kachenoura N, Frouin F, et al. Consistency of aortic distensibility and pulse wave velocity estimates with respect to the Bramwell-Hill theoretical model: a cardiovascular magnetic resonance study. J. Cardiovasc. Magn. Reson. 2011;13:11. Available at: http://jcmr-online.biomedcentral.com/articles/10.1186/1532-429X-13-11.

87. Ibrahim E-SH, Johnson KR, Miller AB, Shaffer JM, White RD. Measuring aortic

pulse wave velocity using high-field cardiovascular magnetic resonance: comparison of techniques. J. Cardiovasc. Magn. Reson. 2010;12:26. Available at: http://jcmr-online.biomedcentral.com/articles/10.1186/1532-429X-12-26.

88. Provan SA, Angel K, Semb AG, et al. Early prediction of increased arterial stiffness in patients with chronic inflammation: A 15-year followup study of 108 patients with rheumatoid arthritis. J. Rheumatol. 2011;38:606–612.

89. Vlachopoulos C, Aznaouridis K, O'Rourke MF, Safar ME, Baou K, Stefanadis C. Prediction of cardiovascular events and all-cause mortality with central haemodynamics: A systematic review and meta-analysis. Eur. Heart J. 2010;31:1865–1871.

90. Nelson AJ, Worthley SG, Cameron JD, et al. Cardiovascular magnetic resonance-derived aortic distensibility: validation and observed regional differences in the elderly. J. Hypertens. 2009;27. Available at: http://journals.lww.com/jhypertension/Fulltext/2009/03000/Cardiovascular_magnetic_resonance_derived_aortic.14.aspx.

91. Laurent S, Cockcroft J, Van Bortel L, et al. Expert consensus document on arterial stiffness: methodological issues and clinical applications. Eur. Heart J. 2006;27:2588–2605. Available at: http://eurheartj.oxfordjournals.org/cgi/doi/10.1093/eurheartj/ehl254.

92. Blacher J, Guerin AP, Pannier B, Marchais SJ, London GM. Arterial Calcifications, Arterial Stiffness, and Cardiovascular Risk in End-Stage Renal Disease. Hypertension 2001;38:938–942. Available at: http://hyper.ahajournals.org/cgi/doi/10.1161/hy1001.096358.

93. Stefanadis C, Wooley CF, Bush CA, Kolibash AJ, Boudoulas H. Aortic distensibility abnormalities in coronary artery disease. Am. J. Cardiol. 1987;59:1300–1304. Available at: http://www.sciencedirect.com/science/article/pii/0002914987909088.

94. Laurent S, Boutouyrie P, Asmar R, et al. Aortic stiffness is an independent predictor of all cause and cardiovascular mortality in hypertensive patients. Hypertension 2001;37:1236–1241. Available at: http://dx.doi.org/10.1161/01.HYP.37.5.1236.

95. Thygesen K, Alpert JS, Jaffe AS, et al. Third universal definition of myocardial infarction. Eur. Heart J. 2012;33:2551–2567.

96. Bhatnagar P, Wickramasinghe K, Williams J, Rayner M, Townsend N. The

epidemiology of cardiovascular disease in the UK 2014. Heart 2015:heartjnl-2015-307516-. Available at: http://heart.bmj.com/content/early/2015/05/06/heartjnl-2015-307516.full.

97. SE S, TA M, BJ G. Unrecognized myocardial infarction. Ann. Intern. Med. 2001;135:801–811. Available at: http://dx.doi.org/10.7326/0003-4819-135-9-200111060-00010.

98. Reimer KA, Jennings RB. The “wavefront phenomenon” of myocardial ischemic cell death. II. Transmural progression of necrosis within the framework of ischemic bed size (myocardium at risk) and collateral flow. Lab. Invest. 1979;40:633–644.

99. Masci PG, Bogaert J. Post myocardial infarction of the left ventricle: the course ahead seen by cardiac MRI. Cardiovasc. Diagn. Ther. 2012;2:113–127.

100. Fishbein MC, Maclean D, Maroko PR. The histopathologic evolution of myocardial infarction. Chest 1978;73:843–849.

101. Ganame J, Messalli G, Masci PG, et al. Time course of infarct healing and left ventricular remodelling in patients with reperfused ST segment elevation myocardial infarction using comprehensive magnetic resonance imaging. Eur. Radiol. 2011;21:693–701.

102. Masci PG, Ganame J, Francone M, et al. Relationship between location and size of myocardial infarction and their reciprocal influences on post-infarction left ventricular remodelling. Eur. Heart J. 2011;32:1640–1648.

103. Springeling T, Uitterdijk A, Rossi A, et al. Evolution of reperfusion post-infarction ventricular remodeling: New MRI insights. Int. J. Cardiol. 2013;169:354–358. Available at: http://dx.doi.org/10.1016/j.ijcard.2013.09.005.

104. Nicod P, Gilpin E, Dittrich H, et al. Influence on prognosis and morbidity of left ventricular ejection fraction with and without signs of left ventricular failure after acute myocardial infarction. Am. J. Cardiol. 1988;61:1165–1171.

105. Steg PG, James SK, Atar D, et al. ESC Guidelines for the management of acute myocardial infarction in patients presenting with ST-segment elevation. Eur. Heart J. 2012;33:2569 LP-2619. Available at: http://eurheartj.oxfordjournals.org/content/33/20/2569.abstract.

106. Ponikowski P, Voors AA, Anker SD, et al. 2016 ESC Guidelines for the diagnosis and treatment of acute and chronic heart failure Gerasimos McMurray, John J. V. Aboyans, Victor Achenbach, Stephan Agewall, Stefan Al-Attar, Nawwar Atherton, John James Bauersachs, Johann John Camm, A. Carerj, Scipione

Ceconi, Claudio Coca, Antonio Elliott, Perry Erol, Çetin Ezekowitz, Justin Fernández- F, editor. Eur. Heart J. 2016;37:2129 LP-2200. Available at: http://eurheartj.oxfordjournals.org/content/37/27/2129.abstract.

107. Agewall S, Beltrame JF, Reynolds HR, et al. ESC working group position paper on myocardial infarction with non-obstructive coronary arteries. Eur. Heart J. 2017;38:143–153. Available at: http://dx.doi.org/10.1093/eurheartj/ehw149.

108. Assomull RG, Lyne JC, Keenan N, Gulati A, Bunce NH, Davies SW. The role of cardiovascular magnetic resonance in patients presenting with chest pain, raised troponin, and unobstructed coronary arteries. Eur Hear. J 2007;28. Available at: http://dx.doi.org/10.1093/eurheartj/ehm113.

109. Kim R, Wu E, Allne R, et al. The Use of Contrast-Enhanced Magnetic Resonance Imaging to Identify Reversible Myocardial Dysfunction. N. Engl. J. Med. 2000;343:1445–1453.

110. Romero J, Kahan J, Kelesidis I, et al. CMR imaging for the evaluation of myocardial stunning after acute myocardial infarction: a meta-analysis of prospective trials. Eur. Heart J. Cardiovasc. Imaging 2013;14:1080–1091.

111. Kloner RA, Ganote CE, Jennings RB. The “no-reflow” phenomenon after temporary coronary occlusion in the dog. J. Clin. Invest. 1974;54:1496–1508.

112. Hamirani Y, Wong A, Kramer C, Salerno M. Effect of Microvascular Obstruction and Intramyocardial Hemorrhage by CMR on LV Remodeling and Outcomes After Myocardial Infarction: A Systematic Review and Meta-Analysis. JACC. Cardiovasc. Imaging 2014;7:940–952.

113. Garg P, Kidambi A, Swoboda PP, et al. The role of left ventricular deformation in the assessment of microvascular obstruction and intramyocardial haemorrhage. Int. J. Cardiovasc. Imaging 2016;0:0. Available at: http://link.springer.com/10.1007/s10554-016-1006-x.

114. Calvieri C, Masselli G, Monti R, Spreca M, Gualdi GF, Fedele F. Intramyocardial hemorrhage: an enigma for cardiac MRI? Biomed Res. Int. 2015;2015:859073.

115. Kwong RY, Chan AK, Brown KA, et al. Impact of Unrecognized Myocardial Scar Detected by Cardiac Magnetic Resonance Imaging on Event-Free Survival in Patients Presenting With Signs or Symptoms of Coronary Artery Disease. 2006.

116. Kaplan MJ. Cardiovascular disease in rheumatoid arthritis. Curr. Opin. Rheumatol. 2006;18:289–297. Available at:

http://www.ncbi.nlm.nih.gov/pubmed/17389882.

117. Avina-Zubieta JA, Choi HK, Sadatsafavi M, Etminan M, Esdaile JM, Lacaille D. Risk of cardiovascular mortality in patients with rheumatoid arthritis: a meta-analysis of observational studies. Arthritis Rheum. 2008;59:1690–1697.

118. Peters MJL, van Halm VP, Voskuyl AE, et al. Does rheumatoid arthritis equal diabetes mellitus as an independent risk factor for cardiovascular disease? A prospective study. Arthritis Rheum. 2009;61:1571–1579.

119. Solomon DH, Goodson NJ, Katz JN, et al. Patterns of cardiovascular risk in rheumatoid arthritis. Ann. Rheum. Dis. 2006;65:1608–1612.

120. Symmons DPM, Gabriel SE. Epidemiology of CVD in rheumatic disease, with a focus on RA and SLE. Nat. Rev. Rheumatol. 2011;7:399–408.

121. Maradit-Kremers H, Crowson CS, Nicola PJ, et al. Increased unrecognized coronary heart disease and sudden deaths in rheumatoid arthritis: a population-based cohort study. Arthritis Rheum. 2005;52:402–411.

122. Mantel A, Holmqvist M, Jernberg T, Wallberg-Jonsson S, Askling J. Rheumatoid arthritis is associated with a more severe presentation of acute coronary syndrome and worse short-term outcome. Eur. Heart J. 2015;36:3413–3422.

123. Martín-Martínez M a., González-Juanatey C, Castañeda S, et al. Recommendations for the management of cardiovascular risk in patients with rheumatoid arthritis: Scientific evidence and expert opinion. Semin. Arthritis Rheum. 2014;44:1–8. Available at: http://dx.doi.org/10.1016/j.semarthrit.2014.01.002.

124. Perk J, De Backer G, Gohlke H, et al. European Guidelines on cardiovascular disease prevention in clinical practice (version 2012). Eur. Heart J. 2012;33:1635–1701.

125. Fent GJ, Greenwood JP, Plein S, Buch MH. The role of non-invasive cardiovascular imaging in the assessment of cardiovascular risk in rheumatoid arthritis: where we are and where we need to be. Ann. Rheum. Dis. 2016:annrheumdis-2016-209744. Available at: http://ard.bmj.com/lookup/doi/10.1136/annrheumdis-2016-209744.

126. Bonfiglio T, EC A. Heart disease in patients with seropositive rheumatoid arthritis: A controlled autopsy study and review. Arch. Intern. Med. 1969;124:714–719. Available at: http://dx.doi.org/10.1001/archinte.1969.00300220066012.

127. LEBOWITZ WB. The Heart in Rheumatoid Arthritis (Rheumatoid Disease)A

Clinical and Pathological Study of Sixty-two Cases. Ann. Intern. Med. 1963;58:102–123. Available at: http://dx.doi.org/10.7326/0003-4819-58-1-102.

128. Svantesson H, Åkesson A, Eberhardt K, Elborgh R. Prognosis in Juvenile Rheumatoid Arthritis with Systemic Onset. Scand. J. Rheumatol. 1983;12:139–144. Available at: http://www.tandfonline.com/doi/abs/10.3109/03009748309102900.

129. Jastrzebska M, Czok ME, Guzik P. Autoimmune diseases, their pharmacological treatment and the cardiovascular system. Cardiol. J. 2013;20:569–576.

130. Watts RA, Carruthers DM, Symmons DP, Scott DG. The incidence of rheumatoid vasculitis in the Norwich Health Authority. Br. J. Rheumatol. 1994;33:832–833.

131. Mäki-Petäjä KM, Elkhawad M, Cheriyan J, et al. Anti-tumor necrosis factor-α therapy reduces aortic inflammation and stiffness in patients with rheumatoid arthritis. Circulation 2012;126:2473–80. Available at: http://circ.ahajournals.org/cgi/content/long/126/21/2473. Accessed September 3, 2015.

132. Hollan I, Prayson R, Saatvedt K, et al. Inflammatory cell infiltrates in vessels with different susceptibility to atherosclerosis in rheumatic and non-rheumatic patients: a controlled study of biopsy specimens obtained at coronary artery surgery. Circ. J. 2008;72:1986–1992.

133. Emami H, Vijayakumar J, Subramanian S, et al. Arterial 18F-FDG uptake in rheumatoid arthritis correlates with synovial activity. JACC Cardiovasc. Imaging 2014;7:959–960. Available at: http://dx.doi.org/10.1016/j.jcmg.2014.03.018.

134. Davis JM 3rd, Roger VL, Crowson CS, Kremers HM, Therneau TM, Gabriel SE. The presentation and outcome of heart failure in patients with rheumatoid arthritis differs from that in the general population. Arthritis Rheum. 2008;58:2603–2611.

135. Prasad M, Hermann J, Gabriel SE, et al. Cardiorheumatology: cardiac involvement in systemic rheumatic disease. Nat. Rev. Cardiol. 2015;12:168–76. Available at: http://dx.doi.org/10.1038/nrcardio.2014.206.

136. Crowson C, Liao K, Davi J, et al. Rheumatoid arthritis and cardiovascular disease. Am. Heart J. 2013;166:623–628.

137. Myasoedova E, Crowson CS, Kremers HM, et al. Lipid paradox in rheumatoid arthritis: the impact of serum lipid measures and systemic inflammation on the risk

of cardiovascular disease. Ann. Rheum. Dis. 2011;70:482–487.

138. Libby P. Role of inflammation in atherosclerosis associated with rheumatoid arthritis. Am. J. Med. 2008;121:S21-31.

139. Ferris HA, Kahn CR. New mechanisms of glucocorticoid-induced insulin resistance: Make no bones about it. J. Clin. Invest. 2012;122:3854–3857.

140. Hafstrom I, Rohani M, Deneberg S, Wornert M, Jogestrand T, Frostegard J. Effects of low-dose prednisolone on endothelial function, atherosclerosis, and traditional risk factors for atherosclerosis in patients with rheumatoid arthritis--a randomized study. J. Rheumatol. 2007;34:1810–1816.

141. Deanfield JE, Halcox JP, Rabelink TJ. Endothelial Function and Dysfunction. Circulation 2007;115:1285 LP-1295. Available at: http://circ.ahajournals.org/content/115/10/1285.abstract.

142. Sandoo A, Veldhuijzen van Zanten JJCS, Metsios GS, Carroll D, Kitas GD. Vascular function and morphology in rheumatoid arthritis: a systematic review. Rheumatology (Oxford). 2011;50:2125–39. Available at: http://www.ncbi.nlm.nih.gov/pubmed/21926155.

143. Vanhoutte PM. Say NO to ET. J. Auton. Nerv. Syst. 2000;81:271–277.

144. Faccini A, Kaski JC, Camici PG. Coronary microvascular dysfunction in chronic inflammatory rheumatoid diseases. Eur. Heart J. 2016;37:1799–1806.

145. Metsios GS, Stavropoulos-Kalinoglou A, Sandoo A, et al. Vascular function and inflammation in rheumatoid arthritis: the role of physical activity. Open Cardiovasc. Med. J. 2010;4:89–96. Available at: http://www.pubmedcentral.nih.gov/articlerender.fcgi?artid=2847820&tool=pmcentrez&rendertype=abstract.

146. Marti CN, Gheorghiade M, Kalogeropoulos AP, Georgiopoulou V V., Quyyumi AA, Butler J. Endothelial dysfunction, arterial stiffness, and heart failure. J. Am. Coll. Cardiol. 2012;60:1455–1469. Available at: http://dx.doi.org/10.1016/j.jacc.2011.11.082.

147. Sattar N, McCarey DW, Capell H, McInnes IB. Explaining how “high-grade” systemic inflammation accelerates vascular risk in rheumatoid arthritis. Circulation 2003;108:2957–2963.

148. Bentzon JF, Otsuka F, Virmani R, Falk E. Mechanisms of plaque formation and rupture. Circ. Res. 2014;114:1852–1866.

149. Yu X-H, Fu Y-C, Zhang D-W, Yin K, Tang C-K. Foam cells in atherosclerosis. Clin. Chim. Acta. 2013;424:245–252.

150. Garner R, Ding T, Deighton C. Management of rheumatoid arthritis. Medicine (Baltimore). 2016;42:237–242. Available at: http://dx.doi.org/10.1016/j.mpmed.2014.02.004.

151. Feldmann M, Brennan FM, Maini RN. Role of cytokines in rheumatoid arthritis. Annu. Rev. Immunol. 1996;14:397–440.

152. Mewar D, Wilson AG. Treatment of rheumatoid arthritis with tumour necrosis factor inhibitors. Br. J. Pharmacol. 2011;162:785–791.

153. Di Giovine FS, Nuki G, Duff GW. Tumour necrosis factor in synovial exudates. Ann. Rheum. Dis. 1988;47:768–772. Available at: http://www.ncbi.nlm.nih.gov/pmc/articles/PMC1003595/.

154. Maini RN, Taylor PC. Anti-cytokine therapy for rheumatoid arthritis. Annu. Rev. Med. 2000;51:207–229.

155. Brennan FM, Chantry D, Jackson A, Maini R, Feldmann M. Inhibitory effect of TNF alpha antibodies on synovial cell interleukin-1 production in rheumatoid arthritis. Lancet (London, England) 1989;2:244–247.

156. Joosten LA, Helsen MM, van de Loo FA, van den Berg WB. Anticytokine treatment of established type II collagen-induced arthritis in DBA/1 mice. A comparative study using anti-TNF alpha, anti-IL-1 alpha/beta, and IL-1Ra. Arthritis Rheum. 1996;39:797–809.

157. Williams RO, Marinova-Mutafchieva L, Feldmann M, Maini RN. Evaluation of TNF-alpha and IL-1 blockade in collagen-induced arthritis and comparison with combined anti-TNF-alpha/anti-CD4 therapy. J. Immunol. 2000;165:7240–7245.

158. Horai R, Saijo S, Tanioka H, et al. Development of chronic inflammatory arthropathy resembling rheumatoid arthritis in interleukin 1 receptor antagonist-deficient mice. J. Exp. Med. 2000;191:313–320.

159. Barnabe C, Martin B-J, Ghali WA. Systematic review and meta-analysis: anti-tumor necrosis factor alpha therapy and cardiovascular events in rheumatoid arthritis. Arthritis Care Res. (Hoboken). 2011;63:522–529.

160. Maki-Petaja KM, Elkhawad M, Cheriyan J, et al. Anti-Tumor Necrosis Factor-alpha Therapy Reduces Aortic Inflammation and Stiffness in Patients with Rheumatoid Arthritis. Circulation 2012. Available at: c:%5CPapers%5CRheumat%5CMakiPetaja 2012 - antiTNF.pdf.

161. Fearon WF, Fearon DT. Inflammation and cardiovascular disease role of the interleukin-1 receptor antagonist. Circulation 2008;117:2577–2579.

162. Mann DL. Inflammatory mediators and the failing heart: past, present, and the foreseeable future. Circ. Res. 2002;91:988–998.

163. Ikonomidis I, Lekakis JP, Nikolaou M, et al. Inhibition of Interleukin-1 by Anakinra Improves Vascular and Left Ventricular Function in Patients With Rheumatoid Arthritis. Circulation 2008;117:2662–2669. Available at: http://circ.ahajournals.org/cgi/doi/10.1161/CIRCULATIONAHA.107.731877.

164. Ikonomidis I, Tzortzis S, Andreadou I, et al. Increased benefit of interleukin-1 inhibition on vascular function, myocardial deformation, and twisting in patients with coronary artery disease and coexisting rheumatoid arthritis. Circ. Cardiovasc. Imaging 2014;7:619–28. Available at: http://www.ncbi.nlm.nih.gov/pubmed/24782115.

165. Genovese MC, Cohen S, Moreland L, et al. Combination therapy with etanercept and anakinra in the treatment of patients with rheumatoid arthritis who have been treated unsuccessfully with methotrexate. Arthritis Rheum. 2004;50:1412–1419.

166. Erhayiem B, Pavitt S, Baxter P, et al. Coronary Artery Disease Evaluation in Rheumatoid Arthritis (CADERA): study protocol for a randomized controlled trial. Trials 2014;15:436. Available at: http://www.pubmedcentral.nih.gov/articlerender.fcgi?artid=4233100&tool=pmcentrez&rendertype=abstract.

167. Giles JT, Malayeri A a., Fernandes V, et al. Left ventricular structure and function in patients with rheumatoid arthritis, as assessed by cardiac magnetic resonance imaging. Arthritis Rheum. 2010;62:940–951. Available at: http://doi.wiley.com/10.1002/art.27349.

168. Niewold TB, Harrison MJ, Paget SA. Anti-CCP antibody testing as a diagnostic and prognostic tool in rheumatoid arthritis. Qjm 2007;100:193–201.

169. Ntusi N a B, Piechnik SK, Francis JM, et al. Diffuse Myocardial Fibrosis and Inflammation in Rheumatoid Arthritis: Insights From CMR T1 Mapping. JACC. Cardiovasc. Imaging 2015;8:526–536. Available at: http://www.sciencedirect.com/science/article/pii/S1936878X1500128X.

170. Kobayashi Y, Giles JT, Hirano M, et al. Assessment of myocardial abnormalities in rheumatoid arthritis using a comprehensive cardiac magnetic

resonance approach: a pilot study. Arthritis Res. Ther. 2010;12:R171. Available at: http://arthritis-research.com/content/12/5/R171.

171. Myasoedova E, Davis JM 3rd, Crowson CS, et al. Brief report: rheumatoid arthritis is associated with left ventricular concentric remodeling: results of a population-based cross-sectional study. Arthritis Rheum. 2013;65:1713–1718.

172. Cioffi G, Viapiana O, Ognibeni F, et al. Prevalence and factors related to inappropriately high left ventricular mass in patients with rheumatoid arthritis without overt cardiac d1 Article O. Prevalence and factors related to inappropriately high left ventricular mass in patients with rheumatoid. J. Hypertens. Oct. 2015;33:2141–2149. Available at: http://ovidsp.ovid.com/ovidweb.cgi?T=JS&CSC=Y&NEWS=N&PAGE=fulltext&D=yrovftq&AN=00004872-201510000-00025.

173. Midtbø H, Gerdts E, Kvien TK, et al. Disease activity and left ventricular structure in patients with rheumatoid arthritis. Rheumatology (Oxford). 2014:511–519. Available at: http://www.ncbi.nlm.nih.gov/pubmed/25224414.

174. Cioffi G, Viapiana O, Ognibeni F, et al. Prevalence and factors related to left ventricular systolic dysfunction in asymptomatic patients with rheumatoid arthritis : A prospective tissue Doppler echocardiography study. Herz 2015;40:989–996.

175. Recio-Mayoral A, Mason JC, Kaski JC, Rubens MB, Harari OA, Camici PG. Chronic inflammation and coronary microvascular dysfunction in patients without risk factors for coronary artery disease. Eur. Heart J. 2009;30:1837–1843.

176. Nagel E. The Future of Cardiovascular Magnetic Resonance. Magnetom Flash 2016;64.

177. Saraste A, Knuuti J. Cardiac PET, CT, and MR: what are the advantages of hybrid imaging? Curr. Cardiol. Rep. 2012;14:24–31.

178. Wollenweber T, Bengel FM. Cardiac Molecular Imaging. Semin. Nucl. Med. 2016;44:386–397. Available at: http://dx.doi.org/10.1053/j.semnuclmed.2014.05.002.

179. Rider OJ, Tyler DJ. Clinical implications of cardiac hyperpolarized magnetic resonance imaging. J. Cardiovasc. Magn. Reson. 2013;15:93. Available at: http://www.pubmedcentral.nih.gov/articlerender.fcgi?artid=3819516&tool=pmcentrez&rendertype=abstract.

180. Stankovic Z, Allen BD, Garcia J, Jarvis KB, Markl M. 4D flow imaging with MRI. Cardiovasc. Diagnosis Ther. Vol 4, No 2 (April 2014) Cardiovasc. Diagnosis

Ther. (MR Imaging Cardiovasc. Dis. 2014. Available at: http://cdt.amegroups.com/article/view/3630.

181. Lee JMS, Shirodaria C, Jackson CE, et al. Multi-modal magnetic resonance imaging quantifies atherosclerosis and vascular dysfunction in patients with type 2 diabetes mellitus. Diabetes Vasc. Dis. Res. 2007;4:44–48.

182. Vogel-Claussen J, Finn JP, Gomes AS, et al. Left ventricular papillary muscle mass: relationship to left ventricular mass and volumes by magnetic resonance imaging. J. Comput. Assist. Tomogr. 2006;30:426–432.

183. Myerson SG, Bellenger NG, Pennell DJ. Assessment of left ventricular mass by cardiovascular magnetic resonance. Hypertension 2002;39:750–755.

184. Fent GJ, Plein S. New Cardiac Magnetic Resonance Reference Ranges for Right Ventricular Volumes and Systolic Function: What's New and Why Should We Care? Circ. Cardiovasc. Imaging 2016;9:e004589.

185. Oliver JJ, Webb DJ. Noninvasive Assessment of Arterial Stiffness and Risk of Atherosclerotic Events ATVB In Focus Noninvasive Assessment of Atherosclerosis: from Structure to Function Noninvasive Assessment of Arterial Stiffness and Risk of Atherosclerotic Events. Arter. Thromb Vasc Biol 2003;23:554–566. Available at: http://atvb.ahajournals.org/content/23/4/554%5Cnhttp://atvb.ahajournals.org//subscriptions/%5Cnhttp://atvb.ahajournals.org/.

186. Larghat AM, Swoboda PP, Biglands JD, Kearney MT, Greenwood JP, Plein S. The microvascular effects of insulin resistance and diabetes on cardiac structure, function, and perfusion: a cardiovascular magnetic resonance study. Eur. Heart J. Cardiovasc. Imaging 2014;15:1368–76. Available at: http://www.pubmedcentral.nih.gov/articlerender.fcgi?artid=4240406&tool=pmcentrez&rendertype=abstract%5Cnhttp://www.ncbi.nlm.nih.gov/pubmed/25117473%5Cnhttp://www.pubmedcentral.nih.gov/articlerender.fcgi?artid=PMC4240406.

187. Young AA, Cowan BR, Streeter D, et al. Evaluation of left ventricular torsion by cardiovascular magnetic resonance. J. Cardiovasc. Magn. Reson. 2012;14:49. Available at: http://jcmr-online.biomedcentral.com/articles/10.1186/1532-429X-14-49.

188. Treibel TA, Fontana M, Maestrini V, et al. Automatic Measurement of the Myocardial Interstitium Synthetic Extracellular Volume Quantification Without Hematocrit Sampling. JACC Cardiovasc. Imaging 2016;9:54–63.

189. Rahman O, Chow K, Carr J, Collins J. Derivation and Validation of Synthetic

Hematocrit Calculation from Blood Pool T1 values at multiple different cardiac blood pools , in both high and low flow states on 3T MRI. Proc. Int. Soc. Magn. Reson. Imaging Med. 2017;25:2763.

190. Teixeira R, Vieira MJ, Goncalves A, Cardim N, Goncalves L. Ultrasonographic vascular mechanics to assess arterial stiffness: a review. Eur. Heart J. Cardiovasc. Imaging 2016;17:233–246.

191. Oishi Y, Mizuguchi Y, Miyoshi H, Iuchi A, Nagase N, Oki T. A novel approach to assess aortic stiffness related to changes in aging using a two-dimensional strain imaging. Echocardiography 2008;25:941–945.

192. Yuda S, Kaneko R, Muranaka A, et al. Quantitative measurement of circumferential carotid arterial strain by two-dimensional speckle tracking imaging in healthy subjects. Echocardiography 2011;28:899–906.

193. Tsai W-C, Sun Y-T, Liu Y-W, et al. Usefulness of vascular wall deformation for assessment of carotid arterial stiffness and association with previous stroke in elderly. Am. J. Hypertens. 2013;26:770–777.

194. Kim S-A, Park S-M, Kim M-N, et al. The relationship between mechanical properties of carotid artery and coronary artery disease. Eur. Heart J. Cardiovasc. Imaging 2012;13:568–73. Available at: http://www.ncbi.nlm.nih.gov/pubmed/22127628.

195. Podgórski M, Grzelak P, Szymczyk K, Szymczyk E, Drozdz J, Stefańczyk L. Peripheral vascular stiffness, assessed with two-dimensional speckle tracking versus the degree of coronary artery calcification, evaluated by tomographic coronary artery calcification index. Arch. Med. Sci. 2015;11:122–129.

196. Bland JM. Statistical Notes: Measurement Error. Br. Med. J. 1996;313:744.

197. Davis TME, Fortun P, Mulder J, Davis WA, Bruce DG. Silent myocardial infarction and its prognosis in a community-based cohort of Type 2 diabetic patients: the Fremantle Diabetes Study. Diabetologia 2004;47:395–399.

198. Sheifer SE, Gersh BJ, Yanez ND 3rd, Ades PA, Burke GL, Manolio TA. Prevalence, predisposing factors, and prognosis of clinically unrecognized myocardial infarction in the elderly. J. Am. Coll. Cardiol. 2000;35:119–126.

199. EB S, JJ C, Sigurdsson S, al et. PRevalence and prognosis of unrecognized myocardial infarction determined by cardiac magnetic resonance in older adults. JAMA 2012;308:890–896. Available at: http://dx.doi.org/10.1001/2012.jama.11089.

200. Sengupta PP, Krishnamoorthy VK, Korinek J, et al. Left ventricular form and

function revisited: applied translational science to cardiovascular ultrasound imaging. J. Am. Soc. Echocardiogr. 2007;20:539–551.

201. Buckberg G, Hoffman JIE, Mahajan A, Saleh S, Coghlan C. Cardiac mechanics revisited: The relationship of cardiac architecture to ventricular function. Circulation 2008;118:2571–2587.

202. Garg P, Kidambi A, Foley JRJ, et al. Ventricular longitudinal function is associated with microvascular obstruction and intramyocardial haemorrhage. Open Hear. 2016;3:e000337. Available at: http://openheart.bmj.com/lookup/doi/10.1136/openhrt-2015-000337.

203. Amundsen BH, Crosby J, Steen PA, Torp H, Slrdahl SA, Stylen A. Regional myocardial long-axis strain and strain rate measured by different tissue Doppler and speckle tracking echocardiography methods: A comparison with tagged magnetic resonance imaging. Eur. J. Echocardiogr. 2009;10:229–237.

204. Delgado V, Mollema SA, Ypenburg C, et al. Relation Between Global Left Ventricular Longitudinal Strain Assessed with Novel Automated Function Imaging and Biplane Left Ventricular Ejection Fraction in Patients with Coronary Artery Disease. J. Am. Soc. Echocardiogr. 2008;21:1244–1250. Available at: http://dx.doi.org/10.1016/j.echo.2008.08.010.

205. Yan RT, Bluemke D, Gomes A, et al. Regional left ventricular myocardial dysfunction as a predictor of incident cardiovascular events: MESA (Multi-Ethnic Study of Atherosclerosis). J. Am. Coll. Cardiol. 2011;57:1735–1744.

206. Nowosielski M, Schocke M, Mayr A, et al. Comparison of wall thickening and ejection fraction by cardiovascular magnetic resonance and echocardiography in acute myocardial infarction. J. Cardiovasc. Magn. Reson. 2009;11:22. Available at: http://www.pubmedcentral.nih.gov/articlerender.fcgi?artid=2717065&tool=pmcentrez&rendertype=abstract.

207. Flett AS, Hasleton J, Cook C, et al. Evaluation of techniques for the quantification of myocardial scar of differing etiology using cardiac magnetic resonance. JACC Cardiovasc. Imaging 2011;4:150–156. Available at: http://dx.doi.org/10.1016/j.jcmg.2010.11.015.

208. DeLong ER, DeLong DM, Clarke-Pearson DL. Comparing the areas under two or more correlated receiver operating characteristic curves: a nonparametric approach. Biometrics 1988;44:837–845.

209. Cicala S, De Simone G, Roman MJ, et al. Prevalence and prognostic

significance of wall-motion abnormalities in adults without clinically recognized cardiovascular disease: The strong heart study. Circulation 2007;116:143–150.

210. Nucifora G, Schuijf JD, Delgado V, et al. Incremental value of subclinical left ventricular systolic dysfunction for the identification of patients with obstructive coronary artery disease. Am. Heart J. 2010;159:148–157. Available at: http://dx.doi.org/10.1016/j.ahj.2009.10.030.

211. Augustine D, Lewandowski a J, Lazdam M, et al. Global and regional left ventricular myocardial deformation measures by magnetic resonance feature tracking in healthy volunteers: comparison with tagging and relevance of gender. J Cardiovasc Magn Reson 2013;15:8. Available at: http://www.ncbi.nlm.nih.gov/pubmed/23331550.

212. Mignot A, Donal E, Zaroui A, et al. Global Longitudinal Strain as a Major Predictor of Cardiac Events in Patients with Depressed Left Ventricular Function: A Multicenter Study. J. Am. Soc. Echocardiogr. 2010;23:1019–1024. Available at: http://www.sciencedirect.com/science/article/pii/S0894731710006486.

213. Antoni ML, Mollema S a., Delgado V, et al. Prognostic importance of strain and strain rate after acute myocardial infarction. Eur. Heart J. 2010;31:1640–1647.

214. Swoboda PP, McDiarmid AK, Erhayiem B, et al. A novel and practical screening tool for the detection of silent myocardial infarction in patients with type 2 diabetes. J. Clin. Endocrinol. Metab. 2016:jc.2016-1318. Available at: http://press.endocrine.org/doi/10.1210/jc.2016-1318.

215. Holland DJ, Marwick TH, Haluska BA, et al. Subclinical LV dysfunction and 10-year outcomes in type 2 diabetes mellitus. 2015:1061–1066.

216. Carluccio E, Biagioli P, Alunni G, et al. Advantages of deformation indices over systolic velocities in assessment of longitudinal systolic function in patients with heart failure and normal ejection fraction. Eur. J. Heart Fail. 2011;13:292–302.

217. Ng ACT, Delgado V, Bertini M, et al. Alterations in multidirectional myocardial functions in patients with aortic stenosis and preserved ejection fraction: a two-dimensional speckle tracking analysis. Eur. Heart J. 2011;32:1542–1550.

218. Reant P, Mirabel M, Lloyd G, et al. Global longitudinal strain is associated with heart failure outcomes in hypertrophic cardiomyopathy. Heart 2016;102:741–747.

219. Amundsen BH, Helle-Valle T, Edvardsen T, et al. Noninvasive myocardial strain measurement by speckle tracking echocardiography: Validation against sonomicrometry and tagged magnetic resonance imaging. J. Am. Coll. Cardiol.

2006;47:789–793.

220. Hor KN, Gottliebson WM, Carson C, et al. Comparison of Magnetic Resonance Feature Tracking for Strain Calculation With Harmonic Phase Imaging Analysis. JACC Cardiovasc. Imaging 2010;3:144–151.

221. Teixeira R, Vieira MJ, Gon??alves A, Cardim N, Gon??alves L. Ultrasonographic vascular mechanics to assess arterial stiffness: A review. Eur. Heart J. Cardiovasc. Imaging 2016;17:233–246.

222. Cavalcante JL, Lima JAC, Redheuil A, Al-Mallah MH. Aortic stiffness: current understanding and future directions. J. Am. Coll. Cardiol. 2011;57:1511–1522.

223. O'Rourke MF, Safar ME, Dzau V. The Cardiovascular Continuum extended: aging effects on the aorta and microvasculature. Vasc. Med. 2010;15:461–468.

224. Erhayiem B, McDiarmid AK, Swoboda PP, et al. Abstract 13101: Subclinical Cardiovascular Abnormalities Exist in Early Rheumatoid Arthritis. Circulation 2015;132:A13101-. Available at: http://circ.ahajournals.org/cgi/content/long/132/Suppl_3/A13101. Accessed March 14, 2016.

225. Provan S a, Semb AG, Hisdal J, et al. Remission is the goal for cardiovascular risk management in patients with rheumatoid arthritis: a cross-sectional comparative study. Ann. Rheum. Dis. 2011;70:812–7. Available at: http://www.ncbi.nlm.nih.gov/pubmed/21288959.

226. Gerlag DM, Raza K, van Baarsen LGM, et al. EULAR recommendations for terminology and research in individuals at risk of rheumatoid arthritis: report from the Study Group for Risk Factors for Rheumatoid Arthritis. Ann. Rheum. Dis. 2012;71:638–641.

227. Rakieh C, Nam JL, Hunt L, et al. Predicting the development of clinical arthritis in anti-CCP positive individuals with non-speci fi c musculoskeletal symptoms : a prospective observational cohort study. Ann. Rheum. Dis. 2015;74:1659–1656.

228. Park HE, Cho G-Y, Kim H-K, Kim Y-J, Sohn D-W. Validation of circumferential carotid artery strain as a screening tool for subclinical atherosclerosis. J. Atheroscler. Thromb. 2012;19:349–56. Available at: http://www.ncbi.nlm.nih.gov/pubmed/22186101.

229. Evans MR, Escalante A, Battafarano DF, Freeman GL, O'Leary DH, Del Rinc??n I. Carotid atherosclerosis predicts incident acute coronary syndromes in rheumatoid arthritis. Arthritis Rheum. 2011;63:1211–1220.

230. Erhayiem B, McDiarmid AK, Swoboda PP, et al. Newly diagnosed, treatment-naive patients with rheumatoid arthritis have early abnormalities of vascular and myocardial function. J. Cardiovasc. Magn. Reson. 2015;17:P285. Available at: http://www.jcmr-online.com/content/17/S1/P285.

231. Karp G, Wolak A, Baumfeld Y, et al. Assessment of aortic stiffness among patients with systemic lupus erythematosus and rheumatoid arthritis by magnetic resonance imaging. Int. J. Cardiovasc. Imaging 2016;32:935–944. Available at: http://link.springer.com/10.1007/s10554-016-0851-y.

232. Cai JM, Hatsukami TS, Ferguson MS, Small R, Polissar NL, Yuan C. Classification of human carotid atherosclerotic lesions with in vivo multicontrast magnetic resonance imaging. Circulation 2002;106:1368–1373.

233. Sokolove J, Brennan MJ, Sharpe O, et al. Brief report: citrullination within the atherosclerotic plaque: a potential target for the anti-citrullinated protein antibody response in rheumatoid arthritis. Arthritis Rheum. 2013;65:1719–1724.

234. Dessein PH, Joffe BI, Veller MG, et al. Traditional and nontraditional cardiovascular risk factors are associated with atherosclerosis in rheumatoid arthritis. J. Rheumatol. 2005;32:435–442.

235. Corrales A, González-Juanatey C, Peiró ME, Blanco R, Llorca J, González-Gay M a. Carotid ultrasound is useful for the cardiovascular risk stratification of patients with rheumatoid arthritis: results of a population-based study. Ann. Rheum. Dis. 2014;73:722–7. Available at: http://www.ncbi.nlm.nih.gov/pubmed/23505241.

236. Haj Hensvold A, Magnusson PKE, Joshua V, et al. Environmental and genetic factors in the development of anticitrullinated protein antibodies (ACPAs) and ACPA-positive rheumatoid arthritis: an epidemiological investigation in twins. Ann. Rheum. Dis. 2015;74:375–380. Available at: http://ard.bmj.com/lookup/doi/10.1136/annrheumdis-2013-203947.

237. Benetos A, Waeber B, Izzo J, et al. Influence of age, risk factors, and cardiovascular and renal disease on arterial stiffness: clinical applications. Am J Hypertens 2002;15:1101–1108. Available at: http://www.ncbi.nlm.nih.gov/entrez/query.fcgi?cmd=Retrieve&db=PubMed&dopt=Citation&list_uids=12460708.

238. Barra LJ, Pope JE, Hitchon C, et al. The effect of rheumatoid arthritis–associated autoantibodies on the incidence of cardiovascular events in a large inception cohort of early inflammatory arthritis. Rheumatology 2017:kew474. Available at: https://academic.oup.com/rheumatology/article-

lookup/doi/10.1093/rheumatology/kew474.

239. Smolen JS, Landewé R, Breedveld FC, et al. EULAR recommendations for the management of rheumatoid arthritis with synthetic and biological disease-modifying antirheumatic drugs : 2013 update. Ann Rheum Dis (Published online first 25th Oct. 2013) 2013:1–18.

240. Kavanaugh A, Fleischmann RM, Emery P, et al. Clinical, functional and radiographic consequences of achieving stable low disease activity and remission with adalimumab plus methotrexate or methotrexate alone in early rheumatoid arthritis: 26-week results from the randomised, controlled OPTIMA study. Ann. Rheum. Dis. 2013;72:64–71.

241. Emery P, Hammoudeh M, FitzGerald O, et al. Sustained Remission with Etanercept Tapering in Early Rheumatoid Arthritis. N. Engl. J. Med. 2014;371:1781–1792.

242. Goekoop-Ruiterman YPM, de Vries-Bouwstra JK, Allaart CF, et al. Clinical and radiographic outcomes of four different treatment strategies in patients with early rheumatoid arthritis (the BeSt study): a randomized, controlled trial. Arthritis Rheum. 2005;52:3381–3390.

243. Low ASL, Symmons DPM, Lunt M, et al. Relationship between exposure to tumour necrosis factor inhibitor therapy and incidence and severity of myocardial infarction in patients with rheumatoid arthritis. Ann. Rheum. Dis. 2017:annrheumdis-2016-209784. Available at: http://ard.bmj.com/lookup/doi/10.1136/annrheumdis-2016-209784.

244. Redheuil A, Wu CO, Kachenoura N, et al. Proximal aortic distensibility is an independent predictor of all-cause mortality and incident CV events: The MESA study. J. Am. Coll. Cardiol. 2014;64:2619–2629.

245. Dumitru RB, Horton S, Hodgson R, et al. A prospective, single-centre, randomised study evaluating the clinical, imaging and immunological depth of remission achieved by very early versus delayed Etanercept in patients with Rheumatoid Arthritis (VEDERA). BMC Musculoskelet. Disord. 2016;17:61. Available at: http://dx.doi.org/10.1186/s12891-016-0915-0.

246. Fransen J, van Riel PLCM. The Disease Activity Score and the EULAR response criteria. Clin. Exp. Rheumatol. 2005;23:S93–S99.

247. Ikonomidis I, Lekakis JP, Nikolaou M, et al. Inhibition of interleukin-1 by anakinra improves vascular and left ventricular function in patients with rheumatoid

arthritis. Circulation 2008;117:2662–2669.

248. Ikdahl E, Rollefstad S, Wibetoe G, et al. Predictive Value of Arterial Stiffness and Subclinical Carotid Atherosclerosis for Cardiovascular Disease in Patients with Rheumatoid Arthritis. J. Rheumatol. 2016. Available at: http://www.jrheum.org/cgi/doi/10.3899/jrheum.160053.

249. Bozkurt B, Kribbs SB, Clubb FJ, et al. Pathophysiologically relevant concentrations of tumor necrosis factor-alpha promote progressive left ventricular dysfunction and remodeling in rats. Circulation 1998;97:1382–1391.

250. Sivasubramanian N, Coker ML, Kurrelmeyer KM, et al. Left ventricular remodeling in transgenic mice with cardiac restricted overexpression of tumor necrosis factor. Circulation 2001;104:826–831.

251. Metsios GS, Stavropoulos-Kalinoglou A, Panoulas VF, et al. Rheumatoid cachexia and cardiovascular disease. Clin. Exp. Rheumatol. 2009;27:985–988. Available at: http://dx.doi.org/10.1038/nrrheum.2010.105.

252. Lancaster GA, Dodd S, Williamson PR. Design and analysis of pilot studies:recommendations for good practice. J. Eval. Clin. Pract. 2004:307–312.

253. Raucci FJ, Parra DA, Christensen JT, et al. Synthetic hematocrit derived from the longitudinal relaxation of blood can lead to clinically significant errors in measurement of extracellular volume fraction in pediatric and young adult patients. J. Cardiovasc. Magn. Reson. 2017;19:1–10.

254. Romano S, Judd RM, Kim RJ, et al. Association of Feature-Tracking Cardiac Magnetic Resonance Imaging Left Ventricular Global Longitudinal Strain with All-Cause Mortality in Patients with Reduced Left Ventricular Ejection Fraction. Circulation 2017;135:2313–2315.

255. Hermans MP, Volkov M, Velden D van der, et al. Anti-citrullinated protein antibodies: a marker of cardiovascular disease and mortality in patients without rheumatoid arthritis. Autoimmune Inflamm. 2017;76:A82.2-A82. Available at: http://ard.bmj.com/lookup/doi/10.1136/annrheumdis-2016-211055.18.

Appendix

Ethical approval letters

NHS
Health Research Authority

NRES Committee Yorkshire & The Humber - Leeds West
First Floor
Millside
Mill Pond Lane
Leeds
LS6 4RA

Telephone: 0113 3050122 Facsimile: 0113 8556191 24 January 2013

Dr John P Greenwood
Consultant Cardiologist, Senior Lecturer
University of Leeds
Academic Unit of Cardiovascular Medicine
G floor, Jubilee Wing
Leeds General Infirmary
LS1 3EX

Dear Dr Greenwood

Study title:	**CE-MARC 2: Optimization of Image Acquisition and Analysis Methods**
REC reference:	**12/YH/0551**
IRAS project ID:	**116093**

Thank you for your letter of 18 January 2013, responding to the Committee's request for further information on the above research and submitting revised documentation.

The further information has been considered on behalf of the Committee by the Chair.

We plan to publish your research summary wording for the above study on the NRES website, together with your contact details, unless you expressly withhold permission to do so. Publication will be no earlier than three months from the date of this favourable opinion letter. Should you wish to provide a substitute contact point, require further information, or wish to withhold permission to publish, please contact the Co-ordinator Mrs Elaine Hazell, nrescommittee.yorkandhumber-leedswest@nhs.uk.

Confirmation of ethical opinion

On behalf of the Committee, I am pleased to confirm a favourable ethical opinion for the above research on the basis described in the application form, protocol and supporting documentation as revised, subject to the conditions specified below.

Ethical review of research sites

NHS sites

The favourable opinion applies to all NHS sites taking part in the study, subject to management permission being obtained from the NHS/HSC R&D office prior to the start of the study (see "Conditions of the favourable opinion" below).

Non-NHS sites

Conditions of the favourable opinion

The favourable opinion is subject to the following conditions being met prior to the start of the study.

Management permission or approval must be obtained from each host organisation prior to the start of the study at the site concerned.

Management permission ("R&D approval") should be sought from all NHS organisations involved in the study in accordance with NHS research governance arrangements.

Guidance on applying for NHS permission for research is available in the Integrated Research Application System or at http://www.rdforum.nhs.uk.

Where a NHS organisation's role in the study is limited to identifying and referring potential participants to research sites ("participant identification centre"), guidance should be sought from the R&D office on the information it requires to give permission for this activity.

For non-NHS sites, site management permission should be obtained in accordance with the procedures of the relevant host organisation.

Sponsors are not required to notify the Committee of approvals from host organisations

Please insert spaces between paragraphs in the section 'What will happen to me if I take part' to improve readability.

It is the responsibility of the sponsor to ensure that all the conditions are complied with before the start of the study or its initiation at a particular site (as applicable).

You should notify the REC in writing once all conditions have been met (except for site approvals from host organisations) and provide copies of any revised documentation with updated version numbers. The REC will acknowledge receipt and provide a final list of the approved documentation for the study, which can be made available to host organisations to facilitate their permission for the study. Failure to provide the final versions to the REC may cause delay in obtaining permissions.

Approved documents

The final list of documents reviewed and approved by the Committee is as follows:

Document	*Version*	*Date*
Advertisement	1.1	
Covering Letter		23 November 2012

Evidence of insurance or indemnity		29 September 2012
Investigator CV		10 August 2012
Letter of invitation to participant		22 November 2012
Participant Consent Form: Healthy volunteers	1.1	18 January 2013
Participant Consent Form	1.1	18 January 2013
Participant Information Sheet: Volunteer	1.1	18 January 2013
Participant Information Sheet	1.1	18 January 2013
Protocol	1.0	05 November 2012
REC application	3.4	23 November 2012
Response to Request for Further Information		18 January 2013

Statement of compliance

The Committee is constituted in accordance with the Governance Arrangements for Research Ethics Committees and complies fully with the Standard Operating Procedures for Research Ethics Committees in the UK.

After ethical review

Reporting requirements

The attached document *"After ethical review – guidance for researchers"* gives detailed guidance on reporting requirements for studies with a favourable opinion, including:

- Notifying substantial amendments
- Adding new sites and investigators
- Notification of serious breaches of the protocol
- Progress and safety reports
- Notifying the end of the study

The NRES website also provides guidance on these topics, which is updated in the light of changes in reporting requirements or procedures.

Feedback

You are invited to give your view of the service that you have received from the National Research Ethics Service and the application procedure. If you wish to make your views known please use the feedback form available on the website.

Further information is available at National Research Ethics Service website > After Review

12/YH/0551 **Please quote this number on all correspondence**

We are pleased to welcome researchers and R & D staff at our NRES committee members' training days – see details at http://www.hra.nhs.uk/hra-training/

With the Committee's best wishes for the success of this project.

Yours sincerely

pp
Dr Rhona Bratt Chair

Email:nrescommittee.yorkandhumber-leedswest@nhs.uk

Enclosures: "After ethical review – guidance for researchers"

Copy to: *Ms Clare E Skinner*
Ms Anne Gowing, Leeds Teaching Hospitals NHS Trust

NHS
Health Research Authority
NRES Committee Yorkshire & The Humber - Leeds West
Room 001, Jarrow Business Centre
Rolling Mill Road
Jarrow
Tyne and Wear
NE32 3DT

Tel: 0191 4283648

18 March 2015

Ms Petra Bijsterveld
Senior Research Nurse & MRI MRF manager
Cardiovascular Imaging
LICAMM
University of Leeds
Leeds Teaching Hospitals NHS Trust

Dear Ms Bijsterveld

Study title:	**MRI Evaluation of Transcatheter and Surgical Aortic Valve Implantation.**
REC reference:	**08/H1307/106**
EudraCT number:	**N/A**
Amendment number:	**5**
Amendment date:	**17 February 2015**
IRAS project ID:	**6033**

The above amendment was reviewed by the Sub-Committee in correspondence.

Summary of Amendment

The applicants seek approval for an increase in the number of participants to be recruited for this study, and for an extension of the recruitment period to September 2016. This long running study requires a large number of participants in relation to the number of completed datasets. This is due to the study population being elderly with many comorbidities, leading to a high dropout rate. The applicants have obtained some further funding to complement the BHF programme grant and wish to continue recruitment as the applicants have not yet obtained the 60 complete datasets required.

Ethical opinion

The members of the Committee taking part in the review gave a favourable ethical opinion of the amendment on the basis described in the notice of amendment form and supporting documentation.

Approved documents

The documents reviewed and approved at the meeting were:

Document	Version	Date
Notice of Substantial Amendment (non-CTIMP)	5	17 February 2015
Research protocol or project proposal	1.5	17 February 2015

NHS
Health Research Authority

NRES Committee South Central - Oxford A

Bristol Research Ethics Committee Centre
Whitefriars
Level 3 Block B
Lewins Mead
Bristol
BS1 2NT

Tel: 0117 342 1387

03 June 2015

Prof Stefan Neubauer
Professor Cardiovascular Medicine
University of Oxford
OCMR, Level 0
John Radcliffe Hospital
OX3 9DU

Dear Prof Neubauer

Study title:	**HCMR - Novel Predictors of Outcome in Hypertrophic Cardiomyopathy**
REC reference:	**14/SC/0190**
Amendment number:	**3**
Amendment date:	**18 May 2015**
IRAS project ID:	**147698**

The above amendment was reviewed by the Sub-Committee in correspondence.

Ethical opinion

The members of the Committee taking part in the review gave a favourable ethical opinion of the amendment on the basis described in the notice of amendment form and supporting documentation.

Approved documents

The documents reviewed and approved at the meeting were:

Document	*Version*	*Date*
Copies of advertisement materials for research participants [Website V4.0 30Apr2015]	4	30 April 2015
Copies of advertisement materials for research participants [Summary of proposed changes to HCMR website_30April2015]	4	30 April 2015
Covering letter on headed paper [1. Cover Letter signed_May2015]	3	20 May 2015
GP/consultant information sheets or letters [GP Letter_UK_V2.0 30Apr2015]	2	30 April 2015
Notice of Substantial Amendment (non-CTIMP) [Amendment Form]	3	18 May 2015
Research protocol or project proposal [Protocol V4.0_2015-04-	4	16 April 2015

16_EU]		

Membership of the Committee

The members of the Committee who took part in the review are listed on the attached sheet.

R&D approval

All investigators and research collaborators in the NHS should notify the R&D office for the relevant NHS care organisation of this amendment and check whether it affects R&D approval of the research.

Statement of compliance

The Committee is constituted in accordance with the Governance Arrangements for Research Ethics Committees and complies fully with the Standard Operating Procedures for Research Ethics Committees in the UK.

We are pleased to welcome researchers and R & D staff at our NRES committee members' training days – see details at http://www.hra.nhs.uk/hra-training/

14/SC/0190:	**Please quote this number on all correspondence**

Yours sincerely

PP
Dr Hugh Davies
Chair

E-mail: nrescommittee.southcentral-oxforda@nhs.net

Enclosures: *List of names and professions of members who took part in the review*

Copy to: *Ms Heather House, Oxford University Hospital NHS Trust, Research and Development Department, Joint Research Office*

NHS
Health Research Authority
NRES Committee Yorkshire & The Humber - Leeds West
Room 001, Jarrow Business Centre
Rolling Mill Road
Jarrow
Tyne and Wear
NE32 3DT

Tel: 0191 4283548

02 March 2015

Petra Bijsterveld
Senior Research Nurse, CMR Research Group
Cardiovascular and Diabetes Research
Sunshine Corridor
Leeds General Infirmary
Great George Street
Leeds
LS1 3EX

Dear Ms Bijsterveld

Study title:	**QUANTITATIVE EVALUATION OF MYOCARDIAL CHARACTERISTICS IN REPERFUSED ST-ELEVATION MYOCARDIAL INFARCTION – A 3 TESLA CARDIOVASCULAR MAGNETIC RESONANCE STUDY**
REC reference:	**12/YH/0169**
Amendment number:	**Minor Amendment to PIS/ICF**
Amendment date:	**13 February 2015**
IRAS project ID:	**101941**

Thank you for your letter of 13 February 2015, notifying the Committee of the above amendment.

The Committee does not consider this to be a "substantial amendment" as defined in the Standard Operating Procedures for Research Ethics Committees. The amendment does not therefore require an ethical opinion from the Committee and may be implemented immediately, provided that it does not affect the approval for the research given by the R&D office for the relevant NHS care organisation.

Documents received

The documents received were as follows:

Document	Version	Date
Notice of Minor Amendment	Minor Amendment to PIS/ICF	13 February 2015
Participant information sheet (PIS) [(and consent form)]	1.2	13 February 2015

Statement of compliance

The Committee is constituted in accordance with the Governance Arrangements for

Research Ethics Committees and complies fully with the Standard Operating Procedures for Research Ethics Committees in the UK.

12/YH/0169:	Please quote this number on all correspondence

Yours sincerely

Miss Christie Ord
REC Assistant

E-mail: nrescommittee.yorkandhumber-leedswest@nhs.net

Copy to: *Anne Gowing, Leeds Teaching Hospitals NHS Trust*

Prof Sven Plein, University of Leeds

Leeds (West) Research Ethics Committee
Room 22
Floor CD, Block 40
King Edward Home
Leeds General Infirmary
Leeds
LSI 3EX
Telephone: 0113 3923181
Facsimile: 0113 3926799
15 January 2010

Professor Paul Emery
ARC Professor
Department of Rheumatology. Second Floor.
Chapel Allerton Hospital, Chapeltown Road
Leeds
LS7 4SA

Dear Professor Emery

Study Title: Inflammatory arthritis disease continuum longitudinal study

REC reference number: 09/1-11307/98 Protocol number: 1

Thank you for your letter of 1 1 January 2010, responding to the Committee's request for further information on the above research and submitting revised documentation.

The further information was considered in correspondence by a sub-committee of the REC A list of the sub-committee members is attached.

Confirmation of ethical opinion

On behalf of the Committee, I am pleased to confirm a favourable ethical opinion for the above research on the basis described in the application form, protocol and supporting documentation as revised, subject to the conditions specified below.

- Ethical review of research sites

The favourable opinion applies to all NHS sites taking part in the study, subject to management permission being obtained from the NHS/HSC R&D office prior to the start of the study (see "Conditions of the favourable opinion" below).

Conditions of the favourable opinion

The favourable opinion is subject to the following conditions being met prior to the start of the study.

Management permission or approval must be obtained from each host organisation prior to the start of the study at the site concerned.

For NHS research sites only, management permission for research ("R&D approval") should be obtained from the relevant care organisation(s) in accordance with NHS research

governance arrangements. Guidance on applying for NHS permission for research is available in the Integrated Research Application System or at http://www.rdforum.nhs.uk. Where the only involvement of the NHS organisation is as a Participant Identification Centre, management permission for research is not required but the R&D office should be notified of the study. Guidance should be sought from the R&D office where necessary.

Sponsors are not required to notify the Committee of approvals from host organisations.

It is the responsibility of the sponsor to ensure that all the conditions are complied with before the start of the study or its initiation at a particular site (as applicable).

Approved documents

The final list of documents reviewed and approved by the Committee is as follows:

Document	Version	Date
Covering Letter		19 November 2009
REC application		20 November 2009
Investigator CV		04 March 2008
Evidence of insurance or indemnity		08 October 2009
Referees or other scientific critique report	1	17 November 2009
GP/Consuttant information Sheets	1	15 October 2009
Protocol	2	05 January 2010
Participant Information Sheet: Cardiovascular study	2	05 January 2010
Participant Information Sheet: Volunteer study	2	05 January 2010
Participant Information Sheet: Main study	2	05 January 2010
Participant Information Sheet: Imaging and bio study	2	05 January 2010
Participant Information Sheet: Synovial biopsy adn bio sub-study	2	05 January 2010

Participant Consent Form: Cardiovascular study	2	05 January 2010
Participant Consent Form: Volunteer study	2	05 January 2010
Participant Consent Form: Main study	2	05 January 2010
Participant Consent Form: Imaging and bio study	2	05 January 2010
Participant Consent Form: Synovial biopsy and bio sub-study	2	05 January 2010
GP/Consultant Information Sheets	2	05 January 2010
Response to Request for Further Information		11 January 2010

Statement of compliance

The Committee is constituted in accordance with the Governance Arrangements for Research Ethics Committees (July 2001) and complies fully with the Standard Operating Procedures for Research Ethics Committees in the UK.

After ethical review

Now that you have completed the application process please visit the National Research Ethics Service website > After Review

You are invited to give your view of the service that you have received from the National Research Ethics Service and the application procedure. If you wish to make your views known please use the feedback form available on the website.
The attached document "After ethical review — guidance for researchers" gives detailed guidance on reporting requirements for studies with a favourable opinion, including:

- Notifying substantial amendments
- Adding new sites and investigators
- Progress and safety reports
- Notifying the end of the study

The NRES website also provides guidance on these topics, which is updated in the light of changes in reporting requirements or procedures.

We would also like to inform you that we consult regularly with stakeholders to improve our service. If you would like to join our Reference Group please email referencegroup@nres.npsa.nhs.uk.

Yours sincerely

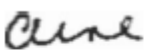

- Dr Rhona Bratt

Chair

Email: Elaine.hazell@leedsth.nhs.uk

Enclosures: List of names and professions of members who were present at the meeting and those who submitted written comments

'After ethical review — guidance for researchers"

Copy to: Ms Rachel De Souza

R&D, Leeds Teaching Hospitals NHS Trust

- Leeds (West) Research Ethics Committee

NHS
Health Research Authority
NRES Committee Yorkshire & The Humber - Leeds West
Room 001, Jarrow Business Centre
Rolling Mill Road
Jarrow
Tyne and Wear
NE32 3DT

Tel: 0191 428 3444

09 April 2015

Mr James Goulding
Clinical Trials Coordinator
Leeds Institute of Rheumatic and Musculoskeletal Medicine
2nd Floor, Chapel Allerton Hospital
Chapeltown Road
Leeds
LS7 4SA

Dear Mr Goulding

Study title:	A Prospective, Single-centre, Randomised Study Evaluating the Clinical, Imaging and Immunological Depth of Remission Achieved by Very Early versus Delayed Etanercept in patients with Rheumatoid Arthritis (VEDERA)
REC reference:	10/H1307/138
Protocol number:	RR10/9592
EudraCT number:	2010-023910-30
Amendment number:	Substantial Amendment 9
Amendment date:	25 February 2015
IRAS project ID:	67634

The above amendment was reviewed by the Sub-Committee in correspondence.

Summary of amendment:

This amendment was submitted to provide an updated protocol with changes such as the cardiovascular sub-study name change to 'CADERA' and the removal of Dr Richard Hodgson as sub-investigator and the addition of Dr Raluca B. Dumitru. Other changes were listed in the 'Summary of Changes' document.

Additionally, the end date for the study was extended to August 2017.

Ethical opinion

The members of the Committee taking part in the review gave a favourable ethical opinion of the amendment on the basis described in the notice of amendment form and supporting documentation.

Approved documents

The documents reviewed and approved at the meeting were:

Document	*Version*	*Date*
Covering letter on headed paper [Letter from James Goulding]		01 April 2015
Notice of Substantial Amendment (CTIMP)	Substantial Amendment 9	25 February 2015
Other [Sponsor Notification]		20 March 2015
Other [Suimmary of amendments]	Substantial Amendment 9	25 February 2015
Participant information sheet (PIS) [VEDERA CV CADERA ICF - Clean]	8.0	25 February 2015
Participant information sheet (PIS) [VEDERA CV CADERA ICF - Tracked Changes]	8.0	25 February 2015
Participant information sheet (PIS) [VEDERA ICF - Clean]	8.0	25 February 2015
Participant information sheet (PIS) [VEDERA ICF - Tracked Changes]	8.0	25 February 2015
Research protocol or project proposal [Clean]	11.0	25 February 2015
Research protocol or project proposal [Tracked Changes]	11.0	25 February 2015

Membership of the Committee

The members of the Committee who took part in the review are listed on the attached sheet.

R&D approval

All investigators and research collaborators in the NHS should notify the R&D office for the relevant NHS care organisation of this amendment and check whether it affects R&D approval of the research.

Statement of compliance

This Committee is recognised by the United Kingdom Ethics Committee Authority under the Medicines for Human Use (Clinical Trials) Regulations 2004, and is authorised to carry out the ethical review of clinical trials of investigational medicinal products.

The Committee is fully compliant with the Regulations as they relate to ethics committees and the conditions and principles of good clinical practice.

The Committee is constituted in accordance with the Governance Arrangements for Research Ethics Committees and complies fully with the Standard Operating Procedures for Research Ethics Committees in the UK.

We are pleased to welcome researchers and R & D staff at our NRES committee members' training days – see details at http://www.hra.nhs.uk/hra-training/

10/H1307/138:	Please quote this number on all correspondence

Yours sincerely

Dr Sheila E. Fisher Chair

E-mail: nrescommittee.yorkandhumber-leedswest@nhs.net

Enclosures: *List of names and professions of members who took part in the review*

Copy to: *Mr Neville Young, Research & Development, Leeds Teaching Hospital Trust*

Dr Maya Buch, University of Leeds

NRES Committee Yorkshire & The Humber - Leeds West

Attendance at Sub-Committee of the REC meeting held by correspondence

Committee Members:

Name	*Profession*	*Present*	*Notes*
Dr Sheila E. Fisher (Chair)	MHRA Committee on Safety of Devices	Yes	
Ms Sarah Kirkland	Research Governance Facilitator	Yes	

Also in attendance:

Name	*Position (or reason for attending)*
Kirstie Penman	Amendments Coordinator

Notes on statistical analysis for chapter 7

Results for the primary outcome (aortic distensibility) in chapter 7 “assessment of Large Artery Involvement in Rheumatoid Arthritis Over Time: Prior to Diagnosis, at Diagnosis and in Established Disease was conducted by intention to treat (ITT) analysis. The overarching principle of ITT analysis is that all patients enrolled and randomised in a randomised control trial are analysed in the groups to which they were originally assigned.

Where baseline CMR data, but no follow up 1 year CMR scan had been conducted, missing data were imputed by multiple imputation with assistance from a biostatistician (EH). Multiple imputation makes some assumptions about missing data- namely that they are missing at random. Importantly, it assumes that they were not missing due to the values themselves (for example because all the missing scans were systematically much higher or lower than the recorded follow up values).

Treatment groups were as follows:

- Group 1: First line ETN-MTX
- Group 2: First-line MTX-T2T ± ETN-MTX

Treatment subgroups were defined as follows:

- Group 1a: First line ETN-MTX responders (24-wk DAS28-ESR ≥2.6)
- Group 1b: First line ETN-MTX non-responders (24-wk DAS-ESR <2.6)
- Group 2a: First line MTX-T2T responders remaining on MTX-T2T (24-wk DAS28-ESR ≥2.6)
- Group 2b: First line MTX-T2T non-responders escalating to ETN-MTX (24-wk DAS-ESR <2.6)

A limitation of this approach is that there were some patients in the group 2 who were not strictly in DAS28-ESR defined remission at week 24 but were not escalated – this decision was based on the judgment of the treating clinician.

For all patients with missing DAS28-ESR at week 24 due to reasons other than withdrawal for lack of efficacy were assumed to be responders in the initial analysis. Data were then re-imputed and reanalysed assuming they were non-responders.

Aortic distensibility values were natural log-transformed prior to analysis. Results in chapter 7 are therefore expressed as ratios between groups.

The imputation model included the following variables at weeks 0, 12, 24, 36 and 48: SJC44, RAI, CRP, ESR, physician VAS, patient general health VAS, patient pain VAS, patient disease activity VAS and early morning stiffness. Aortic distensibility at baseline and 1 year was included. The model also included age, gender, symptom duration, treatment and an indicator for whether the patient was a responder.

Multiple imputation by chained equations was used to create 50 complete datasets, the results from which were combined according to Rubin's rules.

Adjusted analyses were performed via multiple regression with appropriate checks that data met the assumptions of the test.